ISSN 2500-316X (Online)

RUSSIAN TECHNOLOGICAL JOURNAL

РОССИЙСКИЙ ТЕХНОЛОГИЧЕСКИЙ ЖУРНАЛ

Information systems.
Computer sciences.
Issues of information security

Multiple robots (robotic centers) and systems.
Remote sensing and non-destructive testing

Modern radio engineering and telecommunication systems

Micro- and nanoelectronics.
Condensed matter physics

Analytical instrument engineering and technology

Mathematical modeling

Economics of knowledge-intensive and high-tech enterprises and industries.
Management in organizational systems

Product quality management. Standardization

Philosophical foundations of technology and society

12+

www.rtj-mirea.ru

12(2) 2024

ISSN 2500-316X (Online)

RUSSIAN TECHNOLOGICAL JOURNAL

РОССИЙСКИЙ ТЕХНОЛОГИЧЕСКИЙ ЖУРНАЛ

- Information systems. Computer sciences. Issues of information security
- Multiple robots (robotic centers) and systems. Remote sensing and non-destructive testing
- Modern radio engineering and telecommunication systems
- Micro- and nanoelectronics. Condensed matter physics
- Analytical instrument engineering and technology
- Mathematical modeling
- Economics of knowledge-intensive and high-tech enterprises and industries. Management in organizational systems
- Product quality management. Standardization
- Philosophical foundations of technology and society

- Информационные системы. Информатика. Проблемы информационной безопасности
- Роботизированные комплексы и системы. Технологии дистанционного зондирования и неразрушающего контроля
- Современные радиотехнические и телекоммуникационные системы
- Микро- и наноэлектроника. Физика конденсированного состояния
- Аналитическое приборостроение и технологии
- Математическое моделирование
- Экономика наукоемких и высокотехнологичных предприятий и производств. Управление в организационных системах
- Управление качеством продукции. Стандартизация
- Мировоззренческие основы технологии и общества

Russian Technological Journal
2024, Vol. 12, No. 2

Russian Technological Journal
2024, том 12, № 2

https://www.rtj-mirea.ru

https://doi.org/10.32362/2500-316X

ISSN 2500-316X (Online)

Russian Technological Journal 2024, Vol. 12, No. 2

Publication date March 31, 2024.

The peer-reviewed scientific and technical journal highlights the issues of complex development of radio engineering, telecommunication and information systems, electronics and informatics, as well as the results of fundamental and applied interdisciplinary researches, technological and economical developments aimed at the development and improvement of the modern technological base.

Periodicity: bimonthly.
The journal was founded in December 2013. The titles were «Herald of MSTU MIREA» until 2016 (ISSN 2313-5026) and «Rossiiskii tekhnologicheskii zhurnal» from January 2016 until July 2021 (ISSN 2500-316X).

Founder and Publisher:
Federal State Budget
Educational Institution of Higher Education
«MIREA – Russian Technological University»
78, Vernadskogo pr., Moscow, 119454 Russia.

The journal is included into the List of peer-reviewed science press of the State Commission for Academic Degrees and Titles of Russian Federation. The Journal is included in Russian State Library (RSL), Russian Science Citation Index, eLibrary, Socionet, Directory of Open Access Journals (DOAJ), Directory of Open Access Scholarly Resources (ROAD), Google Scholar, Ulrich's International Periodicals Directory.

The registration number ПИ № ФС 77 - 81733 was issued in August 19, 2021 by the Federal Service for Supervision of Communications, Information Technology, and Mass Media of Russia.

The subscription index of *Pressa Rossii*: **79641**.

Russian Technological Journal 2024, том 12, № 2

Дата опубликования 31 марта 2024 г.

Научно-технический рецензируемый журнал освещает вопросы комплексного развития радиотехнических, телекоммуникационных и информационных систем, электроники и информатики, а также результаты фундаментальных и прикладных междисциплинарных исследований, технологических и организационно-экономических разработок, направленных на развитие и совершенствование современной технологической базы.

Периодичность: один раз в два месяца.
Журнал основан в декабре 2013 года. До 2016 г. издавался под названием «Вестник МГТУ МИРЭА» (ISSN 2313-5026), а с января 2016 г. по июль 2021 г. под названием «Российский технологический журнал» (ISSN 2500-316X).

Учредитель и издатель:
федеральное государственное бюджетное
образовательное учреждение высшего образования
«МИРЭА – Российский технологический университет»
119454, РФ, г. Москва, пр-т Вернадского, д. 78.

Журнал входит в Перечень ведущих рецензируемых научных журналов ВАК РФ, в которых должны быть опубликованы основные научные результаты диссертаций на соискание ученой степени кандидата наук и доктора наук, индексируется в РГБ, РИНЦ, eLibrary, Соционет, Directory of Open Access Journals (DOAJ), Directory of Open Access Scholarly Resources (ROAD), Google Scholar, Ulrich's International Periodicals Directory.

Регистрационный номер и дата принятия решения о регистрации СМИ ПИ № ФС 77 - 81733 от 19.08.2021 г.
СМИ зарегистрировано Федеральной службой по надзору в сфере связи, информационных технологий и массовых коммуникаций (Роскомнадзор).

Индекс по объединенному каталогу «Пресса России» **79641**.

https://www.rtj-mirea.ru

Editorial Board

Редакционная коллегия

Contents

Содержание

Information systems. Computer sciences. Issues of information security

Информационные системы. Информатика. Проблемы информационной безопасности

UDC 004.042
https://doi.org/10.32362/2500-316X-2024-12-2-7-15

RESEARCH ARTICLE

Methods for analyzing the impact of software changes on objective functions and safety functions

Alexander A. Legkodumov [1, @],
Boris N. Kozeyev [2, @],
Vladimir V. Belikov [3],
Andrey V. Korolkov [3]

[1] *SFB Laboratory, Moscow, 127083 Russia*
[2] *ALFA-BANK, Moscow, 107078 Russia*
[3] *MIREA – Russian Technological University, Moscow, 119454 Russia*
[@] *Corresponding author, e-mail: studkkso0416@mail.ru, kozeev.boris2018@yandex.ru*

Abstract

Objectives. This paper examines the various approaches to analyzing the impact of software changes, and suggests a new method using function control flows. Impact analysis of software change can require the investment of a lot of time and competence on the part of the expert conducting it. There is no detailed description of methodology for analyzing the impact of changes and it is not established at a legislative level. The proposed method has three aims: reducing the level of requirements for an expert when conducting software research; localizing code areas to establish defects in information protection functions; and reducing the time spent on analyzing the impact of changes.

Methods. The study analyzes the common methods for analyzing software changes with a description of their positive and negative sides. The possibility of analyzing changes in the control flow of software functions is considered as an alternative to line-by-line comparison of the full volume of source codes. Represented as tree-shaped graphs, the control flows of different versions of the same software are subject to a merging procedure. The final result is analyzed by an expert from the research organization.

Results. The research results of the software change analysis methods are presented with a description of their disadvantages. A description is given of the method for change analysis using function control. This complements existing methods, while eliminating their disadvantages. The study also analyzes the possibility of using this method beyond the tasks defined in the introduction.

Conclusions. The use of methods to localize the most vulnerable code sections is considered one of the most promising areas for analyzing change impact. In addition to searching for vulnerable code sections, it is important to evaluate the effectiveness of the control flow comparison method in the analysis of source code when transferred to another code base.

Keywords: static analysis, cryptographic protection tool, change impact analysis, graph merging, program code analysis

• **Submitted:** 02.08.2023 • **Revised:** 25.09.2023 • **Accepted:** 05.02.2024

For citation: Legkodumov A.A., Kozeyev B.N., Belikov V.V., Korolkov A.V. Methods for analyzing the impact of software changes on objective functions and safety functions. *Russ. Technol. J.* 2024;12(2):7–15. https://doi.org/10.32362/2500-316X-2024-12-2-7-15

Financial disclosure: The authors have no a financial or property interest in any material or method mentioned.

The authors declare no conflicts of interest.

НАУЧНАЯ СТАТЬЯ

Методы анализа влияния изменений программного обеспечения на целевые функции и функции безопасности

А.А. Легкодумов [1,@],
Б.Н. Козеев [2,@],
В.В. Беликов [3],
А.В. Корольков [3]

[1] *СФБ Лаборатория, Москва, 127083 Россия*
[2] *АЛЬФА-БАНК, Москва, 107078 Россия*
[3] *МИРЭА – Российский технологический университет, Москва, 119454 Россия*
[@] *Автор для переписки, e-mail: studkkso0416@mail.ru, kozeev.boris2018@yandex.ru*

Резюме

Цели. В статье рассматриваются различные подходы к выполнению процедуры анализа влияния изменений программного обеспечения (ПО) на его безопасность, а также предложен новый метод проведения процедуры анализа, использующий потоки управления функций. Анализ влияния изменений ПО – достаточно трудоемкая процедура, требующая значительных временных затрат и наличия необходимой компетенции у проводящего ее эксперта. Методика проведения анализа влияния изменений ПО не имеет детального описания и не закреплена на законодательном уровне. Цель предлагаемого метода – снижение уровня требований к эксперту, проводящему исследование ПО; локализация областей кода для исследования на наличие дефектов в функциях, обеспечивающих защиту информации; сокращение времени, затрачиваемого на проведение анализа влияния изменений.

Методы. Проанализированы наиболее распространенные методы анализа изменений: построчное сравнение, система управления версиями, выполнение автоматизированных текстов. Приведено описание положительных и отрицательных сторон методов анализа. Рассмотрена возможность анализа изменений потока управления функциями ПО как альтернатива стандартному построчному сравнению полного объема исходных текстов. После построения потоки управления различных версий одного ПО, представленные в виде древовидных графов, проходят процедуру объединения. Конечный результат анализируется экспертом.

Результаты. Приведены результаты исследования методов анализа изменений ПО с описанием недостатков. Представлено описание метода проведения анализа изменений, использующего поток управления функций, который дополняет существующие методы, устраняя их представленные недостатки. Проанализирована возможность применения данного метода за рамками задач, определенных во введении.

Выводы. Использование методов, локализующих наиболее уязвимые участки кода, выделено как одно из наиболее перспективных направлений для проведения анализа влияния изменений. Помимо поиска уязвимых участков кода, важной является оценка эффективности метода сравнения потоков управления в анализе исходного кода при его переходе на другую кодовую базу.

Ключевые слова: статический анализ, средство криптографической защиты, анализ влияния изменений, объединение графов, анализ программного кода

• **Поступила:** 02.08.2023 • **Доработана:** 25.09.2023 • **Принята к опубликованию:** 05.02.2024

Для цитирования: Легкодумов А.А., Козеев Б.Н., Беликов В.В., Корольков А.В. Методы анализа влияния изменений программного обеспечения на целевые функции и функции безопасности. *Russ. Technol. J.* 2024;12(2):7–15. https://doi.org/10.32362/2500-316X-2024-12-2-7-15

Прозрачность финансовой деятельности: Авторы не имеют финансовой заинтересованности в представленных материалах или методах.

Авторы заявляют об отсутствии конфликта интересов.

INTRODUCTION

Software is deeply integrated into the life of modern man. It is used in medical equipment, cars, banks, airplanes, phones, and many other areas. Much of today's software interacts with the personal data (PD) of its users or may even be installed at a critical facility (CF) allowing interaction with highly valuable data. Compromised CF or theft of PD can result in infrastructure destruction, facility control failure, theft of user resources, and other negative consequences. The security of user data and infrastructure requires embedding certified information security equipment (CISE). This can be specialized software designed to protect private information [1]. In order to protect against new threats, new information security features are constantly being added to the source codes of the information security software, or existing ones are changed. After such a change, special examination of CISE needs to be carried out. The need for such examination is justified by orders of the Federal Service for Technical and Export Control (FSTEC)[1] and the Federal Security Service of Russia.[2]

Developing and maintaining any software is a continuous process wherein the existing functionality is constantly changing. New functions are added, coding styles are updated, optimizations are made, and errors are corrected. Any change made to the software or hardware product (hereinafter referred to as a product) may have an unpredictable impact on a certain part or even on all functions performed by the product. The more changes made to the product, the more difficult it is to trace their impact. In order to detect the changes made, and to establish their nature and quality, a special study called change impact analysis (CIA) [2] is conducted. This is performed, in order to test the software used and to determine the degree of risks associated with any changes made.

Note: in the following text, the expert referred to is an employee of a testing laboratory involved in the CISE change impact analysis.

CIA is a labor-intensive procedure. A significant amount of work is performed manually by the expert and the developer of the protection system. Based on the results of CIA, the aim of the expert is to obtain answers to the following questions:

1. Which program modules and functionalities would be affected by the specific change and how exactly?
2. Would this implementation affect the functionality of the application or individual application modules?

Orders No. 55 of the Federal Security Service of Russia and No. 66 of FSTEC the CISE state that CIA is required after each change. In this way a significant number of changes may accumulate between two versions of the same product, thus increasing the working time of the expert. Thus, the complexity and the amount of resources spent on CIA is additionally affected. Furthermore, a special study

[1] Paragraph 71 of the FSTEC Order No. 55 from April 03, 2018 "Regulation on the Information Protection Equipment Certification System." The paragraph of the Order specifies that the developer of an information protection system should conduct tests of the information protection system involving a testing laboratory (in Russ.). https://fstec.ru/dokumenty/vse-dokumenty/prikazy/prikaz-fstek-rossii-ot-3-aprelya-2018-g-n-55. Accessed May 02, 2023.

[2] Paragraph 41 of the Order of the Federal Security Service of Russia No. 66 dated February 09, 2005 "Regulations on the Development, Production, Implementation, and Operation of Encryption (Cryptographic) Means of Information Protection (Regulations PKZ-2005)." The paragraph specifies that all changes in the design of cryptographic information protection means and their manufacturing technology should be coordinated by the manufacturer of cryptographic information protection means with a specialized organization and the Federal Security Service of Russia (in Russ.). http://pravo.gov.ru/proxy/ips/?docbody=&prevDoc=102900265&backlink=1&nd=102097894&rdk=0. Accessed May 02, 2023.

is required to be conducted by an expert from a third-party organization, unfamiliar with the software and organization of the internal operation of the CISE functions. All the above constitutes the main problem of change analysis [3].

The expert conducting CIA should be highly qualified. They are required to possess:

- an understanding of the software operation;
- knowledge of the programming language in which the product is developed;
- an understanding of the operation of libraries used in the product implementation;
- the ability to search for changed code sections and analyze these sections to evaluate the impact of changes on the product functionality.

The paper considers different approaches to conducting CIA. It presents a method aimed at optimizing the analysis, in order to reduce the level of requirements of the expert and reducing the time needed to obtain meaningful results. When used in this paper, meaningful results are understood to be finding code changes and determining their impact on the CISE quality characteristics.

1. ANALYSIS OF EXISTING CIA METHODS

1.1. Line-by-line comparison

Line-by-line comparison is a method by which an expert performs a line-by-line comparison of different source code versions of the same product, in order to find and evaluate differences. The procedure can be performed using software source code comparison tools such as *Beyond Compare*[3], *Araxis Merge*[4] or the Linux built-in *diff* utility. Source code modification for this method consists of deleting, adding, or changing a line. In most practical cases, the changes found during line-by-line comparison are erroneous insertions which have no effect on functions implemented by the product. Changes which can be classified as erroneous can be divided as follows:

- changing the names of functions or variables;
- removing or adding line breaks;
- deleting or adding comments;
- deleting or adding code lines which do not relate to the functionality implemented by the product (if only not regulated by requirements).

The latter represents idle code sections [4]. This may be code which only participates in developer tests or operates in a certain environment. In addition to erroneous occurrences, this method is relatively ineffective in situations when the product code base switches to another programming language. In this case, any line could be marked as mismatched by automatic analysis tools.

The advantage of this method is that it covers the entire volume of software source code, thus enhancing the possibility of detecting a vulnerability when compared to automated analysis [5]. However, line-by-line analysis is a very costly procedure requiring a lot of expert man-hours along with an in-depth knowledge of the programming language.

1.2. Version control systems

In order to reduce the amount of work performed "manually" by the expert of the research organization, the development company may provide additional materials together with the research materials. These may be, for example, the history of changes generated by a version control system. In modern practice, a version control system is used to optimize the organization of work of several developers on any given product.

This system consists of software to facilitate the management of changing information. This allows changes in the program code to be tracked. It also enables version control, organizing the simultaneous work of several developers, supporting several development directions, and ensuring their interaction. The use of information about source code modifications focuses the attention of the expert and simplifies its understanding.

The advantage of this method is that the change report can be built in automatic mode. There is no need for a separate search of every change by using the line-by-line comparison of two source code versions [6]. However, this advantage contains its main disadvantage. Due to the widespread use of version control systems, the history of changes is available when developing most software. Despite this, the examination can be difficult since the quality of the description of changes depends directly on the employee engaged in describing the changes made during the development. The generated report or change history may provide incomplete or even incorrect information which may hinder a correct CIA.

1.3. Automated tests

Another CIA method implies comparing the test results of two versions of the same software. This method enables checking and confirming that the logic of functions has not changed. This method allows any changes leading to the appearance of defects in the operation of product functions and safety functions to be tracked [7].

[3] https://www.scootersoftware.com/. Accessed May 02, 2023.

[4] https://www.araxis.com/merge/index.en. Accessed May 02, 2023.

The advantages of this method include the possibility of automating testing of a large amount of data. However, any conclusion based on test results cannot be considered reliable, since the developer may add undocumented features to the software. The tests are based on known product features and cannot signal the presence of a software anomaly. Although automated test systems are quite capable of finding errors when changes are implemented incorrectly, the automated test approach may show incomplete or incorrect results in the context of the tests being performed [8]. Depending on the code size being tested and the quality of changes being made, the test set or regression testing, as another approach, lose out to CIA in terms of the amount of resources spent and accuracy [9]. The advantage of CIA is the possibility of testing separate code sections while ignoring the rest of the protection system. Thus, testing modified software using common practices may not be enough to ensure compliance with security requirements. Some code parts may require double checking, deeper analysis, or another approach to testing [10]. The disadvantages of the method also include additional work on creating or modernizing tests for software, if existing functionality has been added or removed. In rare cases, experts of research organizations have to work with incomplete source code, excluding the possibility of conducting CIA using tests.

2. METHOD FOR CONDUCTING CIA

The main problem with CIA is the amount of resources required to conduct it, whether in terms of time required by experts or software knowledge. In order to reduce the time required to analyze test results or carry out line-by-line comparison, the difference in the product logic and the relationships between the functions of the first and second versions of the product may be analyzed [11]. Analysis using the proposed method is divided into the following steps:

- performing static analysis of software to obtain data;
- building the function call sequence based on the data obtained as a result of static analysis [12];
- representing the function call sequence in the form of a tree-shaped graph [13];
- combining the tree-shaped graphs of two versions.

The static analysis of source codes should result in the following data:

- data types used;
- class structures;
- function call sequence [14].

The resulting root graph representing the software control flow shows the first function in the control flow as a root. The graph nodes are other functions which participate in the call chain [15]. In the process of merging the plotted tree-shaped graphs, deleted or added nodes are selected. Based on data obtained from the new graph, the expert can develop hypotheses.

The following hypotheses are selected for testing:

- the node is deleted, implying the functionality is excluded from the software or transferred to another node;
- the node is added, implying a new functionality has been added to the software or it is a transferred functionality from a remote node;
- the order of node calling is changed, meaning changes in the data processing logic have taken place.

We shall consider the following example. Figures 1 and 2 show the sequences of function calls in the form of root graphs G_1 and G_2. The *main* node is the initial call of all other software functions. The func_N node represents any function implemented in the software, where N is a number from 1 to the maximum possible number of function calls.

The result of merging graphs G_1 and G_2 is shown in Fig. 3.

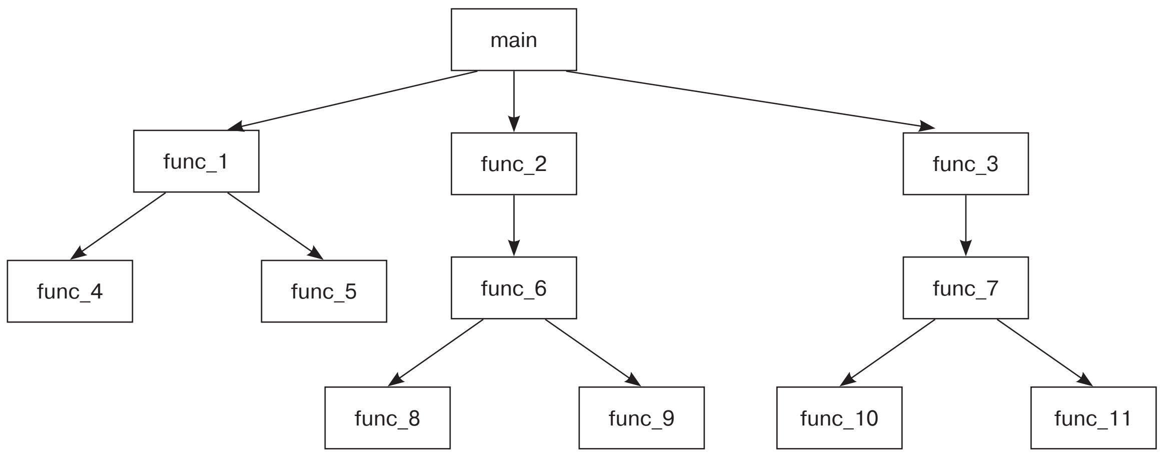

Fig. 1. Flow of function calls for the old software version represented as a tree-shaped graph

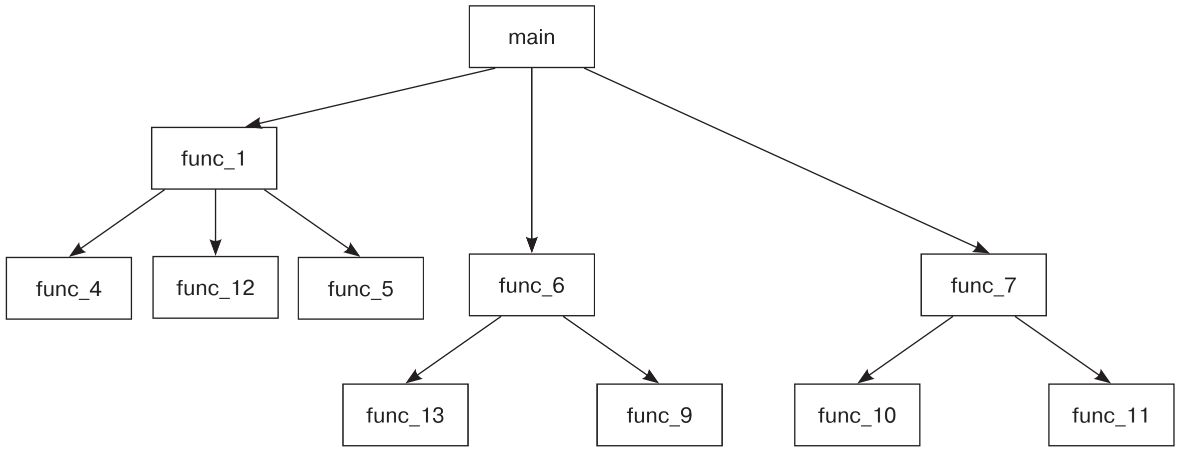

Fig. 2. Flow of function calls for the new software version represented as a tree-shaped graph

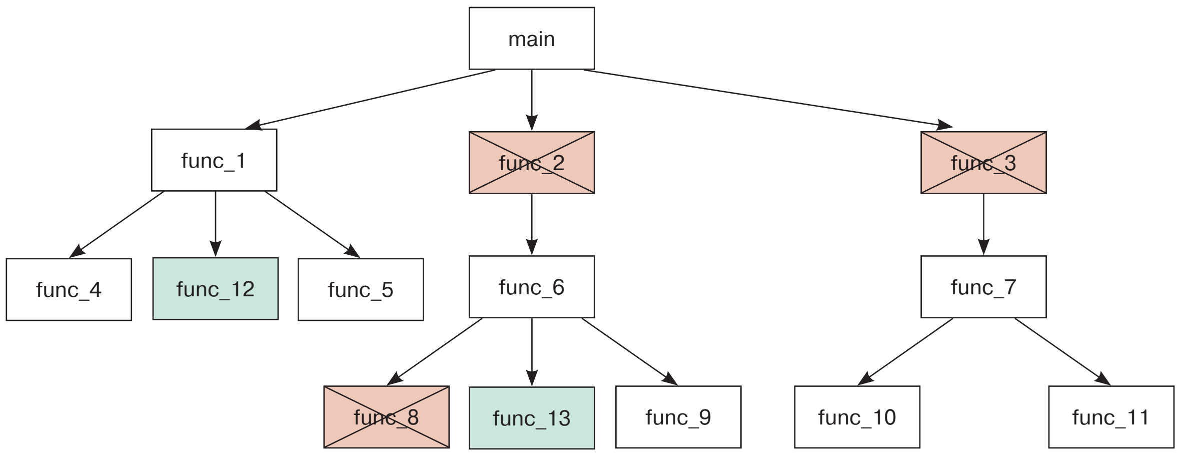

Fig. 3. Result of merging two graphs

Based on the data obtained, the following hypotheses are proposed for testing:

- the func_12 node is added to the left branch. Hypothesis: the node implements new functionality;
- the middle branch has undergone most changes. The func_2 and func_8 nodes are removed. Hypothesis: new func_13 node has either new functionality or implements the capabilities of func_2 and func_8;
- the top func_3 node in the right branch is removed. Hypothesis: the functionality is removed completely or moved to the nodes below it.

Thus, the task is localized and reduced to the task of analyzing versions of specific functions with no direct interaction with the software source code:

- in the left branch, the impact is determined by analyzing operation of func_12;
- in the middle branch, the impact is established by analyzing the result of comparing func_2 and func_8 nodes with func_13 node;
- in the right branch, the impact is established by measuring the significance of the functionality implemented by func_3 and checking the code (using the search program) for the presence of the func_3 implementation in the nodes below it.

CONCLUSIONS

This paper considers the most common methods and tools used to conduct CIA. It also presents the concept of a new method aimed at remedying the disadvantages of the existing methods for studying the impact of software changes on its security. The advantage of the method is in its ability to calculate code sections which have undergone the biggest changes even before the expert interacts with the source code directly.

In addition to its use by experts in research organizations, this method can also be implemented in software development companies, in order to track anomalies in software logic during the development phase.

Further research will focus on using the method in CIA related to transition to a new code base, as well as on improving the accuracy of identifying vulnerable nodes when tainted data is used in the analysis.

Authors' contributions

A.A. Legkodumov—justification of the research concept, development of the research methodology, writing a prototype of the program implementing the method, and writing the text of the article.

B.N. Kozeyev—literature review, analysis and generalization of literature data, conducting research on open source code, and editing the article.

V.V. Belikov—collection and systematization of data, formulation of conclusions, analysis of research results, and editing the article.

A.V. Korolkov—creation of the research model, planning the research, analysis of the research results, and editing the article.

REFERENCES

1. Karpov Yu.G. *Model checking. Verifikatsiya parallel'nykh i raspredelennykh programmnykh system* (*Model checking. Verification of Parallel and Distributed Software Systems*). St. Petersburg: BHV-Petersburg; 2010. 560 p. (in Russ.). ISBN 978-5-9775-0404-1
2. Belikov D.V. The use of static source code analysis in software development and testing. *Studencheskii forum = Student Forum.* 2021;41:90–93 (in Russ.).
3. Belikov D.V. Methods for conducting static analysis of program code. *Studencheskii forum = Student Forum.* 2022;13(192):15–18 (in Russ.).
4. Kazarin O.V., Skiba V.Yu. About one method of verification of settlement programs. *Bezopasnost' informatsionnykh tekhnologii = IT Security* (*Russia*). 1997;3:40–33 (in Russ.).
5. Shchedrin D.A. Application of machine learning methods and analysis of static code of intelligent systems. *Nauchno-issledovatel'skii tsentr "Technical Innovations" = Scientific Journal "Research Center Technical Innovations."* 2023;16:28–32 (in Russ.).
6. Ivannikov V.P., Belevantsev A.A., Borodin A.E., Ignatiev V.N., Zhurikhin D.M., Avetisyan A.I., Leonov M.I. Static analyzer Svace for finding of defects in program source code. *Trudy Instituta sistemnogo programmirovaniya RAN = Proceedings of the Institute for System Programming of the RAS*. 2014;26(1):231–250 (in Russ.). https://doi.org/10.15514/ISPRAS-2014-26(1)-7
7. Viktorov D.S., Samovolina E.V., Mokeeva O.A. The effectiveness of static analysis for finding software defects. *Vestnik Voennoi akademii vozdushno-kosmicheskoi oborony = Bulletin of the Military Academy of Aerospace Defense*. 2021;6:25–39 (in Russ.).
8. Buryakova N.A., Chernov A.V. Classification of partially formalized and formal models and methods of software verification. *Inzhenernyi Vestnik Dona = Eng. J. Don*. 2010;4:129–134 (in Russ.).
9. Efimov A.I. The problem of technological security of software for weapons systems. *Bezopasnost' informatsionnykh tekhnologii = IT Security* (*Russia*). 1994;3–4:22–33 (in Russ.).
10. Efimov A.I., Palchun B.P., Ukhlinov L.M. Methodology for constructing tests for checking technological safety *of programming automation tools based on their functional diagrams. Voprosy zashchity informatsii = Information Security Questions*. 1995;3:30:52–54 (in Russ.).
11. Glukhikh M.I., Itsykson V.M., Tsesko V.A. Using dependencies to improve precision of code analysis. *Aut. Control Comp. Sci*. 2012;46(7):338–344. https://doi.org/10.3103/S0146411612070097
[Original Russian Text: Glukhikh M.I., Itsykson V.M., Tsesko V.A. Using dependencies to improve precision of code analysis. *Modelirovanie i Analiz Informatsionnykh Sistem*, 2011;18(4):68–79 (in Russ.).]
12. Malikov O.R. Automatic detection of vulnerabilities in the source code of programs. *Izvestiya TRTU*. 2005;4:48–53 (in Russ.).
13. Nesov V.S., Malikov O.R. Using information about linear dependencies to detect vulnerabilities in the source code of programs. *Trudy Instituta sistemnogo programmirovaniya RAN = Proceedings of the Institute for System Programming of the RAS*. 2006;9:51–57 (in Russ.).
14. Vorotnikova T.Yu. Reliable code: static analysis of program code as a means of improving the reliability of software for information systems. *Informatsionnye tekhnologii v UIS = Information Technologies in the UIS*. 2020;2:22–27 (in Russ.).
15. Fritz C., Arzt S., Rashofer S., et al. Highly Precise Taint Analysis for Android Applications. *Technical Report TUD-CS-2013-0113.* EC SPRIDE. May 2013. 14 p. Available from URL: http://www.bodden.de/pubs/TUD-CS-2013-0113.pdf

СПИСОК ЛИТЕРАТУРЫ

1. Карпов Ю.Г. *Model checking. Верификация параллельных и распределенных программных систем*. СПб.: БХВ-Петербург; 2010. 560 с. ISBN 978-5-9775-0404-1
2. Беликов Д.В. Использование статического анализа исходного кода в разработке и тестировании программного обеспечения. *Студенческий форум*. 2021;41:90–93.
3. Беликов Д.В. Методы проведения статического анализа программного кода. *Студенческий форум*. 2022;13(192):15–18.
4. Казарин О.В., Скиба В.Ю. Об одном методе верификации расчетных программ. *Безопасность информационных технологий*. 1997;3:40–33.
5. Щедрин Д.А. Применение методов машинного обучения и анализа статического кода интеллектуальных систем. *Научно-исследовательский центр «Technical Innovations»*. 2023;16:28–32.
6. Иванников В.П., Белеванцев А.А., Бородин А.Е., Игнатьев В.Н., Журихин Д.М., Аветисян А.И., Леонов М.И. Статический анализатор Svace для поиска дефектов в исходном коде программ. *Труды Института системного программирования РАН*. 2014;26(1):231–250. https://doi.org/10.15514/ISPRAS-2014-26(1)-7
7. Викторов Д.С., Самоволина Е.В., Мокеева О.А. Эффективность статического анализа для поиска дефектов программного обеспечения. *Вестник Военной академии воздушно-космической обороны.* 2021;6:25–39.
8. Бурякова Н.А., Чернов А.В. Классификация частично формализованных и формальных моделей и методов верификации программного обеспечения. *Инженерный Вестник Дона*. 2010;4:129–134.
9. Ефимов А.И. Проблема технологической безопасности программного обеспечения систем вооружения. *Безопасность информационных технологий*. 1994;3–4:22–33.
10. Ефимов А.И., Пальчун Б.П., Ухлинов Л.М. Методика построения тестов проверки технологической безопасности инструментальных средств автоматизации программирования на основе их функциональных диаграмм. *Вопросы защиты информации*. 1995;3(30):52–54.
11. Глухих М.И., Ицыксон В.М., Цесько В.А. Использование зависимостей для повышения точности статического анализа программ. *Моделирование и анализ информационных систем*. 2011;18(4):68–79.
12. Маликов О.Р. Автоматическое обнаружение уязвимостей в исходном коде программ. *Известия Таганрогского радиотехнического университета* (*Известия ТРТУ*). 2005;4:48–53.
13. Несов В.С., Маликов О.Р. Использование информации о линейных зависимостях для обнаружения уязвимостей в исходном коде программ. *Труды Института системного программирования РАН*. 2006;9:51–57.
14. Воротникова Т.Ю. Надежный код: статический анализ программного кода как средство повышения надежности программного обеспечения информационных систем. *Информационные технологии в УИС*. 2020;2:22–27.
15. Fritz C., Arzt S., Rashofer S., et al. Highly Precise Taint Analysis for Android Applications. *Technical Report TUD-CS-2013-0113.* EC SPRIDE. May 2013. 14 p. URL: http://www.bodden.de/pubs/TUD-CS-2013-0113.pdf

About the authors

Alexander A. Legkodumov, Cryptographic Analysis Specialist, SFB Laboratory (56/2, Mishina ul., Moscow, 127083 Russia). E-mail: studkkso0416@mail.ru. https://orcid.org/0000-0002-2562-4333

Boris N. Kozeyev, Chief Specialist, ALFA-BANK (27, Kalanchevskaya ul., Moscow, 107078 Russia). E-mail: kozeev.boris2018@yandex.ru. https://orcid.org/0009-0009-0993-8082

Vladimir V. Belikov, Cand. Sci. (Military), Docent, Assistant Professor, Department of Information Security, Institute of Artificial Intelligence, MIREA – Russian Technological University (78, Vernadskogo pr., Moscow, 119454 Russia). E-mail: belikov_v@mirea.ru. Scopus Author ID 57983605100, https://orcid.org/0000-0003-1423-1072

Andrey V. Korolkov, Cand. Sci. (Eng.), Senior Researcher, Head of the Department of Information Security, Institute of Artificial Intelligence, MIREA – Russian Technological University (78, Vernadskogo pr., Moscow, 119454 Russia). E-mail: korolkov@mirea.ru. RSCI SPIN-code 3849-6868.

Об авторах

Легкодумов Александр Алексеевич, специалист инженерно-криптографического анализа, ООО «СФБ Лаборатория» (127083, Россия, Москва, ул. Мишина, д. 56, стр. 2). E-mail: studkkso0416@mail.ru. https://orcid.org/0000-0002-2562-4333

Козеев Борис Николаевич, главный специалист, АО «АЛЬФА-БАНК» (107078, Москва, ул. Каланчевская, д. 27). E-mail: kozeev.boris2018@yandex.ru. https://orcid.org/0009-0009-0993-8082

Беликов Владимир Вячеславович, к.воен.н., доцент, доцент кафедры информационной безопасности, Институт искусственного интеллекта ФГБОУ ВО «МИРЭА – Российский технологический университет» (119454, Россия, Москва, пр-т Вернадского, д. 78). E-mail: belikov_v@mirea.ru. Scopus Author ID 57983605100, https://orcid.org/0000-0003-1423-1072

Корольков Андрей Вячеславович, к.т.н., старший научный сотрудник, заведующий кафедрой информационной безопасности, Институт искусственного интеллекта ФГБОУ ВО «МИРЭА – Российский технологический университет» (119454, Россия, Москва, пр-т Вернадского, д. 78). E-mail: korolkov@mirea.ru. SPIN-код РИНЦ 3849-6868.

Translated from Russian into English by Kirill V. Nazarov
Edited for English language and spelling by Dr. David Mossop

UDC 004.056
https://doi.org/10.32362/2500-316X-2024-12-2-16-27

RESEARCH ARTICLE

Analysis of information flow security using software implementing business logic based on stored database program blocks

Aleksey A. Timakov @

MIREA – Russian Technological University, Moscow, 119454 Russia
@ *Corresponding author, e-mail: timakov@mirea.ru*

Abstract
Objectives. Verification of software security is typically performed using dynamic and static analysis tools. The corresponding types of analysis do not usually consider the business logic of the software and do not rely on data access control policies. A modern approach to resolving this problem is to implement language-based information flow control. Despite a large amount of research, mechanisms for information flow control in software are not widely used in practice. This is because they are complex and impose increased demands on developers. The aim of the work is to transfer information flow control from the language level to the level of formal verification. This will enable the functions of controlling data integrity and confidentiality in software to be isolated into a separate task, which can be resolved by information security analysts.
Methods. The research is based on general formal security methods for computer systems and formal verification methods. The algorithm developed by the author for checking security specifications and resolving security violations uses temporal logic of actions.
Results. The technology is presented as a step-by-step approach to resolving specific tasks, including the following: designing a database (DB) for storing and processing sensitive information; analyzing dependencies and identifying relevant sets of program blocks in the DB; generating TLA+ specifications for the identified program blocks; labeling specifications according to global security policy rules and additional constraints; applying the specification verification algorithm, and resolving security violations while providing recommendations for software developers. The procedure also involves analyzing labeled data, in order to control the spread of verified program block output values in external software modules.
Conclusions. The technology presented herein does not require developers to include redundant annotations describing security policy rules. The function of analyzing information flows with reference to predefined access restrictions is moved to a separate stage of the software development life cycle.

Keywords: information flows, information flow control, formal verification, language platform, security policy, abstract semantics, non-interference

• **Submitted:** 11.05.2023 • **Revised:** 03.10.2023 • **Accepted:** 07.02.2024

For citation: Timakov A.A. Analysis of information flow security using software implementing business logic based on stored database program blocks. *Russ. Technol. J.* 2024;12(2):16–27. https://doi.org/10.32362/2500-316X-2024-12-2-16-27

Financial disclosure: The author has no a financial or property interest in any material or method mentioned.

The author declares no conflicts of interest.

НАУЧНАЯ СТАТЬЯ

Технология анализа безопасности информационных потоков в программном обеспечении, реализующем бизнес-логику с использованием хранимых программных блоков баз данных

А.А. Тимаков @

МИРЭА – Российский технологический университет, Москва, 119454 Россия
@ *Автор для переписки, e-mail: timakov@mirea.ru*

Резюме
Цели. Проверка свойств безопасности программного обеспечения (ПО) при построении информационных систем с высоким уровнем доверия, как правило, осуществляется с использованием инструментов динамического и статического анализа. Соответствующие виды анализа обычно не учитывают бизнес-логику ПО и не опираются на политику управления доступом к данным. Современным направлением решения проблемы является контроль информационных потоков. Несмотря на большое количество проведенных исследований, механизмы контроля информационных потоков в ПО пока не находят широкого применения на практике, поскольку обладают значительной сложностью и диктуют повышенные требования к разработчикам. Целью работы является перенос контроля информационных потоков с языкового уровня на уровень формальной верификации и выделение функции контроля целостности и конфиденциальности данных в ПО в самостоятельную задачу, решаемую аналитиками информационной безопасности.
Методы. Исследование опирается на общие формальные методы безопасности компьютерных систем и методы формальной верификации. Разработанный автором алгоритм проверки спецификаций использует аппарат темпоральной логики действий.
Результаты. Представлена технология, предполагающая поэтапное решение частных задач: проектирование базы данных (БД) для хранения и обработки подлежащей защите информации, анализ зависимостей и выделение релевантного множества программных блоков БД, генерация спецификаций TLA+ выделенных программных блоков БД, разметка спецификаций в соответствии с правилами глобальной политики безопасности и дополнительными ограничениями, применение алгоритма проверки спецификаций и устранение нарушений инварианта безопасности с внесением рекомендаций для разработчиков ПО, применение процедуры анализа помеченных данных для контроля распространения выходных значений верифицированных программных блоков БД во внешних программных модулях.
Выводы. Представленная технология не требует от разработчиков внесения избыточных аннотаций, описывающих правила политики безопасности. Функция анализа информационных потоков с привязкой к заданным в системе ограничениям доступа выносится на отдельный этап жизненного цикла разработки ПО.

Ключевые слова: информационные потоки, контроль информационных потоков, формальная верификация, языковая платформа, политика безопасности, абстрактная семантика, информационное невлияние

• **Поступила:** 11.05.2023 • **Доработана:** 03.10.2023 • **Принята к опубликованию:** 07.02.2024

Для цитирования: Тимаков А.А. Технология анализа безопасности информационных потоков в программном обеспечении, реализующем бизнес-логику с использованием хранимых программных блоков баз данных. *Russ. Technol. J.* 2024;12(2):16–27. https://doi.org/10.32362/2500-316X-2024-12-2-16-27

Прозрачность финансовой деятельности: Автор не имеет финансовой заинтересованности в представленных материалах или методах.

Автор заявляет об отсутствии конфликта интересов.

INTRODUCTION

The conditions for assigning automated systems to certain protection classes are determined by evaluation standards. At present, such security requirements are formulated in terms of "General Criteria for Assessing the Security of Information Technologies"[1] and include functional and trust requirements [1]. Based on an analysis of the regulatory documents,[2, 3, 4] it follows that there are three important categories of conditions to be taken into account when determining the protection class: control of legal trajectories and media of information distribution[5]; control of hidden channels; and formal proof of the effectiveness of the implemented protection mechanisms or security of computing.

At the application level, verifying computing security is most difficult. In practice, a complete solution to this problem has not been achieved, even in the context of controlling legal information dissemination trajectories. Information dissemination trajectories in software (software) which conform to the rules provided by its logic can be obtained from the control flow graph. This is provided that the control flow has integrity. In order to ensure data confidentiality and integrity in software, a combination of formal, semi-formal and informal techniques is used at different stages of system development. Some of these techniques include dynamic and static code analysis, symbolic (cosymbolic) execution, formal verification, and fuzzing testing.[6] Additional protective measures such as randomization of dynamic memory offsets, stack execution protection, control-flow integrity control, among others, can be applied at the platform and compiler level. Although the checks implemented using the above methods play an essential role in ensuring information protection, they mostly do not take into account the specifics of processed data and business logic of the application. Formal methods which take into account the specifics of data include methods based on information flow control (IFC).

Any technology of computing security analysis based on instrumentation in software (IFC) has four commonly accepted components: alphabet of restrictive labels; formal security conditions (semantics security); security condition checking (enforcing mechanism) mechanism; and implementation. The full-fledged implementation of the instrumentation in an information system implies coverage of all four components.

The difficulty of describing security policy at the application and special software level is due to two factors: firstly, the need to take into account the access control rules implemented at the system level, and secondly, the need to take into account additional restrictions, usually checked directly in the program code. Studies devoted to the description of security policy at the level of program code can be found in [2].

Most of the studies concerning computational security (IFC) [3–6], take the concept of information noninterference as a basis. In the case of software, the essence is reduced to verifying the absence of influence of sensitive (untrusted—in the context of integrity control) input values on sensitive (trusted—in the context of integrity control) output values. The necessary formal definitions will be presented below. The literature also describes other approaches to the definition of computational security: staticity of intruder knowledge [7], non-inference [8], and others.

Verification methods are most often realized at the language level in the form of separate types of static (dynamic) analysis. The methods of static analysis of information flows based on safe (secure type system) type systems have gained special popularity [9, 10]. They enable the principle of safe composition to be applied which is essential in view of the large size of the verified code of industrial applications.

Well-known implementations of IFC include JIF [11], Joana [12], and Paragon [13].

A comprehensive review of the results already achieved in this subject area is presented in [2–4].

Despite its long history, IFC in software remains only a subject of academic research. The reason is the complexity of procedures for marking source code (source code markup) with safety (security) labels and interpreting the results obtained (warnings).

1. METHODOLOGICAL BASIS

The hypothetical basis of this article is that in order to transfer the research of instrumentation methods (IFC) into practice, the function of analyzing

[1] GOST R ISO/IEC 15408-1-2002. State Standard of the Russian Federation. *Information technology. Security techniques. Evaluation criteria for IT security*. Part 1. Moscow: IPK Izdatelstvo standartov; 2002 (in Russ.).

[2] Order of the Federal Service for Technical and Export Control of Russia No. 31 dated March 14, 2014. "On Approval of Requirements for Information Protection in Automated Control Systems for Production and Technological Processes at Critically Important Facilities, Potentially Hazardous Facilities, as well as Facilities Presenting an Increased Risk to Human Life and Health and to the Natural Environment" (in Russ.). https://fstec.ru/dokumenty/vse-dokumenty/prikazy/prikaz-fstek-rossii-ot-14-marta-2014-g-n-31. Accessed March 12, 2023.

[3] GOST R 56939-2016. National Standard of the Russian Federation. *Information protection. Secure software development. General requirements*. Moscow: Standartinform; 2018 (in Russ.).

[4] GOST R 51583-2014. National Standard of the Russian Federation. *Information protection. Sequence of protected operational system formation. General provisions*. Moscow: Standartinform; 2018 (in Russ.).

[5] Legal trajectories and environments for information dissemination mean the trajectories and environments envisioned by the system developer for user access to data, as well as data exchange between users and individual system components.

[6] Fuzzing testing is a software testing technique of giving incorrect, unexpected, or random data as input to an application.

information flows with reference to access restrictions set in the system needs to be positioned at a separate stage of the software development life cycle. This can be achieved by turning to the theory of formal verification of software properties.

Before proceeding to a description of the proposed technology, we note that the idea of using the theory of formal program verification in the field of instrumentation (IFC) is not new. Significant results were obtained by Clarkson et al. [14]. In particular, the authors extended the apparatuses of linear temporal logic (LTL) and branching time logic (computational tree logic, CTL) by quantizers (quantifiers) over computation trajectories. As a result, properties of information flow security were formulated (based on the notion of information non-influence noninterference), which, in fact, are hyperproperties. The papers also outline an approach to verifying these properties using model playback (model checking tools) tools. The essence of the approach involves a description of the Kripke structure for the program to be verified, description of security properties using HyperLTL formulas—LTL extension and subsequent generation and verification of the automata model.[7] Describing an industrial application in the form of a Kripke structure may in practice be a difficult task. The authors of this study and the corresponding prototype themselves note the impossibility of scaling the application area of the developed toolkit to systems of medium complexity (the number of states does not exceed 1000). In [15], an interesting way of representing safety (security) properties of information flows as standard safety properties is proposed. This method is based on the idea of transforming the program being checked using an own composition and certain standard (inference rules) rules of inference of the system of safe types (secure type system). The limitations here include a certain difficulty in interpreting the verification results, since the procedure requires modification of the original program, and the remaining labor-intensity of analyzing programs with a large number of states.

In order to overcome the limitations of formal verification, the present study also borrows the previously mentioned approach based on secure type systems. However, in contrast to [14] and [15], a transition from operational semantics to a simplified abstract semantics of information flows is proposed for modeling computations. In addition, we introduce a restriction related to developers' compliance with the principle of minimizing the attack surface. This, inter alia, implies compact storage of sensitive information (in a limited set of tables) and the desire to clearly separate critical and non-critical services of the system. The physical separation of services based on the levels of confidentiality and integrity of processed data is now becoming possible. This is due to the rejection of monolithic architecture of business applications and the wide development of platforms supporting modular development. The type inference rules in our study are assumed to be replaced by rules of abstract information flow semantics. The rejection of operational semantics in favor of abstract semantics in modeling computations allows a significant reduction in the number of states of the automata model to be achieved, and the security properties of information flows in the form of standard reliability (safety) properties to be formulated. All this enables a mechanism for checking software security properties (in the sense of information flows) to be implemented on the basis of widely used in practice tools for creating program specifications and playing TLA+ and TLC models (TLA checker).

In this study, an intruder is defined as any system user who is not an administrator. The intruder knows the source code, can interact with the program, and has access to output values generated at all stages of execution and possessing a security label corresponding to his own label. We also believe that the intruder is unable to exploit hidden probabilistic information channels and time channels.

[7] In these studies, Büchi automata are taken as a basis.

2. METHOD OF INFORMATION FLOW SECURITY ANALYSIS

As already mentioned, the purpose of the technology developed is to detect and eliminate prohibited information flows in the software of enterprise-level automated information systems. The previously mentioned MAC (IFC) implementations mainly rely on the system of safe types (secure type systems) and static analysis (static analysis is a separate compilation step). Safe (secure) types in such platforms define security policy rules along with rules of data conversion and restrictions on the amount of allocated memory dictated by standard types. For example, an extended variable type might look like this: int x {Alice –> Bob}. This means that the owner of the data stored in variable x is Alice, and reading is allowed to Alice, Bob, and any other users acting on their behalf. Thus, the known IFC implementations already mentioned assume that the software developer is assigned additional functions of marking up the source code and interpreting security warnings generated by the static analyzer. The proposed technology is based on the idea of automatic generation of specifications based on the source code of database (DB) program blocks (services) with their subsequent verification by security specialists—analysts [16]. The stages of the analysis are presented in Fig. 1.

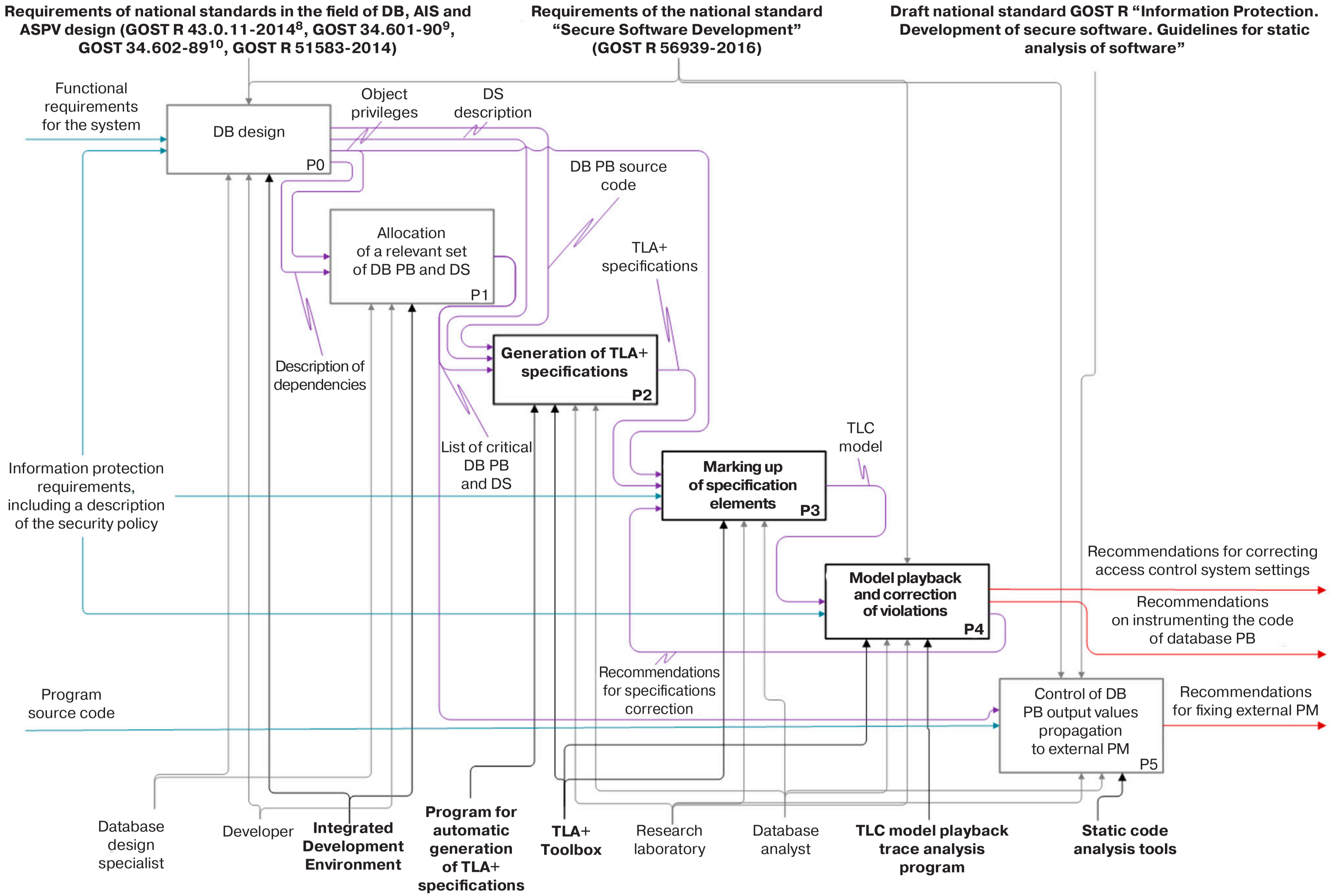

Fig. 1. Stages of analysis. PM—program module, PB—program block, DS—data source, AIS—automated information system, ASPV—automated system in a protected version

[8] GOST R 43.0.11-2014. National Standard of the Russian Federation. *Informational ensuring of equipment and operational activity. Database in technical activities*. Moscow: Standartinform; 2018 (in Russ.).

[9] GOST 34.601-90. Interstate Standard. *Information technology. Set of standards for automated systems. Automated systems. Stages of development*. Moscow: Standartinform; 2009 (in Russ.).

[10] GOST 34.602-89. Interstate Standard. *Information technology. Set of standards for automated systems. Technical directions for automated system making*. Moscow: Standartinform; 2009 (in Russ.).

The stored database program blocks (*PL/SQL* blocks) in the context of technology represent a convenient mechanism for implementing business logic. These modules, as a rule, are characterized by small code size, absence of redundant calculations, and focus on working with data.

A subset of the *PL/SQL*, language is used in the description of the technology, and its BNF-grammar[11] is presented below:

(values) v ::= $n \mid b$

(declarations) d ::= x **number** | $x_1\ x_2$ | $d_1;d_n$ | **type** x_r **is object** $(x_{f1}\ x_1,\ldots x_{fn}\ x_n)$ | **type** x_t **is table of** x | **exception** x | **procedure** $x_p(x_1,\ldots x_n)$ **as** d **begin** c_1 [**exception**] c_2 **end;**| **function** $x_{fn}(x_1,\ldots x_n)$ **return** x_{rt} **as** d **begin** c_1 [**exception** c_2] **end;** |...

(expressions) e ::= $v \mid x \mid x_1.x_2 \mid e_1 \odot e_2 \mid x(e_1,\ldots e_2) \mid \ldots$

(conditions) cnd ::= $e_1 * e_2 \mid cnd_1 \circledast cnd_2$

(statements) c ::= $x := e \mid c_1;c_2 \mid x_f(x_1 \rightarrow e_1,\ldots x_n \rightarrow e_n)$ | **if** e **then** c_1 **else** c_2 | **while** e **do** c | **end if** | **end while** | $c_1 \vee c_2$ | **select** $e_1,\ldots e_n$ **into** $x_1,\ldots x_n$ **from** $x_{t1},\ldots x_{tn}$ **where** cnd | **insert into** $x_t\ (x_1,\ldots x_n)$ **values** $(e_1,\ldots e_n)$ | **update** x_t **set** $x_1 = e_1,\ldots x_n = e_n$ **where** cnd | **delete from** x_t **where** cnd| **throw** x_{exc} | **when** x_{exc} **then** c | **null**| **return**$(x_{out} \rightarrow e)$ |...

(program) p ::= **Declare** d **begin** c_1 [**exception** c_2] **end;**

2.1. Database design

The first stage of analysis is database design. It should be performed in such a way that confidential data is placed compactly—in a limited set of tables. This requirement does not contradict the generally accepted principles of secure development, while at the same time allows us to isolate critical calculations from the general *PL/SQL* code more effectively.

2.2. Allocation of a relevant set of database program blocks and data sources

The next step is to select *PL/SQL* procedures and functions which implement critical computations, i.e., computations over confidential data and data requiring a high level of trust. An integral function of modern databases is the management of direct and transitive dependencies.[12, 13, 14] They are used by the system kernel to check the states of objects before their calls and to avoid critical errors at runtime.[15] Such mechanisms work in approximately the same way. In *Oracle* DBMS, in order to obtain the direct and indirect dependencies associated with some table T, the following commands may be executed:

execute deptree_fill('TABLE', 'T');
select * **from** deptree.

The next three steps: generation, markup, and application of the specification validation algorithm, are the key and most labor-intensive ones.

2.3. Generation of TLA+ specifications

Let *PC* be the security label of the instruction counter (program counter). It defines the implicit information flows occurring in conditional **if** statements and **while** loops; *c* is the current instruction in the process associated with the user session; *M* is the abstract state of the computing environment, which defines the mapping of variables (local and global), input and output flows to their corresponding restrictive labels; *n* is the total number of user sessions. Then the execution of program blocks in the DBMS environment can be described by the system of state transitions (state transition system) in the following form:

$$\left\langle \left\langle \left\langle PC1, c1 \right\rangle \ldots \left\langle PCn, cn \right\rangle \right\rangle, M \right\rangle.$$

The generation of specifications describing the behavior of such a system is performed using the "*Generation of TLA+ specifications based on database program blocks*" software tool, in accordance with the abstract semantics of information flows [2].

As an example, consider the rule of calculating an abstract expression and the assignment rule. The result of an abstract expression $\odot$, is calculated as the minimum (least) upper bound of the labels of the operands included in it:

[11] Backus–Naur formisa formal system for describing syntax.

[12] https://docs.oracle.com/cd/A84870_01/doc/server.816/a76965/c19depnd.htm. Accessed March 12, 2023.

[13] https://www.postgresql.org/docs/current/catalog-pg-depend.html. Accessed March 12, 2023.

[14] https://learn.microsoft.com/en-us/sql/ssms/object/object-dependencies?view=sql-server-ver16.AccessedMarch12, 2023.

[15] Database program environment is not monolithic, and in the process of database instance operation separate objects: tables, program blocks, views, etc., may undergo changes that are critical for the operation of other dependent objects.

$$(\text{E-OPER})\frac{\langle e1, M\rangle \Downarrow p1 \quad \langle e2, M\rangle \Downarrow p2}{\langle e1 \odot e2, M\rangle \Downarrow p1 \sqcup p2}.$$

The resulting labels for comparison expressions * and logical expressions ⊛ are calculated in the same way. As a result of the assignment operation, the abstract state of the computing environment changes according to the label of the value to be assigned and the label of the instruction counter in the current session:

$$(\text{C-ASSIGN})\frac{\langle e,M\rangle \Downarrow p}{\begin{array}{c}\langle\langle\langle\ldots\rangle\ldots\langle PC, x{:=}e\rangle\ldots\langle\ldots\rangle\rangle, M\rangle \to \\ \to \langle\langle\langle\ldots\rangle\ldots\langle PC,\text{null}\rangle\ldots\langle\ldots\rangle\rangle, M[x \mapsto p \sqcup pc1\ldots pcn]\rangle\end{array}}.$$

Rules of type EXT are used to check information flows associated with the elements-stocks possessing stationary security labels. These include output streams, attributes of relations, which can be accessed outside the context of calls of the checked program blocks. *Inv* conditions correspond to the security (safety) invariant:

$$(\text{C-ASSIGN-EXT})\frac{\langle e,M\rangle \Downarrow p \quad \langle x,M\rangle \Downarrow px \quad \text{inv: } p \sqcup pc1\ldots pcn \sqsubseteq px}{\begin{array}{c}\langle\langle\langle\ldots\rangle\ldots\langle PC, x{:=}e\rangle\ldots\langle\ldots\rangle\rangle, M\rangle \to \\ \to \langle\langle\langle\ldots\rangle\ldots\langle PC,\text{null}\rangle\ldots\langle\ldots\rangle\rangle, M\rangle\end{array}}.$$

Transitions between parallel sessions are represented as equally probable. This is a fair assumption for the chosen intruder model and the corresponding information non-influence (noninterference) scheme. They are described by global rules in the following form:

$$(\text{GLOB-1})\frac{O(d) = ci \qquad \langle PCi, ci, M\rangle \to \langle PCk, ck, M'\rangle}{\langle\langle\langle PC1, c1\rangle\ldots\langle PCn, cn\rangle\rangle, M\rangle \xrightarrow[1/n]{i} \langle\langle\langle PC1, c1\rangle\ldots\langle PCi-1, ci-1\rangle\langle PCk, ck\rangle\ldots\langle PCn, cn\rangle\rangle, M'\rangle},$$

$$(\text{GLOB-2})\frac{O(d) = ci \qquad \langle PCi, ci, M\rangle \to \langle PCi, M\rangle}{\langle\langle\langle PC1, c1\rangle\ldots\langle PCn, cn\rangle\rangle, M\rangle \xrightarrow[1/n]{i} \langle\langle\langle PC1, c1\rangle\ldots\langle PCi-1, ci-1\rangle\langle PCi+1, ci+1\rangle\ldots\langle PCn, cn\rangle\rangle, M\rangle}.$$

2.4. Layout (Marking up) of specification elements

Specification markup is performed on the basis of the described security policy requirements and valid access restrictions. In order to perform this step, the modified language for describing security policies *Paralocks* [13] is used. Its main advantages include the ability to embed data declassification conditions into policy expressions (or labels), flexibility, and the ability to integrate with various access control systems (role-based, mandate-based, mandatory, etc.). Arguments regarding the necessity of interfacing the IFC mechanisms implemented at the level of special (application) software and system-level access control mechanisms, as well as a comparative analysis of known security policy description languages that justify the choice of *Paralocks*, are given in [2].

Formally, the security label P_k is defined by a first-order predicate logic formula of the following form: $P_k \triangleq C_1 \wedge C_2 \wedge \ldots$, here C_n is a separate expression of information flow admissibility: $\forall x_1,\ldots,x_m.l_1(\cdot) \wedge l_2(\cdot) \wedge l_3(\cdot)\ldots \Rightarrow Flow(u)$, $Flow(u)$ is a predicate denoting the data flow to u (u is a bound variable or constant denoting a user), l_1 … l_n are conditions (or locks) whose fulfillment is required for $Flow(u)$ to be true. Predicates l_1 … l_n can be parametric or non-parametric. The set of possible locks depends on the access restrictions set at the system level and additional restrictions realized by the application software.

As an example, let us consider the policy requirement: “A flow to an arbitrary user x is possible if: (a) the *guest* role is set for x and the *w_hours* lock is open—the attempt is made during business hours, or (b) the *account* role is set for x.” Logically it can be represented as:

$$\forall x.\left(w\_hours \wedge guest(x) \Rightarrow Flow(x)\right) \wedge$$
$$\wedge\left(account(x) \Rightarrow Flow(x)\right).$$

For the convenience of analyzing the traces leading to the occurrence of prohibited information flows, a separate software tool with a graphical user interface was developed: “*Analysis of TLC model playback traces built on the basis of TLA+ specifications of database program blocks and leading to the violation of the invariant of information flows security*.” Labels are displayed in accordance with the simplified notation, in which the example under consideration appears as follows:

x : account(x)
x : guest(x), t_expire

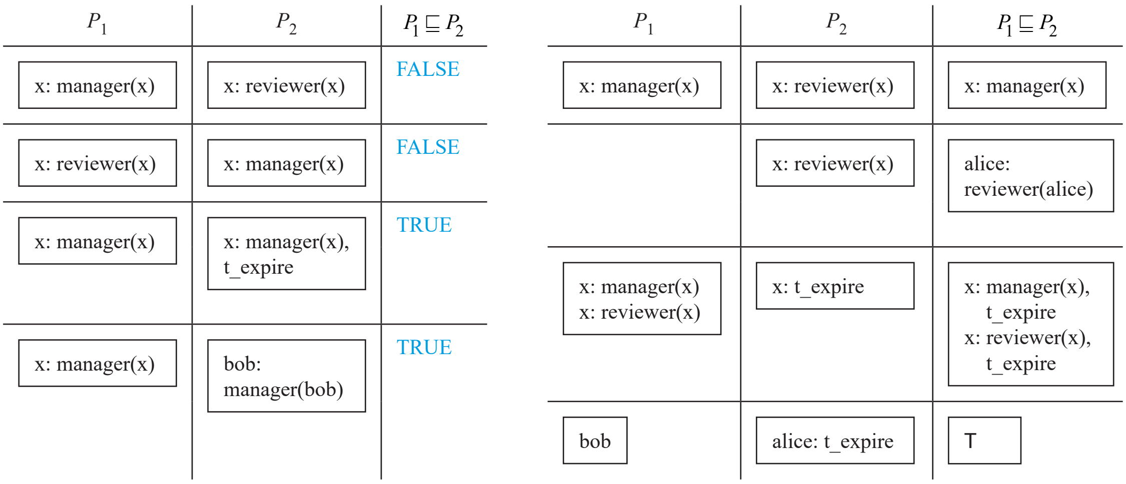

Fig. 2. Work of the label comparison operator and calculation of the minimum upper boundary

A partial order relation $\sqsubseteq$ on the set of security labels is defined as follows:

$$P_1 \sqsubseteq P_2, \text{ if } \forall c_2 \in P_2 : \exists c_1 \in P_1 : c_1 \sqsubseteq c_2. \qquad (1)$$

From a logical point of view $P_1 \sqsubseteq P_2$ can be interpreted as

$$P_1 \models P_2. \qquad (2)$$

In [17] it is shown that condition (1) is necessary and sufficient for the truth of expression (2). The comparison of security label proposals in [17] is described algorithmically, through a set of rules.

Figure 2, using simplified notation, shows several examples of how the comparison operator works on a set of labels and calculates the least upper bound.

The confidentiality level of the data used by the program may not only decrease, but also increase in the process of their processing. In order to take this into account, the *Paralocks* language syntax is extended with a one-parameter *Unknown* lock. It permits rules of classification to be specified by content (*what*)[16] for separate elements. *Unknown* lock can be used in the left part (premise) of a policy clause of some element, if in the course of calculations the policy of the element should become stricter when some additional information is disclosed.[17] For example, a policy of the form “Salary (of an employee) can be read only by a specialist of the financial department” provided that the attributes identifying the employee are: *emp_id*, *email*, *lname*, can be expressed as:

$$\forall x.(Unknown(emp\_id) \wedge$$
$$\wedge\, Unknown(email) \wedge Unknown(lname) \Rightarrow$$
$$\Rightarrow Flow(x)) \wedge account\_emp(x) \Rightarrow Flow(x).$$

Using TLA+ formulas, finite sets of possible proposals of security policies (labels) and policies themselves can be defined.[18] Using the TLA PS (proof system), we prove that the set of policies with a partial order relation defined on it forms a complete algebraic lattice.

2.5. Model playback and correction of irregularities of the safety invariants

The property of progress-dependent information noninterference (PDIN) [3] is adopted as a formal condition of computational security. In contrast to strict information noninterference, intermediate states are subject to verification. No restrictions are imposed on the values of internal variables (inaccessible for observation).

Definition 1. *Program P satisfies the progress-dependent information noninterference property for initial and final mappings of a set of variables to a set of security labels M_1 and M_2—*$\mathrm{PDIN}(P)_{M_1,M_2}$*, if for any two states S_1 and S_2 of the computation environment consisting of a low equivalence relation with respect to some security level L at mapping M_1:* (a) *each computation step is accompanied by the generation of the same observed values with respect to level L or leads to a divergence for both states;* (b) *corresponding final*

[16] It is assumed that data classification is characterized by the same aspects: *when*, *who*, *what*, *where*, as for declassification.

[17] It is also allowed the approach when the classification conditions are not taken into account, i.e., the strictest policy $(account\_emp(x) \Rightarrow Flow(x))$ is initially selected for the element. At the same time, in case of false positives (when there are no grounds for classification), the reverse declassification procedure is applied.

[18] https://github.com/timimin/plif. Accessed March 12, 2023.

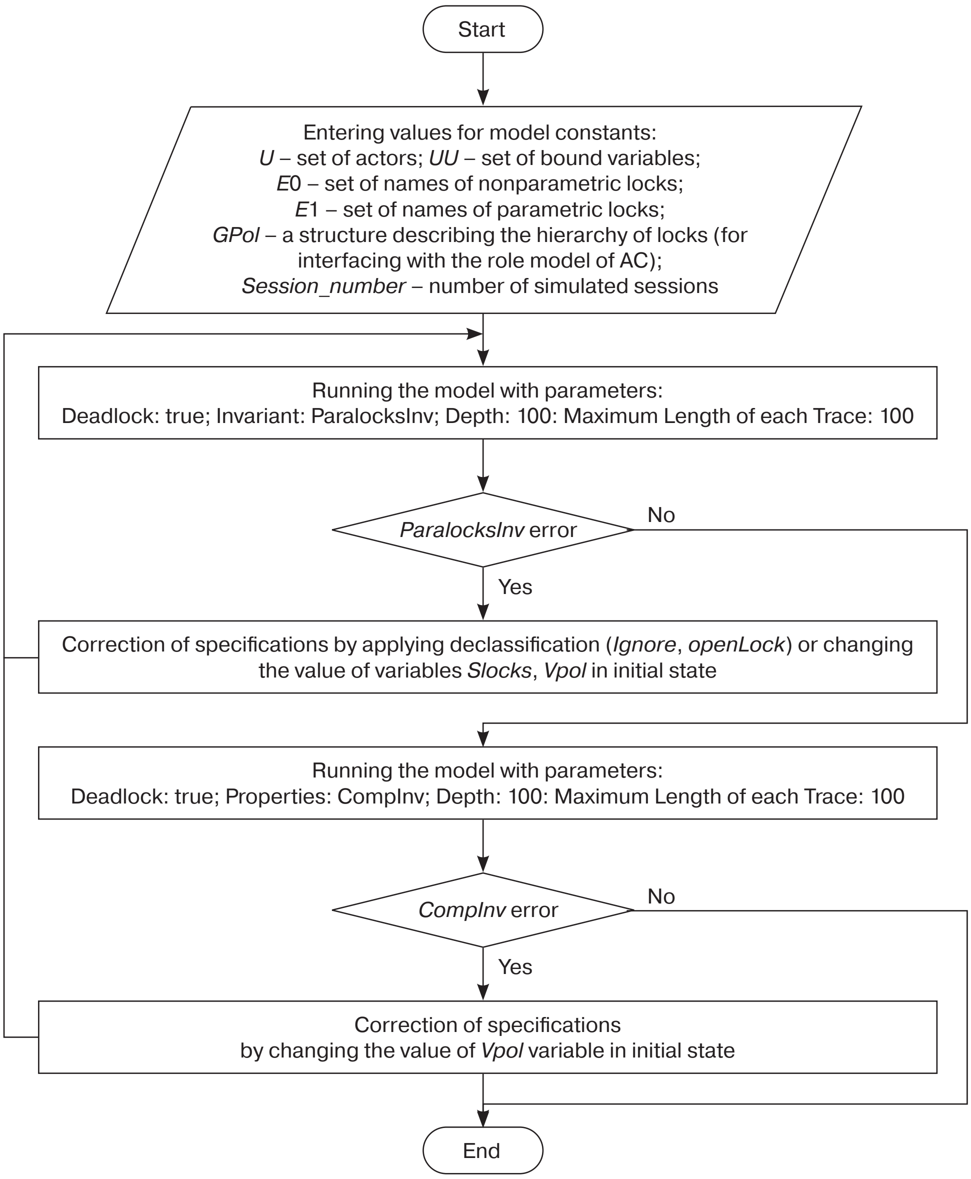

Fig. 3. Specification verification algorithm. AC—access control

states S_1' and S_2' of the computation environment consist of a low equivalence relation with respect to some security level L at mapping M_2:

$$\mathrm{PDIN}(P)_{M_1,M_2} \triangleq \forall L, S_1, S_2, o_1, o_2 : S_1 \eqsim_{M_1,L} S_2 \wedge$$
$$\wedge\, P(S_1) \downarrow \left\langle S_1', o_1 \right\rangle \wedge P(S_2) \downarrow \left\langle S_2', o_2 \right\rangle \Rightarrow$$
$$\Rightarrow o_1 \approx_{L(d)} o_2 \wedge S_1' \eqsim_{M_2,L} S_2'.$$

The expression $o_1 \approx_{L(d)} o_2$ denotes the equivalence of the observed behaviors with respect to the level L (taking into account the declassification [18]). Two states of the computation environment are assumed to be in a low equivalence relation with respect to a given privacy level L, if all pairs of similarly labeled elements with label not exceeding L have the same values. Condition (b) is easily verified for individual expressions and *PL/SQL* commands using the abstract semantics rules defined for them, and is important for formal proof of the security of computation in general under flow-sensitive conditions and the absence of restrictions on the number of executable blocks in one session.

Algorithm. The preliminary step of the algorithm (Fig. 3) defines constants which specify the number of simulated sessions, the set of user names, the set of user (bound) variables, the set of single-parameter locks, and the set of non-parameter locks, etc. When the model is replayed, the main security invariant *ParalocksInv* (guaranteeing that condition (a) of Definition 1 is met for individual commands and expressions) and the action property *CompInv* (guaranteeing that the initial and final mappings of the set of global variables to the set of labels are equivalent). If *ParalocksInv* is violated, a data declassification procedure may be applied. It usually implies code correction or changing the privileges of accessing database objects. In the event of an error caused by the violation of the *CompInv* property, the label of the corresponding global variable—table column—is incremented in the initial state.[19] Bringing the labels of global variables to stationary values allows the fulfillment of condition (a) of Definition 1 to be verified for individual *PL*/*SQL* commands and expressions for all possible initial and final abstract states M_1 and M_2. This, in turn, is required to prove the correctness of the computation model checking algorithm.

Proof of convergence of the algorithm and fulfillment of security conditions of infinite computations in an unlimited number of user sessions in accordance with the definition of PDIN at successful completion of the algorithm is given in [5].

2.6. Control of distribution of output values of verified database program blocks in external program modules

Control of the propagation of output values of verified procedures and functions in application software is performed using standard taint tracking analysis by means of tools such as *CodeQL* [19].

CONCLUSIONS

The key stages of the technology herein presented have been tested on training examples. Despite a certain loss of analysis accuracy, due to abstraction inevitable for formal verification, the possibility of graphical interpretation of problematic calculation traces using a utility entitled "*Analysis of TLC model playback traces built on the basis of TLA+ specifications of database program blocks and leading to violation of information flows security invariant*" developed with the author's participation significantly simplifies the task of identifying false alarms.

The development of comprehensive methodological recommendations on the application of data reclassifi cation (declassification and classification) procedures is a promising area for further research. At the present time, the general principles of reclassification have been formulated and a number of schemes have been proposed. However, they require adaptation to the described technology. It is recommended that separate research on the last stage of the proposed procedure be conducted.

[19] Fulfillment of the *CompInv* property can be achieved in a finite number of iterations because the policy alphabet is a finite lattice and the transition functions of the global variable policy computation are monotonically increasing.

REFERENCES

1. Devyanin P.N., Telezhnikiv V.I., Khoroshilov A.V. Building a methodology for secure system software development on the example of operating systems. *Trudy Instituta sistemnogo programmirovaniya RAN = Proceedings of the Institute for System Programming of the RAS* (*Proceedings of ISP RAS*). 2021;33(5):25–40 (in Russ.). https://doi.org/10.15514/ISPRAS-2021-33(5)-2
2. Timakov A.A. Information flow control in software DB units based on formal verification. *Program. Comput. Soft*. 2022;48(4):265–285. https://doi.org/10.1134/S0361768822040053
3. Hedin D., Sabelfeld A. A Perspective on Information-Flow Control. In: *Software Safety and Security*. 2012;33:319–347. https://doi.org/10.3233/978-1-61499-028-4-319
4. Kozyri E., Chong S., Myers A.C. Expressing Information Flow Properties. *Foundations and Trends® in Privacy and Security*. 2022;3(1):1–102. http://doi.org/10.1561/3300000008
5. Volpano D., Smith G. Probabilistic noninterference in a concurrent language. *Journal of Computer Security* (*JCS*). 1999;7(2):231–253. http://doi.org/10.3233/JCS-1999-72-305
6. Sabelfeld A., Sands D. Probabilistic noninterference for multi-threaded programs. In: *Proceedings 13th IEEE Computer Security Foundations Workshop* (*CSFW-13*). 2000. P. 200–214. https://doi.org/10.1109/CSFW.2000.856937
7. Askarov A., Chong S. Learning is Change in Knowledge: Knowledge-Based Security for Dynamic Policies. In: *Proceedings 25th IEEE Computer Security Foundations Symposium* (*CSF 2012*). 2012. P. 308–322. https://doi.org/10.1109/CSF.2012.31
8. Sutherland D. A model of information. In: *Proceedings of the 9th National Security Conference*. 1986. P. 175–183.
9. Volpano D., Irvine C., Smith G. Sound type system for secure flow analysis. *Journal of Computer Security* (*JCS*). 1996;4(2–3):167–187.
10. Mantel H., Sudbrock H. Types vs. PDGs in information flow analysis. In: Albert E. (Ed.). *Logic-Based Program Synthesis and Transformation. The 22nd International Symposium, LOPSTR 2012. Proceedings.* Springer. 2012. P. 106–121. https://doi.org/10.1007/978-3-642-38197-3_8
11. Myers A.C., Liskov B. A decentralized model for information flow control. *ACM SIGOPS Operating Systems Review.* 1997;5:129–142. https://doi.org/10.1145/268998.266669
12. Graf J., Hecker M., Mohr M., Snelting G. Checking applications using security APIs with JOANA. In: *8th International Workshop on Analysis of Security APIs*. *Proceedings.* 2015. P. 118–129.
13. Broberg N., van Delft B., Sands D. Paragon for practical programming with information-flow control. In: Shan C. (Ed.). *Programming Languages and Systems: The 11th Asian Symposium*, APLAS 2013. *Proceedings.* Springer. 2013. P. 217–232. https://doi.org/10.1007/978-3-319-03542-0_16
14. Clarkson M.R., Finkbeiner B., Koleini M., Micinski K.K., Rabe M.N., Sánchez C. Temporal logics for hyperproperties. In: Abadi M., Kremer S. (Eds.). *Principles of Security and Trust: The Third International Conference*, POST 2014. *Proceedings.* Berlin, Heidelberg: Springer; 2014. P. 265–284. https://doi.org/10.1007/978-3-642-54792-8_15
15. Terauchi T., Aiken A. Secure information flow as a safety problem. In: Hankin C., Siveroni I. (Eds.). In: *Static Analysis: The 12th International Static Symposium*, SAS 2005. *Proceedings*. Berlin, Heidelberg: Springer. 2005. P. 352–367. https://doi.org/10.1007/11547662_24
16. Timakov A.A. Scenario of Information Flow Analysis Implementation in PL/SQL Program Units with PLIF Platform. *Program. Comput. Soft.* 2023;49(4):215–231. https://doi.org/10.1134/S0361768823040114

[Original Russian Text: Timakov A.A. Scenario of Information Flow Analysis Implementation in PL/SQL Program Units with PLIF Platform. *Programmirovanie.* 2023;4:215–231 (in Russ.).]

17. Broberg N., Sands D. Paralocks: Role based information flow control and beyond. In: *Proceedings of the Conference Record of the Annual ACM Symposium on Principles of Programming Languages*. 2010. P. 431–444. https://doi.org/10.1145/1706299.1706349
18. Sabelfeld A., Sands D. Declassification: Dimensions and principles. *Journal of Computer Security* (*JCS*). 2009;17(5):517–548. http://doi.org/10.3233/JCS-2009-0352
19. Youn D., Lee S., Ryu S. Declarative static analysis for multilingual programs using CodeQL. *Software: Practice and Experience*. 2023;53(7):1472–1495. https://doi.org/10.1002/spe.3199

About the author

Aleksey A. Timakov, Cand. Sci. (Eng.), Associate Professor, Department of Information Security, Institute of Artificial Intelligence, MIREA – Russian Technological University (78, Vernadskogo pr., Moscow, 119454 Russia). E-mail: timakov@mirea.ru. Scopus Author ID 57809572100, RSCI SPIN-code 3163-2170, https://orcid.org/0000-0003-4306-789X

Об авторе

Тимаков Алексей Анатольевич, к.т.н., доцент, доцент кафедры информационной безопасности, Институт искусственного интеллекта ФГБОУ ВО «МИРЭА – Российский технологический университет» (119454, Россия, Москва, пр-т Вернадского, д. 78). E-mail: timakov@mirea.ru. Scopus Author ID 57809572100, SPIN-код РИНЦ 3163-2170, https://orcid.org/0000-0003-4306-789X

Translated from Russian into English by Lyudmila O. Bychkova
Edited for English language and spelling by Dr. David Mossop

UDC 621.396.69
https://doi.org/10.32362/2500-316X-2024-12-2-28-38

RESEARCH ARTICLE

Diagnostics of structural integrity violations of avionics during impact tests

Saygid U. Uvaysov,
Aleksey V. Dolmatov @,
The H. Vo,
Ngoc T. Luu,
Cong D. Nguyen

MIREA – Russian Technological University, Moscow, 119454 Russia
@ Corresponding author, e-mail: dolmatov@mirea.ru

Abstract

Objectives. With the continuous development of modern radio equipment in the field of aviation and space instrumentation, the requirements for accuracy, stability, and reliability of electronic equipment operated on spacecraft are also on the increase. Spacecraft avionic units (SAU) operate under special conditions and malfunctions, as a rule, are impossible to repair. SAU are hermetically sealed structures, making it difficult to assess their technical condition. The aim of this study is to increase the efficiency and reliability of detecting latent defects in SAU using the diagnostic method involving exposure to mechanical shocks.

Methods. Based on known methods, a new diagnostic method is proposed which simulates mechanical processes under shock effects at the design stage. The aim is to evaluate the presence of various latent defects in SAU. In a serviceable state, the amplitude-frequency characteristics (frequency response) of SAU differ from the frequency response of SAU with defects which affect mechanical characteristics. It was for this reason that the diagnostic model of evaluating the technical condition of SAU without removal of devices was developed.

Results. This work simulates the mechanical processes in SAU in a serviceable state in the presence of a variety of defect. It also involves experimental studies of mechanical characteristics in both serviceable and faulty states. After measuring the mechanical characteristics under the impact of shock loads, the data obtained is compared with simulation results in the presence of various defects. The comparison result is a report on the technical condition of SAU.

Conclusions. The method of diagnosing SAU under mechanical shock impact enhances the efficiency of diagnosing latent defects during the production and operation of SAU.

Keywords: diagnostics, mechanical shock impact, spacecraft avionic units

• **Submitted:** 05.05.2023 • **Revised:** 31.10.2023 • **Accepted:** 06.02.2024

For citation: Uvaysov S.U., Dolmatov A.V., Vo Th.H., Luu N.T., Nguyen C.D. Diagnostics of structural integrity violations of avionics during impact tests. *Russ. Technol. J.* 2024;12(2):28–38. https://doi.org/10.32362/2500-316X-2024-12-2-28-38

Financial disclosure: The authors have no a financial or property interest in any material or method mentioned.

The authors declare no conflicts of interest.

НАУЧНАЯ СТАТЬЯ

Диагностика нарушений целостности конструкций бортовых радиоэлектронных средств при испытаниях на ударные воздействия

С.У. Увайсов,
А.В. Долматов @,
Т.Х. Во,
Н.Т. Лыу,
К.Д. Нгуен

МИРЭА – Российский технологический университет, Москва, 119454 Россия
@ Автор для переписки, e-mail: dolmatov@mirea.ru

Резюме
Цели. С непрерывным развитием современных технических средств в области авиации и космического приборостроения постоянно повышаются требования к точности, устойчивости и надежности электронной аппаратуры, эксплуатируемой на космических аппаратах. Блоки бортовых радиоэлектронных средств космических аппаратов (БРЭСКА) эксплуатируются в особых условиях. В случае возникновения неисправности ее устранение, как правило, оказывается невозможным. Блоки БРЭСКА представляют собой герметично закрытые конструкции, поэтому их демонтаж для оценки технического состояния затруднен. Целью исследования является повышение эффективности и достоверности выявления латентных дефектов в блоках БРЭСКА путем использования метода диагностирования при воздействии механических ударов.
Методы. На основании известных методов в работе предложен новый метод диагностирования с использованием моделирования механических процессов при ударных воздействиях на этапе проектирования блоков БРЭСКА для оценки наличия различных латентных дефектов. В исправном состоянии блоки БРЭСКА имеют амплитудно-частотные характеристики (АЧХ), отличные от АЧХ блоков БРЭСКА, имеющих различные дефекты, отражающиеся на механических характеристиках. С учетом этого разработана диагностическая модель, оценивающая техническое состояние блоков БРЭСКА без демонтажа устройств в процессе диагностирования.
Результаты. В работе проведено моделирование механических процессов в блоках БРЭСКА в исправном состоянии и при наличии различных дефектов, а также экспериментальные исследования механических характеристик в исправном и неисправном состояниях. После проведения измерений механических характеристик при воздействии ударных нагрузок полученные данные сравниваются с результатами моделирования при наличии различных дефектов. Результатом сравнения является отчет о техническом состоянии блока БРЭСКА.
Выводы. Разработанный метод диагностирования блоков БРЭСКА при ударных механических воздействиях позволяет повысить эффективность диагностирования латентных дефектов в процессе производства и эксплуатации БРЭСКА.

Ключевые слова: диагностирование, ударные механические воздействия, блок бортовых радиоэлектронных средств космических аппаратов

• **Поступила:** 05.05.2023 • **Доработана:** 31.10.2023 • **Принята к опубликованию:** 06.02.2024

Для цитирования: Увайсов С.У., Долматов А.В., Во Т.Х., Лыу Н.Т., Нгуен К.Д. Диагностика нарушений целостности конструкций бортовых радиоэлектронных средств при испытаниях на ударные воздействия. *Russ. Technol. J.* 2024;12(2):28–38. https://doi.org/10.32362/2500-316X-2024-12-2-28-38

Прозрачность финансовой деятельности: Авторы не имеют финансовой заинтересованности в представленных материалах или методах.

Авторы заявляют об отсутствии конфликта интересов.

INTRODUCTION

Under external destabilizing factors or in the process of aging, a change in the technical state of any radio-electronic product occurs [1, 2]. Malfunctions of spacecraft avionic units (SAU) can occur due to errors made at the stages of production or operation. These errors can result in the disruption of the physical structure and material composition, as well as in the instability of product parameters. Each error is capable of resulting in sudden or gradual failures during operation [3]. Statistics show that some electronic devices may have defects including latent ones during most of their life cycle (from production to disposal) [4–6]. Therefore, the detection and elimination of latent defects plays a very important role in maintaining the stability and performance of the equipment.[1]

The aim of this paper is to develop a new method for diagnostic modeling based on studying the SAU amplitude-frequency response (AFR) under shock impact. The simulation results along with information on the technical condition of the equipment being studied herein represent the initial data used for comparison with similar products in the absence or presence of defected SAU.

Establishing the technical condition of printed board assemblies (PBAs) or units of radio-electronic means (REM) can be performed manually using simple devices such as multimeters, oscilloscopes, and frequency meters. However, when mass inspections are required, this diagnostics process takes a lot of time and is inefficient.

Today, non-destructive methods of diagnostics are widely used at production enterprises during testing as part of the process of output control [7, 8]. Such a method for diagnosing SAU under mechanical shock loads can increase the efficiency and reliability of defect detection without disintegration of objects [9]. However, it is worth noting certain factors which need to be taken into account, in order to obtain a reliable diagnostic result:

- computer simulation of research objects must be performed with a high level of accuracy in terms of describing the physical structure, the parameters of structural materials, and materials of electro-radio elements (ERE) [10];
- support for the specified accuracy of shock simulation on the vibration test bench, and correct accelerometer placement [11].

All electronic products, whether PBA or SAU, have their own resonant frequencies.[2,3] In a good technical condition, the product displays a certain natural frequency spectrum. The appearance of defects in SAU is accompanied by a change in its own resonant frequencies. Based on this principle, the method of diagnostics under shock impact on SAU is proposed.[4]

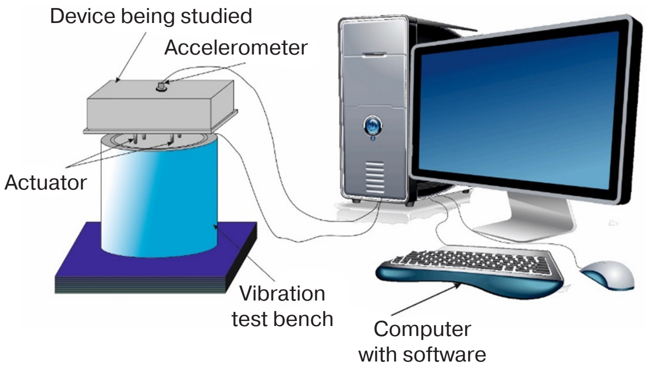

Fig. 1. The shock test bench for SAU

A shock test bench (Fig. 1) consists of a computer system with software which analyzes technical parameters of the device under study. This system is connected to the vibration test bench, in order to determine vibration characteristics using an accelerometer. The vibrational shock effect of the vibration test bench on one axis in an upward and downward direction is recorded by a sensor. This sensor then sends this information to the computer [12]. The response produced by the vibration test bench has a certain amplitude and frequency ranging from 2 Hz to 10000 Hz. The shape of the shock can be specified as a trapezoidal, sawtooth, triangular, or half-sinusoidal pulse.

DETERMINING SAU TECHNICAL CONDITION DURING SHOCK TESTS

The aim of this paper is to determine a method for diagnosing SAU during shock tests. The structural diagram is shown in Fig. 2. The general principle of the method consists of mathematical modeling of SAU characteristics in the serviceable and faulty state. The information regarding the modeling results is used for comparison with the results obtained by experimental characterization of the real device [13, 14].

The SAU diagnostics consists of two main stages:

1. Development of a diagnostic model based on SAU characteristics and parameters and creation of a database (units 1–7). The database is a set of SAU AFRs calculated at serviceable and faulty states.

[1] Malkin V.S. *Technical diagnostics*. 2nd ed., revised and supplemented. St. Petersburg: Lan; 2013. 272 p. (in Russ.).

[2] Zelenskiy V.A., Sukhachev K.I. *Fundamentals of design, technology and reliability of radio electronic means:* Textbook. Samara: Samara University; 2020. 146 p. (in Russ.).

[3] Muromtsev D.Yu., Tyurin I.V., Belousov O.A., Kurnosov R.Yu. *Design of functional assemblies and modules of radio-electronic means:* Textbook for Universities. 2nd ed., St. Petersburg: Lan; 2021. 252 p. (in Russ.).

[4] Muromtsev D.Yu., Belousov O.A., Tyurin I.V., Kurnosov R.Yu. *Design of REM units*. 4th ed. St. Petersburg: Lan; 2023. 288 p. (in Russ.).

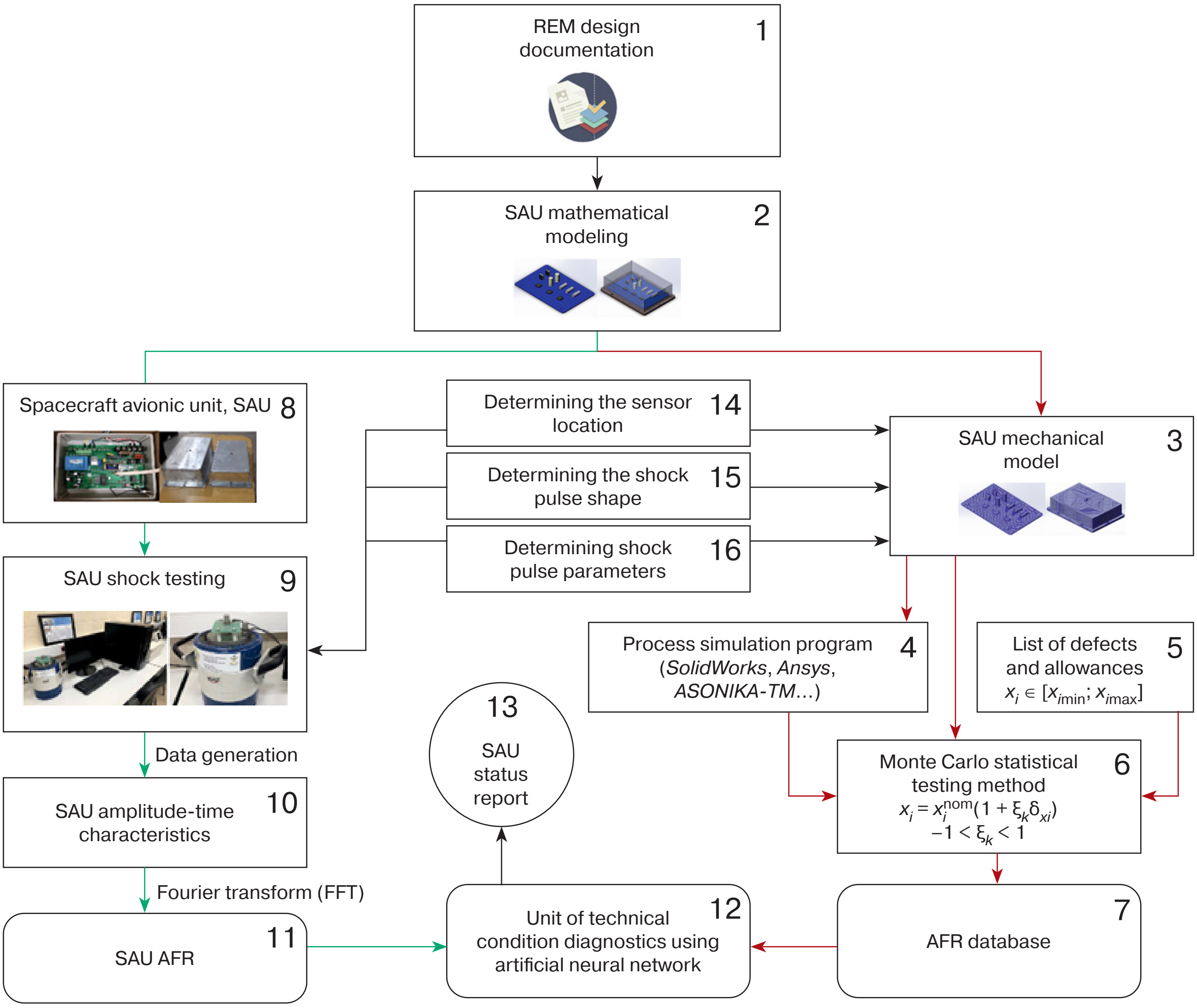

Fig. 2. Structural diagram of the method for diagnosing SAU during shock tests

2. Experimental tests of real SAU samples conducted using a vibration test bench (units 8–11). The resulting data is processed and compared (unit 12) with a set of AFR data. Then a report on the SAU technical condition is created (unit 13).

At the initial stage, the mathematical and diagnostic models of the SAU structure are developed (units 1–3 in Fig. 2). When creating the mathematical model, attention must be paid to specifying geometric and physical-mechanical parameters of the structure and EREs accurately. The placement of EREs on PBA must correspond to the given schematic diagram. During modeling, attention must be paid to the location of accelerometer on the unit, since the sensor weight can affect SAU mechanical characteristics.

Mechanical processes in SAU can be modeled using various software products, in order to establish their mechanical properties and physical structure. Such products are: *SolidWorks*[5], *Ansys*[6], *Nastran*[7], *ASONIKA-TM*[8], and others. [15]. These modeling programs allow users to obtain mechanical characteristics in SAU structures with a high level of accuracy (unit 4 in Fig. 2).

When preparing the initial data for simulating mechanical processes in SAU, the following factors must be taken into account:

- determining the sensor location, in order to obtain the result of shock impact on the object (the displacement amplitude at the sensor location is maximum at its own resonant frequency) (unit 14);

[5] https://www.solidworks.com/. Accessed December 19, 2023.

[6] https://www.ansys.com/. Accessed December 19, 2023.

[7] https://www.autodesk.com/products/nastran/overview. Accessed December 19, 2023.

[8] https://asonika-online.ru/products/asonika-tm/ (in Russ.). Accessed December 19, 2023.

- determining the pulse shape specified in the modeling program. These may be trapezoidal, triangular, sawtooth, or sinusoidal [16]. Studies have shown the trapezoidal pulse to be optimal (unit 15);
- determining pulse parameters including pulse amplitude and duration, at which the physical structure is not destroyed and SAU characteristics are not disturbed (unit 16). The value range of the pulse amplitude must correspond to the research object structure. The minimum value of the shock pulse amplitude $A_{\text{min effect}}$ must not be less than the value $A_{\text{min pract}}$ that can be obtained by the sensor. The maximum value $A_{\text{max effect}}$ should not be greater than the value of the experimental amplitude $A_{\text{min theor}}$ resulting in natural structure destruction:

$$[A_{\text{min effect}}; A_{\text{max effect}}] \in [A_{\text{min pract}}; A_{\text{max theor}}],$$

where $A_{\text{min pract}}$ is the lower boundary of amplitude values (determined by the measuring instrument characteristic); $A_{\text{max theor}}$ is the upper boundary of amplitude values.

The most common mechanical SAU defects addressed in the paper include:

- loosening of the SAU PBA screws;
- cracks in structural elements (cracking of printed circuit boards (PCBs), etc.);
- deformation of structural elements (PCB deformation, rivet fastening curvature, and etc.);
- tearing off a part of or the whole ERE from PBA;
- passive ERE contact on the printed circuit board with other structural elements (may occur in conditions of the SAU high density).

The calculation result of the diagnostic model for mechanical processes is a set of SAU AFRs for specified typical defects stored and presented on the computer (unit 7 in Fig. 2). Each AFR corresponds to a certain faulty state or its set of defects.

In the aims of enhancing diagnostic efficiency and reducing the probability of errors (incorrect defect recognition, non-existent defects) [17], the simulated mechanical processes take into account allowances $[x_{i\min}; x_{i\max}]$ within which the values x_i, $i = \overline{1, n}$ for physical-mechanical and geometric parameters of structural elements change (unit 6 in Fig. 2). Here, the Monte Carlo simulation modeling method is used [18]. Thus, the parameter value (physical-mechanical or geometric) for the SAU structure is determined using the following formula:

$$x_i = x_i^{\text{nom}}(1 + \xi_k \delta_{xi}),$$

where x_i is current value of the ith parameter at kth realization; x_i^{nom} is nominal value of the ith parameter; ξ_k is random variable ($-1 < \xi_k < 1$) output by the random number generator; δ_{xi} is relative allowance of the ith parameter. At the final stage, experimental SAU characteristics are determined. The experiment is conducted on the vibration test bench (unit 9 in Fig. 2) integrated with a computer to obtain the product AFR through the sensor installed in the center of the SAU cover (unit 10 in Fig. 2).

The resulting characteristic is the data set of discrete AFR values used to calculate the transition from the time domain to the frequency domain via the fast Fourier transform (FFT) (unit 11). Fast Fourier transform formula is the following:

$$F(\omega) = \int_{-\infty}^{+\infty} f(t) e^{-j\omega t} dt,$$

where t is time, $f(t)$ is the normal distribution density function, ω is the signal cyclic frequency, and j is the imaginary unit.

This result is used for comparison with the previously created AFR set (unit 7) using an artificial neural network applied to the search task (ensemble learning introduced neural network) implemented in the Python language environment.

As a result, a report on SAU technical condition is created. When defects are detected using the described methodology, they can be remedied at the production enterprise. Should SAU AFR not coincide with any AFR stored in the database prior to defect confirmation, additional research or final expert decisions will be required.

The diagnostic result using this method may be achieved with a high level of efficiency in the case of simulation modeling of a large defect database. It also provides a high level of accuracy when setting geometric and physical-mechanical parameters of SAU design. In addition, it increases the economic efficiency of diagnostics when used in serial production.

EXPERIMENTAL STUDIES OF THE PROPOSED METHOD

In order to verify the proposed method, an experimental SAU prototype was created.[9] It represents a closed body with dimensions shown in Fig. 3. The unit body is made of pressed aluminum. The body elements are fastened together using screw connections.

Inside the body, the printed circuit board (WAVGAT authorization Store, China) of 100 × 150 mm in size is placed on a fixed stand using a retaining screw (Fig. 4).

[9] GOST R 52762-2007. National Standard of the Russian Federation. *Mechanical environment stability test methods for machines, instruments and other industrial products. Test methods for bumps to enclosure of products*. Moscow: Standardinform; 2007. 19 p. (in Russ.).

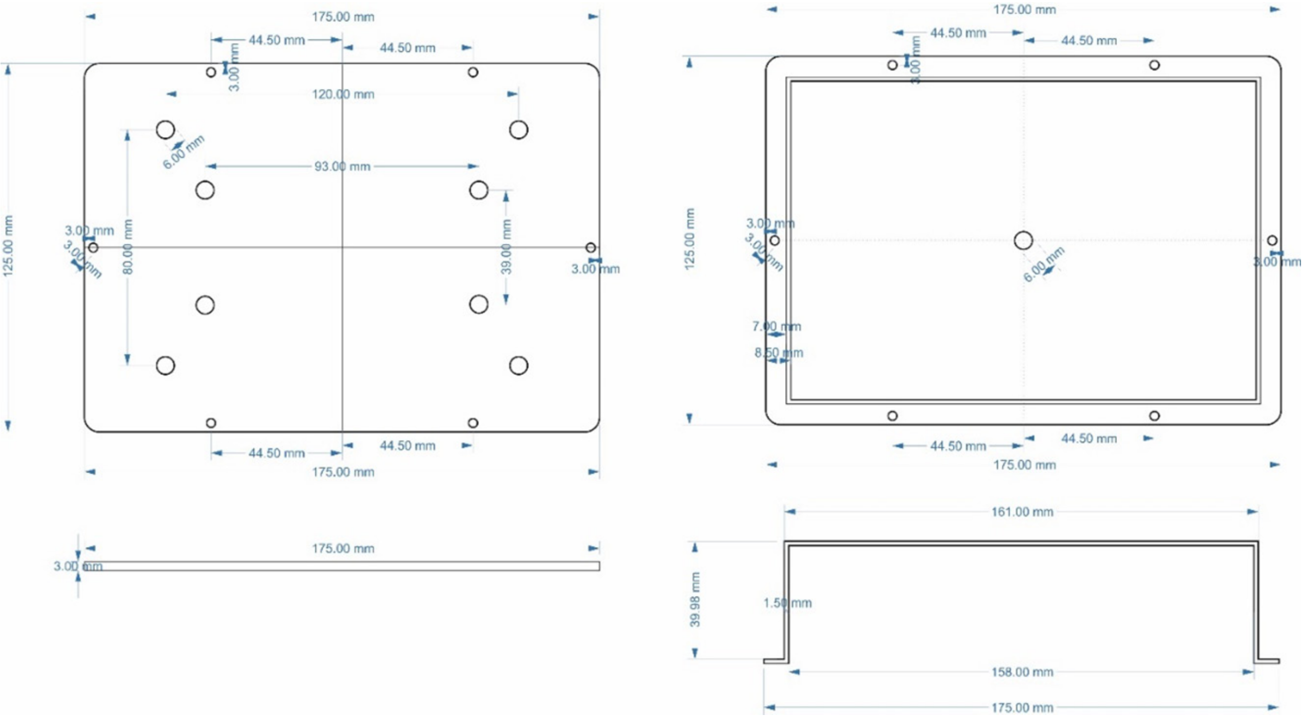

Fig. 3. Drawing of SAU body (bottom and cover)

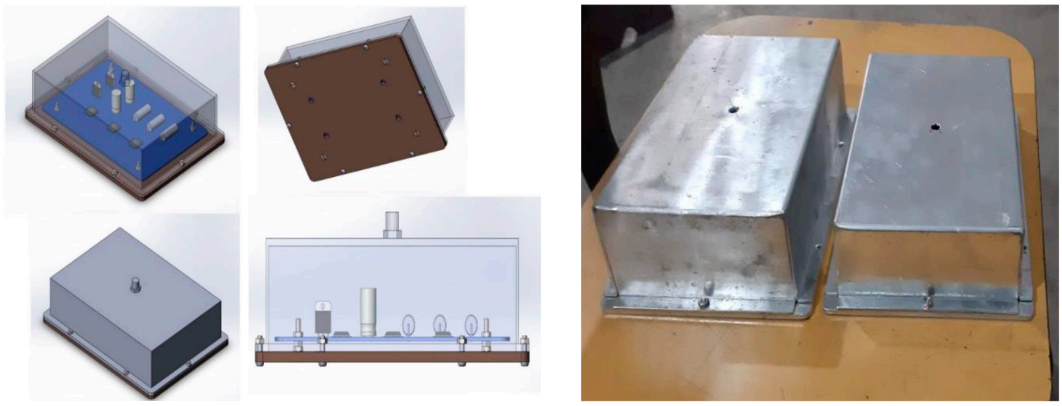

(a) (b)

Fig. 4. View of SAU model (a) and the real sample (b)

The device being studied is placed on a vibration test bench (IMV Corporation, Japan) connected to the computer by means of software (Fig. 5). The sensor used to measure SAU mechanical characteristics refers to the VP-32 type.[10]

Experimental studies of SAU are carried out under trapezoidal impulse shock with acceleration $A = 30$ m/s^2, shock duration $T = 0.04$ s. Possible defects are described in Table 1.

Fig. 5. The appearance of the vibration test bench

[10] https://ostec-test.ru/catalog/equipment/datchiki-vibratsii/vibropreobrazovatel-uskoreniya-vp-32/ (in Russ.). Accessed December 19, 2023.

Table 1. Description of SAU defects

Defect	Defect description	Image
No defects	Serviceable state	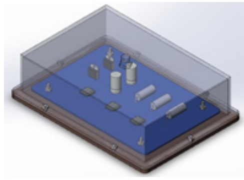
Defect 1	Loosening of PBA screws	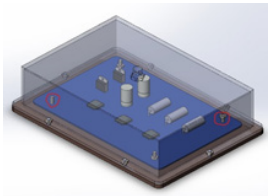
Defect 2	Absence of resistor	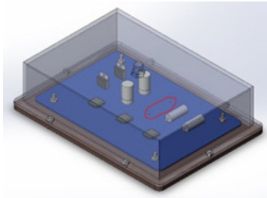
Defect 3	Absence of transistor and capacitor	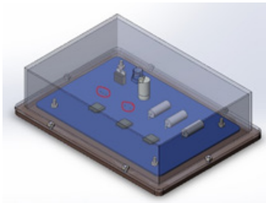

The experimental measurement results of the mechanical characteristics obtained on the SAU prototype represent AFR for each of its defects (Fig. 6). This shows a distinct AFR result: the natural resonant frequency values at the control point, where the sensor is installed, for SAU with a defect differ from those in the serviceable state. The results are recorded in the AFR database for SAU different technical states (Table 2). They can be used for diagnostic analysis of SAU technical condition in the future.

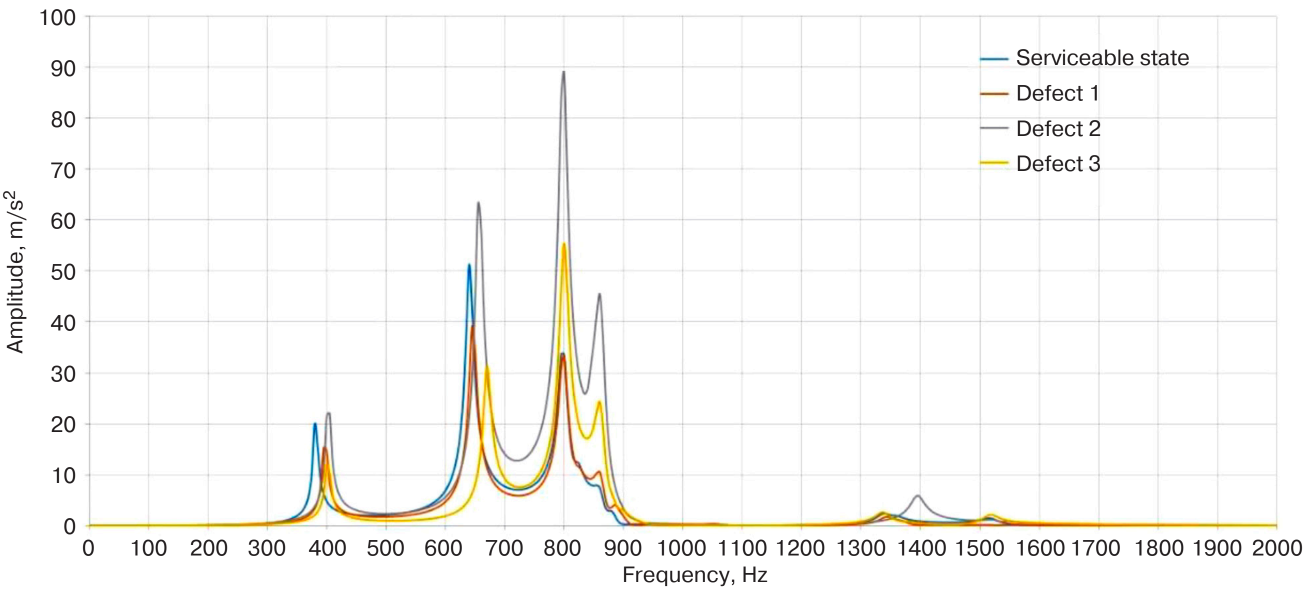

Fig. 6. Spectral characteristics for differing SAU states

Table 2. Database for SAU different states

Frequency, Hz	Serviceable state	Defect 1	Defect 2	Defect 3
0	0.0038	0.0024	0.0023	0.0021
5	0.0038	0.0024	0.0024	0.0022
10	0.0038	0.0024	0.0023	0.0021
15	0.0037	0.0023	0.0021	0.0020
20	0.0034	0.0022	0.0018	0.0018
25	0.0031	0.0020	0.0014	0.0014
30	0.0028	0.0017	0.0010	0.0011
……	…………	…………	…………	………….
1970	0.0089	0.0166	0.0770	0.0694
1975	0.0087	0.0162	0.0749	0.0675
1980	0.0085	0.0158	0.0729	0.0656
1985	0.0083	0.0153	0.0708	0.0637
1990	0.0081	0.0149	0.0688	0.0618
1995	0.0079	0.0145	0.0668	0.0600
2000	0.0077	0.0140	0.0648	0.0582

CONCLUSIONS

The method for diagnosing SAU under mechanical shock loads proposed in this paper allows for SAU defects to be diagnosed and detected efficiently. Further studies will facilitate the detection of all possible types of defects using this method, and can assist in developing both an algorithm and diagnostic techniques. The research results could be implemented into the educational process of MIREA – Russian Technological University and other universities.

Authors' contribution. All authors equally contributed to the research work.

REFERENCES

1. Brumsteyn Yu.M., Vybornova O.N. Analysis of some models for group risk management. *Prikaspiiskii zhurnal: Upravlenie i vysokie tekhnologii = Caspian Journal: Management and High Technologies*. 2015;4:64–72 (in Russ.).
2. Sysuev V.A., Polkanov S.A., Lysenko Yu.S. Analysis of modern methods of protection of on-board electronic devices from external mechanical influences. In: *Proceedings of the International Symposium "Reliability and Quality*." 2020. V. 2. P. 39–41 (in Russ.).
3. Balizh K.S., Eremeev P.M., Simakhina E.A. Analysis of the causes of faults and failures for design of space equipment. In: *The 45th Academic Space Conference, Dedicated to the Memory of Academician S.P. Korolev and Other Outstanding Russian Scientists – Pioneers of Space Exploration* (*Korolev Academic Space Conference*): collection of abstracts. Moscow: Bauman Press; 2021. V. 2. P. 396–398 (in Russ.).
4. Golushko D.A., Trusov V.A., Yurkov N.K., Brostilov S.A., Brostilova T.Yu., Rybakov I.M. Hardware Software complex for testing electronic devices on the effect of vibration. *Prikaspiiskii zhurnal: Upravlenie i vysokie tekhnologii = Caspian Journal: Management and High Technologies*. 2016;1:151–160 (in Russ.).

5. Klestov S.A. Classification of defects in electronic equipment. In: *Intelligent Systems of the 4th Industrial Revolution:* Collection of Materials of the V International Forum. Tomsk. 2023. P. 52–53 (in Russ.).
6. Romanov A.M., Nelyutskov M.A., Ryazyapov I.N. Analysis of defects in radio-electronic devices, methods and means of their detection. In: *Proceedings of the International Symposium "Reliability and Quality*." 2023. V. 1. P. 413–414 (in Russ.).
7. Sartakov S.S. Analysis of methods and means of testing electronic equipment of aircraft. In: *Actual Problems of Radio Electronics and Telecommunications:* Materials of the All-Russian Scientific and Technical Conference. Samara; 2020. P. 206–207 (in Russ.).
8. Pham L.Q.Kh., Dao A.Q., Uvaysov S.U., Chernoverskaya V.V., Bushmeleva K.I. Determination of the effective level of single shock pulses for detecting defects in printed board assemblies of electronic devices. *Vestnik Mezhdunarodnogo universiteta prirody, obshchestva i cheloveka "Dubna." Seriya: Estestvennye i inzhenernye nauki = Bulletin of Dubna International University for Nature, Society, and Man. Series: "Natural and Engineering Sciences.* 2020;3(48):46–54 (in Russ.).
9. Nelyutskov M.A., Marchenko V.V., Lysenko A.V., Tan'kov G.V., Rybakov I.M. Shock pulses as a test method of radio-electronic means. In: *Proceedings of the International Symposium "Reliability and Quality*." 2020. V. 2. P. 238–240 (in Russ.).
10. Kofanov Yu.N., Sotnikova S.Yu. Improving the accuracy of modeling based on identification. *Innovatsii na osnove informatsionnykh i kommunikatsionnykh tekhnologii = Innovations Based on Information and Communication Technologies*. 2015;1:176–178 (in Russ.).
11. Kondrashov D.E. Decision support system for diagnostics of electronic means based on the analysis of shock effects. In: *Problems and Solutions of Automation of the 21st Century:* Materials of the Sixth National Scientific and Practical Student Conference. Surgut. 2023. P. 93–98 (in Russ.).
12. Lyshov S.M., Ivanov I.A., Uvaysov S.U. Methodology for determining the threshold value of the similarity criterion by experimental characteristics. In: *Reliability and Quality: Proceedings of the International Symposium*. 2013. V. 2. P. 372–374 (in Russ.).
13. Bushmeleva K.I., Kondrashov D.E., Uvaysov S.U., Pham L.Q.H. Automated system of diagnostics of radio-electronic means based on shock effects. In: *Innovative, Information and Communication Technologies:* Proceedings of the 17th International Scientific and Practical Conference. 2020. P. 384–389 (in Russ.).
14. Kondrashov D.E., Bushmeleva K.I., Uvaysov S.U., Demchenko S.K. Methods of diagnostics of electronic means based on the analysis of shock effects by means of machine learning algorithms. In: *Innovative, Information and Communication technologies:* Proceedings of the 18th International Scientific and Practical Conference. Sochi. 2021. P. 190–195 (in Russ.).
15. Shalumov A.S. ASONIKA – Russian CAD electronics in terms of virtual tests. *Elektronika: Nauka, tekhnologiya, biznes = Electronics: Science, Technology, Business*. 2022;3:82–83 (in Russ.). https://doi.org/10.22184/1992-4178.2022.214.3.82.83
16. Rezchikova E.V., Luong Q.L. Vibration protection of on-board electronic equipment from external influences. *Kontrol'. Diagnostika = Testing. Diagnostics*. 2021;24(11):22–30 (in Russ.). https://doi.org/10.14489/td.2021.11.pp.022-030
17. Irzaev G.H. Provision and evaluation of testability of the design of complex radio-electronic meansdevices at the stages of their design. *Kontrol'. Diagnostika = Testing. Diagnostics*. 2023;26(5):34–41 (in Russ.). https://doi.org/10.14489/td.2023.05.pp.034-041
18. Kashnikova A.P., Belyaeva M.B. The Monte Carlo method in the problems of modeling processes and systems. *Modern Science*. 2021;(1–2):358–362 (in Russ.).

СПИСОК ЛИТЕРАТУРЫ

1. Брумштейн Ю.М., Выборнова О.Н. Анализ некоторых моделей группового управления рисками. *Прикаспийский журнал: Управление и высокие технологии*. 2015;4:64–72.
2. Сысуев В.А., Полканов С.А., Лысенко Ю.С. Анализ современных методов защиты бортовых радиоэлектронных устройств от внешних механических воздействий. *Труды международного симпозиума «Надежность и качество»*. 2020. Т. 2. С. 39–41.
3. Балиж К.С., Еремеев П.М., Симахина Е.А. Анализ причин сбоев и отказов при проектировании аппаратуры космического назначения. *XLV Академические чтения по космонавтике, посвященные памяти академика С.П. Королёва и других выдающихся отечественных ученых – пионеров освоения космического пространства:* сборник тезисов. М.: Издательство МГТУ им. Н.Э. Баумана; 2021. Т. 2. С. 396–398.
4. Голушко Д.А., Трусов В.А., Юрков Н.К., Бростилов С.А., Бростилова Т.Ю., Рыбаков И.М. Программно-аппаратный комплекс для проведения испытаний изделий электронной техники на воздействие вибрации. *Прикаспийский журнал: управление и высокие технологии*. 2016;1:151–160.
5. Клестов С.А. Классификация дефектов радиоэлектронной аппаратуры. *Интеллектуальные системы 4-й промышленной революции. Сборник материалов V Международного форума.* Томск. 2023. С. 52–53.
6. Романов А.М., Нелюцков М.А., Рязяпов И.Н. Анализ дефектов РЭС, методов и средств их обнаружения. *Труды международного симпозиума «Надежность и качество»*. 2023. Т. 1. С. 413–414.
7. Сартаков С.С. Анализ методов и средств испытаний радиоэлектронного оборудования воздушных судов. *Актуальные проблемы радиоэлектроники и телекоммуникаций:* материалы Всероссийской научно-технической конференции. Самара. 2020. С. 206–207.

8. Фам Л.К.Х., Дао А.К., Увайсов С.У., Черноверская В.В., Бушмелева К.И. Определение эффективного уровня одиночных ударных импульсов для выявления дефектов печатных узлов электронных средств. *Вестник Международного университета природы, общества и человека «Дубна». Серия: Естественные и инженерные науки*. 2020;3(48):46–54.
9. Нелюцков М.А., Марченко В.В., Лысенко А.В., Таньков Г.В., Рыбаков И.М. Ударные импульсы как метод испытаний радиоэлектронных средств. *Труды международного симпозиума «Надежность и качество»*. 2020. Т. 2. С. 238–240.
10. Кофанов Ю.Н., Сотникова С.Ю. Повышение точности моделирования на основе идентификации. *Инновации на основе информационных и коммуникационных технологий*. 2015;1:176–178.
11. Кондрашов Д.Е. Система поддержки принятия решений диагностики электронных средств на основе анализа ударных воздействий. *Проблемы и решения автоматизации XXI века:* Материалы VI Национальной научно-практической студенческой конференции. Сургут. 2023. С. 93–98.
12. Лышов С.М., Иванов И.А., Увайсов С.У. Методика определения порогового значения критерия подобия по экспериментальным характеристикам. *Труды Международного симпозиума «Надежность и качество»*. 2013. Т. 2. С. 372–374.
13. Бушмелева К.И., Кондрашов Д.Е., Увайсов С.У., Фам Л.К.Х. Автоматизированная система диагностики радиоэлектронных средств на основе ударных воздействий. *Инновационные, информационные и коммуникационные технологии:* сборник трудов XVII Международной научно-практической конференции. 2020. С. 384–389.
14. Кондрашов Д.Е., Бушмелева К.И., Увайсов С.У., Демченко С.К. Методика диагностики электронных средств на основе анализа ударных воздействий посредством алгоритмов машинного обучения. *Инновационные, информационные и коммуникационные технологии:* сборник трудов XVIII Международной научно-практической конференции. Сочи. 2021. Р. 190–195.
15. Шалумов А.С. АСОНИКА – российская САПР электроники в части виртуальных испытаний. *Электроника: Наука, технология, бизнес*. 2022;3:82–83. https://doi.org/10.22184/1992-4178.2022.214.3.82.83
16. Резчикова Е.В., Лыонг К.Л. Виброзащита бортовой электронной аппаратуры от внешних воздействий. *Контроль. Диагностика*. 2021;24(11):22–30. https://doi.org/10.14489/td.2021.11.pp.022-030
17. Ирзаев Г.Х. Обеспечение и оценка контролепригодности конструкции сложных радиоэлектронных средств на этапах их проектирования. *Контроль. Диагностика*. 2023;26(5):34–41. https://doi.org/10.14489/td.2023.05.pp.034-041
18. Кашникова А.П., Беляева М.Б. Метод Монте-Карло в задачах моделирования процессов и систем. *Modern Science*. 2021;(1–2):358–362.

About the authors

Saygid U. Uvaysov, Dr. Sci. (Eng.), Professor, Head of the Department of Design and Production of Radioelectronic Devices, Institute of Radio Electronics and Informatics, MIREA – Russian Technological University (78, Vernadskogo pr., Moscow, 119454 Russia). E-mail: uvajsov@mirea.ru. Scopus Author ID 55931417100, ResearcherID H-6746-2015, RSCI SPIN-code 3801-4816, https://orcid.org/0000-0003-1943-6819

Aleksey V. Dolmatov, Cand. Sci. (Eng.), Associate Professor, Department of Design and Production of Radioelectronic Devices, Institute of Radio Electronics and Informatics, MIREA – Russian Technological University (78, Vernadskogo pr., Moscow, 119454 Russia). E-mail: dolmatov@mirea.ru, RSCI SPIN-code 3887-2405, https://orcid.org/0000-0003-2969-2971

The H. Vo, Postgraduate Student, Department of Design and Production of Radioelectronic Devices, Institute of Radio Electronics and Informatics, MIREA – Russian Technological University (78, Vernadskogo pr., Moscow, 119454 Russia). E-mail: thehai.ttrd@gmail.com. https://orcid.org/0009-0009-7240-4374

Ngoc T. Luu, Postgraduate Student, Department of Design and Production of Radioelectronic Devices, Institute of Radio Electronics and Informatics, MIREA – Russian Technological University (78, Vernadskogo pr., Moscow, 119454 Russia). E-mail: alex05vn@gmail.com. https://orcid.org/0009-0001-8779-7563

Cong D. Nguyen, Postgraduate Student, Department of Design and Production of Radioelectronic Devices, Institute of Radio Electronics and Informatics, MIREA – Russian Technological University (78, Vernadskogo pr., Moscow, 119454 Russia). E-mail: ngcongduc9x@gmail.com. https://orcid.org/0009-0000-9237-156X

Об авторах

Увайсов Сайгид Увайсович, д.т.н., профессор, заведующий кафедрой конструирования и производства радиоэлектронных средств, Институт радиоэлектроники и информатики ФГБОУ ВО «МИРЭА – Российский технологический университет» (119454, Россия, Москва, пр-т Вернадского, д. 78). E-mail: uvajsov@mirea.ru. Scopus Author ID 55931417100, ResearcherID H-6746-2015, SPIN-код РИНЦ 3801-4816, https://orcid.org/0000-0003-1943-6819

Долматов Алексей Вячеславович, к.т.н., доцент, кафедра конструирования и производства радиоэлектронных средств, Институт радиоэлектроники и информатики ФГБОУ ВО «МИРЭА – Российский технологический университет» (119454, Россия, Москва, пр-т Вернадского, д. 78). E-mail: dolmatov@mirea.ru. SPIN-код РИНЦ 3887-2405, https://orcid.org/0000-0003-2969-2971

Во Тхе Хай, аспирант, кафедра конструирования и производства радиоэлектронных средств, Институт радиоэлектроники и информатики ФГБОУ ВО «МИРЭА – Российский технологический университет» (119454, Россия, Москва, пр-т Вернадского, д. 78). E-mail: thehai.ttrd@gmail.com. https://orcid.org/0009-0009-7240-4374

Лыу Нгок Тиен, аспирант, кафедра конструирования и производства радиоэлектронных средств, Институт радиоэлектроники и информатики ФГБОУ ВО «МИРЭА – Российский технологический университет» (119454, Россия, Москва, пр-т Вернадского, д. 78). E-mail: alex05vn@gmail.com. https://orcid.org/0009-0001-8779-7563

Нгуен Конг Дык, аспирант, кафедра конструирования и производства радиоэлектронных средств, Институт радиоэлектроники и информатики ФГБОУ ВО «МИРЭА – Российский технологический университет» (119454, Россия, Москва, пр-т Вернадского, д. 78). E-mail: ngcongduc9x@gmail.com. https://orcid.org/0009-0000-9237-156X

Translated from Russian into English by Kirill V. Nazarov
Edited for English language and spelling by Dr. David Mossop

UDC 519.718:004.722
https://doi.org/10.32362/2500-316X-2024-12-2-39-47

RESEARCH ARTICLE

Analysis of the structural reliability of communication networks supporting protective switching mechanisms for one protected section and one backup section

Kirill A. Batenkov [1, @],
Aleksandr B. Fokin [2]

[1] *MIREA – Russian Technological University, Moscow, 119454 Russia*
[2] *Academy of Federal Guard Service of Russian Federation, Orel, 302015 Russia*
[@] *Corresponding author, e-mail: pustur@yandex.ru*

Abstract
Objectives. The service level agreement is an important tool used in building reasonable relations between subscribers and operators of telecommunication networks. This includes the quality of services provided. One key component is reliability as assessed by the availability factor. The most suitable model for assessing the reliability of the service provided is a random graph model based on the service contour. This is the set of technical resources involved in the provision of this service. In this formulation, the assessment of the reliability of the service is based on the reliability of elements which constitute the telecommunications network (graph), nodes (vertices) and communication lines (edges). At the same time, the availability factors of nodes and lines are determined by the design features of the distribution environment, as well as the technical means used to organize them. The purpose of this work is to develop an approach to analyzing the reliability of telecommunication networks which support protective switching mechanisms for one protected and one backup sections.
Methods. The following methods are used: theory of random graphs, matrices, probabilities and computer modeling.
Results. The elements of the route, both basic and reserving, are divided into three groups. The first indicates permanent unchangeable parts of the paths, the second group identifies the reserved sections, and the third group indicates the reserving sections. At the same time, each of the reserved and reserving sections is formed on the basis of specified preferences. They are usually aimed at increasing the resulting reliability, although other rules may be used. In the case of protective switching schemes for one protected section and one backup sections, a variant of forming routes used for further calculations of the reliability indicator is shown.
Conclusions. Using the example of a backbone network, the study shows that the use of protective switching mechanisms for the case of one required transmission route demonstrates a significant increase in reliability, with the exception of the use of protective switching in sections. This is primarily due to the topology features of the network under consideration.

Keywords: communication network, graph, connectivity probability, protective switching, reliability, service, availability factor

• **Submitted:** 03.07.2023 • **Revised:** 20.09.2023 • **Accepted:** 09.02.2024

For citation: Batenkov K.A., Fokin A.B. Analysis of the structural reliability of communication networks supporting protective switching mechanisms for one protected section and one backup section. *Russ. Technol. J.* 2024;12(2):39–47. https://doi.org/10.32362/2500-316X-2024-12-2-39-47

Financial disclosure: The authors have no a financial or property interest in any material or method mentioned.

The authors declare no conflicts of interest.

НАУЧНАЯ СТАТЬЯ

Анализ структурной надежности сетей связи с механизмами защитного переключения для одного защищаемого и одного резервного участков

К.А. Батенков [1, @],
А.Б. Фокин [2]

[1] *МИРЭА – Российский технологический университет, Москва, 119454 Россия*
[2] *Академия Федеральной службы охраны Российской Федерации, Орёл, 302015 Россия*
[@] *Автор для переписки, e-mail: pustur@yandex.ru*

Резюме

Цели. Известно, что соглашение об уровне обслуживания является важным инструментом выстраивания разумных отношений между абонентами и операторами телекоммуникационных сетей, в т.ч. в части качества предоставляемых услуг, одной из составляющих которого является надежность, оцениваемая коэффициентом готовности. Наиболее подходящей моделью для оценки надежности предоставляемой услуги оказывается случайная графовая модель, строящаяся на основе контура обслуживания – совокупности технических средств, участвующих в оказании данной услуги. В данной постановке оценка надежности услуги отталкивается от надежности составляющих телекоммуникационную сеть (граф) элементов – узлов (вершин) и линий связи (ребер). При этом коэффициенты готовности узлов и линий определяются конструктивными особенностями среды распространения и организующих их технических средств. Целью работы является разработка подхода к анализу надежности телекоммуникационных сетей, поддерживающих механизмы защитного переключения для одного защищаемого и одного резервного участков, позволяющего на основе компьютерного моделирования проводить сравнение подобных механизмов.

Методы. Использованы методы теории случайных графов, матриц, вероятностей и компьютерного моделирования.

Результаты. Предложено разбивать на три группы элементы маршрута (как основные, так и резервирующие): первая группа указывает на постоянные неизменяемые части путей, вторая – идентифицирует резервируемые участки, а третья группа указывает на резервирующие участки. При этом каждый из резервируемых и резервирующих участков формируется на основе заданных предпочтений и обычно направлен на увеличение результирующей надежности, хотя возможно использование и других правил. Для схем защитного переключения для одного защищаемого и одного резервного участков показан вариант формирования маршрутов, используемых для дальнейших расчетов показателя надежности путем компьютерного моделирования.

Выводы. На примере магистральной сети путем компьютерного моделирования показано, что использование механизмов защитного переключения для случая одного требуемого маршрута передачи демонстрирует существенный рост надежности, за исключением применения защитного переключения на участках, что связано, прежде всего, с особенностями топологии рассматриваемой сети.

Ключевые слова: сеть связи, граф, вероятность связности, защитное переключение, надежность, услуга, коэффициент готовности

• **Поступила:** 03.07.2023 • **Доработана:** 20.09.2023 • **Принята к опубликованию:** 09.02.2024

Для цитирования: Батенков К.А., Фокин А.Б. Анализ структурной надежности сетей связи с механизмами защитного переключения для одного защищаемого и одного резервного участков. *Russ. Technol. J.* 2024;12(2):39–47. https://doi.org/10.32362/2500-316X-2024-12-2-39-47

Прозрачность финансовой деятельности: Авторы не имеют финансовой заинтересованности в представленных материалах или методах.

Авторы заявляют об отсутствии конфликта интересов.

INTRODUCTION

The service level agreement (SLA) is an important tool for building reasonable relations between subscribers and telecommunication network operators [1]. At the same time, both international recommendations and Russian standards suggest its use in the information and telecommunication technology sectors. In accordance with this agreement, both parties reach a certain understanding of the service provided, as well as its quality, responsibility, priority and other factors.

The basic structure of an SLA for any communication service includes nine sections. The section containing service level information necessarily contains information on the service quality indicators, as well as the values of the indicators guaranteed to the subscriber by the operator (GOST R 55389-2012[1]). The most significant of these are the indicators which characterize the readiness of the service. Both direct indicators, for example, downtime or MTBF, and indirect indicators, such as availability factor, which is the most commonly used reliability indicator can be used. Sometimes simpler deterministic indicators are used which characterize the connectivity of an equivalent graph modeling the original telecommunication network or even the service [2].

The choice of this as a key indicator is because it simply and clearly eliminates misunderstandings between users and operators. It is specified in the form of a share (percentage) of the service uptime at the corresponding access point to the service.

The values of the availability factor guaranteed by the operator, as well as other indicators, are established on the basis of existing federal and industry documents. For example, there are standards which regulate local telephone services (GOST R 53727-2009[2]), tone frequency channels,[3] network and line paths.[4,5] However, the situation concerning dynamically developing modern telecommunication services is not entirely satisfactory. One usually has to be content with the legislative values of Russian or foreign telecom operators, formalized on the basis of the experience of operation of their telecommunication networks (Rec. E. 860[6]). An example would be the International Telecommunication Union recommendations for optical transport networks (Rec. G. 8201[7]) or multimedia services (Rec. G. 1010[8]).

In such a situation, it is extremely important for the service provider to estimate the availability factor of the service requested by the user. The main obstacle is the large measurement interval required to obtain reliable experimental estimates, increasing significantly as availability factors increase. The application of calculation relations, enabling us to calculate such estimates on the basis of a certain set of initial data available to the telecom operator, allows us to analyze its capabilities from the point of view of end-user requests made in advance.

[1] GOST R 55389-2012. National Standard of the Russian Federation. *System of National Standards for quality of telecommunication services. Service Level Agreement* (*SLA*). Moscow: Standartinform; 2019. 12 p. (in Russ.).

[2] GOST R 53727-2009. National Standard of the Russian Federation. *Quality of service "Local telephone communication." Quality indices*. Moscow: Standartinform; 2011. 11 p. (in Russ.).

[3] *Regulations for electrical parameters of tone frequency channels of main and intra-area primary networks*. Approved by the Ministry of Communications of the Russian Federation 15.04.96. Moscow: MK-Polygraph; 1996. 96 p. (in Russ.).

[4] *Regulations for electrical parameters of network paths of main and intra-area primary networks*. Part I. Approved by the Ministry of Communications of the Russian Federation 08.01.1997. Moscow: MK-Polygraph; 1996. 134 p. (in Russ.).

[5] *Regulations for electrical parameters of network paths of main and intra-area primary networks*. Part II. Approved by the Ministry of Communications of the Russian Federation 08.01.1997. Moscow: MK-Polygraph; 1996. 168 p. (in Russ.).

[6] Rec. E. 860. *Framework of a service level agreement*. Geneva: ITU-T; 2003. 30 p. https://www.itu.int/rec/T-REC-E.860-200206-I/en. Accessed February 26, 2024.

[7] Rec. G. 8201. *Error performance parameters and objectives for multi-operator international paths within optical transport networks*. Geneva: ITU-T; 2012. 24 p. https://www.itu.int/rec/T-REC-G.8201. Accessed February 26, 2024.

[8] Rec. G. 1010. *End-user multimedia QoS categories*. Geneva: ITU-T; 2002. 18 p. https://www.itu.int/rec/T-REC-G.1010/en. Accessed February 26, 2024.

1. RELIABILITY OF THE NETWORK AND ITS COMPONENTS

The most suitable model for assessing the reliability of the service provided is a random graph model [3], based on the service loop. This is set of technical resources involved in the provision of this service [1, 4]. In this formulation, the service reliability assessment is clearly based on the reliability of the elements constituting the telecommunication network (graph): nodes (vertices) and communication lines (edges) [5]. In this case, methods which require specified subgraphs, for example, paths [6] or sections [7], in the structure of the initial graph are often used.

The availability factors of nodes and lines are determined by the design features of the propagation environment and their organizing technical facilities (Rec. G. 911[9]) [8]. However, the operator usually does not have a detailed description of such features, so simplified models are used.

Applied network equipment, such as optical cross-connectors and I/O multiplexers, consists of a significant number of different elements. Each is characterized by its own MTBF and recovery time (Rec. G. 911) [9]. MTBF T_0 of network equipment is expressed as a dimension of time or number of failures per unit time, usually taken as 10^9 h, or approximately 114155 years. The average recovery time T_r, on the other hand, is expressed in hours. The availability factor corresponds to the probability of connectivity p of the corresponding node or line: $p = \frac{T_r}{T_0}$.

Link failures can be caused either by optical cable failure, or by failures of optical amplifiers or WDM (wavelength division multiplexing—multiplexing with wavelength division multiplexing, spectral multiplexing) systems. A commonly accepted assumption is that failures of individual fibers in an optical cable occur simultaneously, since they are most often caused by digging faults leading to failure of all fibers at once. For a cable, the mean time-to-failure T_0 is given as a measure of the burst length corresponding to the average cable length d_0 exposed to a single cut per year. This condition can be explained by the increasing probability of a cable break as its length d increases. Longer sections potentially have more opportunities of being damaged by external influences. The average MTBF of an optical cable, expressed in hours, is determined by the expression [9]

$$T_0 = 8760\frac{d_0}{d}.$$

The mean time T_r of cable restoration includes time of fault localization, access to the cable, damage repair and commissioning, including testing of information exchange quality.

A list of average MTBF and recovery times for the most commonly used network equipment is presented in [9]. To some extent, these values are too highly averaged and may differ among equipment manufacturers. They may change even more so over time due to the improvement of the element base. Nevertheless, their application is justified from the point of view not of obtaining the absolute values of the calculated reliability indicators of telecommunication networks, but as a tool for comparing the mechanisms of fault tolerance due to the proximity of the indicators to real typical values. The MTBF for modern equipment is often even lower than the data provided [10]. The reason, apparently, is the complication of the electronic components base.

Next we consider a bidirectional communication line connecting two nodes by cable segments interspersed with optical amplifiers at a distance of about 100 km. The communication line is clearly operable when all its constituent elements are ready. Assuming statistical independence of their failures, the line availability factor p_{line} can be calculated using the formula:

$$p_{\text{line}}(d) = (1 - 6.088 \cdot 10^{-6} d) \cdot 0.999952^{\left\lfloor \frac{d}{100} \right\rfloor} \cdot 0.999988^2. \quad (1)$$

2. SAFETY SWITCHING MECHANISMS

The availability factor of an individual communication line is calculated simply using the model of serial connection of elements as a basis. However, in real telecommunication networks characterized by alternative routes, the situation is much more complicated [11]. In this case, protective switching mechanisms [12], or backup circuits, play an important role in the final reliability of connections.

This paper considers the impact of telecommunication network characteristics on final reliability from the position of the most commonly used indicator: availability factor. Issues relating to the efficiency of switching to backup channels require further clarification [13]. The methods of protection switching (protection) for one main route (Rec. G. 808[10]) [14] are considered as basic mechanisms of fault tolerance provision. There is also a protection switching architecture with one protected

[9] Rec. G. 911. *Parameters and calculation methodologies for reliability and availability of fibre optic systems* (*Previously CCITT Recommendation*). Geneva: ITU-T; 1994. 39 p. https://www.itu.int/rec/T-REC-G.911/en. Accessed February 26, 2024.

[10] Rec. G. 808. *Terms and definitions for network protection and restoration*. Amendment 1. 2018–03. Geneva: ITU-T; 2018. 20 p. https://www.itu.int/rec/T-REC-G.808/en. Accessed February 26, 2024.

section and one backup section (1 : 1 or 1 + 1), as well as six varieties of protected sections of network elements: line, node, route, segment, ring, p-cycle [9]. Each of the varieties has its own properties from the point of view of technical realization. However, from the point of view of reliability analysis based on random graphs, it is sufficient to consider the protected section as a set of vertices and edges of the graph, the use of which is permitted only on the main route. In this case, the use of rings or p-cycles is also reduced to such types of backup by simple transformations.

3. ARCHITECTURE OF INFORMATION TRANSMISSION ROUTES

Path elements, both basic and reserving, can be characterized in three groups (Fig. 1). The first indicates permanent unchangeable parts of the paths and is defined as a vector $\mathbf{s} = \{s_i\}_{i=\overline{1,l+v}}$ of the initial graph elements, where s_i = 1, if ith graph element (edge or vertex) is contained in the given path, and s_i = 0, if not. l is the number of edges in the graph v is the number of vertices in the graph. The second group identifies the reserved sections and is represented in the form of a matrix $\mathbf{S} = \{s_{i,j}\}_{\substack{i=\overline{1,l+v},\\ j=\overline{1,n}}}$ each column of which is equivalent to one of the n where similarly $s_{i,j}$ = 1, if the ith element is contained in the jth path, and $s_{i,j}$ = 0, if not. The third group indicates the reserving sections, and it is written in the form of a matrix $\mathbf{T} = \{t_{i,j}\}_{\substack{i=\overline{1,l+v},\\ j=\overline{1,m}}}$, each column of which is equivalent to one of the m reserving sections. Here likewise $t_{i,j}$ = 1, if the ith element is contained in the jth path, and $t_{i,j}$ = 0, if not. Each backup and reserving section is formed on the basis of given preferences, and is usually aimed at increasing the resulting reliability, Other rules may also be used.

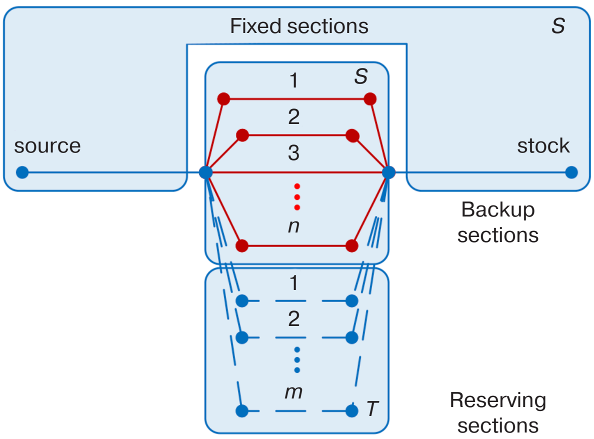

Fig. 1. Architecture of information transmission routes with protection switching mechanisms

Thus, in the general case for protective switching architectures it is reasonable to consider n basic routes of transmission of information as a basis. They are usually defined in the form of simple circuits with independent protected sections with maximum availability factors. Protected sections have maximum availability factors. Then the matrix of backup sections is selected on the basis of the maximum value of the availability factor between the given elements of the initial graph, taking into account their independence and that they are not included in the fixed part of the route

$$\mathbf{S}^{\langle 1\rangle} = \left\{ \mathbf{W}^{\langle j\rangle} : \max\left[\mathbf{s} + \mathbf{W}^{\langle j\rangle}\right] = 1, \max_{j=\overline{1,s}} \prod_{i=1}^{l+v} p_i w_{i,j} \right\},$$

$$\mathbf{S}^{\langle i\rangle} = \left\{ \mathbf{W}^{\langle j\rangle} : \max\left[\mathbf{s} + \operatorname{sign}(\mathbf{S1}_{i-1}) + \mathbf{W}^{\langle j\rangle}\right] = 1, \max_{j=\overline{1,s}} \prod_{i=1}^{l+v} p_i w_{i,j} \right\}, \; i = \overline{2,n},$$

where $\mathbf{W} = \{w_{i,j}\}_{\substack{i=\overline{1,l+v},\\ j=\overline{1,s}}}$ is the matrix of paths between the source and the drain of backup sections; $w_{i,j}$ = 1, if the ith element is contained in the jth path and $w_{i,j}$ = 0 if it is not contained; $\mathbf{p} = \{p_i\}_{i=\overline{1,l+v}}$ is the vector of probabilities of connectivity (operability) of edges and vertices; p_i is the probability of connectivity (availability factor) of the ith element.

Here, each column $\mathbf{S}^{\langle i\rangle}$ of the reserved sites matrix is formed from a column $\mathbf{W}^{\langle j\rangle}$ of the path matrix. This column at the same time does not have repeated elements in the previous main paths already used. This can be verified by the general condition $\max\left[\mathbf{s} + \operatorname{sign}(\mathbf{S1}_{i-1} + \mathbf{W}^{\langle j\rangle}\right]$, and has the maximum connectivity probability (availability factor) among the possible alternative paths. It can be expressed as $\max_{j=\overline{1,s}} \prod_{i=1}^{l+v} p_i w_{i,j}$.

Directly, the main routes are represented as a path matrix $\mathbf{R}$:

$$\mathbf{R} = \mathbf{s1}_n^{\mathrm{T}} + \mathbf{S}.$$

Similarly, in a general case, m routes containing backup sections are defined in the form of simple chains with independent backup, wherein reserving sections have a maximum availability factor. Then the matrix of redundant sections is chosen based on the maximum value of the availability factor between the given elements of the initial graph. This takes into account their independence and that they are not included in the fixed part of the route and backup sections

$$\mathbf{T}^{\langle 1\rangle}=\left\{\mathbf{W}^{\langle j\rangle}:\max\left[\operatorname{sign}(\mathbf{R1}_n)+\mathbf{W}^{\langle j\rangle}\right]=1,\ \max_{j=\overline{1,s}}\prod_{i=1}^{l+v}p_i w_{i,j}\right\},$$

$$\mathbf{T}^{\langle i\rangle}=\left\{\mathbf{W}^{\langle j\rangle}:\max\left[\operatorname{sign}(\mathbf{R1}_n)+\operatorname{sign}(\mathbf{T1}_{i-1})+\mathbf{W}^{\langle j\rangle}\right]=1,\ \max_{j=\overline{1,s}}\prod_{i=1}^{l+v}p_i w_{i,j}\right\},\ i=\overline{2,m}.$$

Here, each column $\mathbf{T}^{\langle i\rangle}$ of the reserving sections matrix is formed from a column $\mathbf{W}^{\langle j\rangle}$ of the path matrix which simultaneously has no repeated elements in the already used previous main and reserve paths. This can be checked by the general condition $\max\left[\mathbf{s}+\operatorname{sign}(\mathbf{S1}_{i-1}+\mathbf{W}^{\langle j\rangle}\right]$, and has the maximum connectivity probability (availability factor) of the possible alternative paths given by the expression $\max_{j=\overline{1,s}}\prod_{i=1}^{l+v}p_i w_{i,j}$.

The backup routes themselves are also represented as a path matrix **U**:

$$\mathbf{U}=\mathbf{s1}_m^{\mathrm{T}}+\mathbf{T}.$$

4. PROTECTIVE SWITCHING ARCHITECTURE FOR ONE PROTECTED AND ONE BACKUP SECTION

For one protected section and one redundant section (1 + 1 or 1 : 1 schemes) (Fig. 2), the original main path is supplemented by a backup path with the same source and stock, with no elements of the protected section of the main path. It also has the maximum availability factor from all possible options. Thus, the matrices of backup **S** and reserving **T** sections are reduced into vectors. The simple circuit matrix **R** contains two columns, the first of which $\mathbf{R}^{\langle 1\rangle}$ points to the primary path, and the second one $\mathbf{R}^{\langle 2\rangle}$ to the reserving path:

$$\mathbf{R}^{\langle 1\rangle}=\mathbf{s}+\mathbf{S},$$

$$\mathbf{R}^{\langle 2\rangle}=\mathbf{s}+\mathbf{T}.$$

5. EXAMPLE OF ANALYZING THE RELIABILITY OF THE MAIN NETWORK

The cable structure of the backbone network of southern Russia (Fig. 3) is available on the official site of the International Telecommunication Union.[11] Fig. 3 also shows the numbered equivalent graph G(12, 21). The onnectivity probability according to GOST R 53111–2008[12] can be interpreted as the availability factor and characterizes reliability.

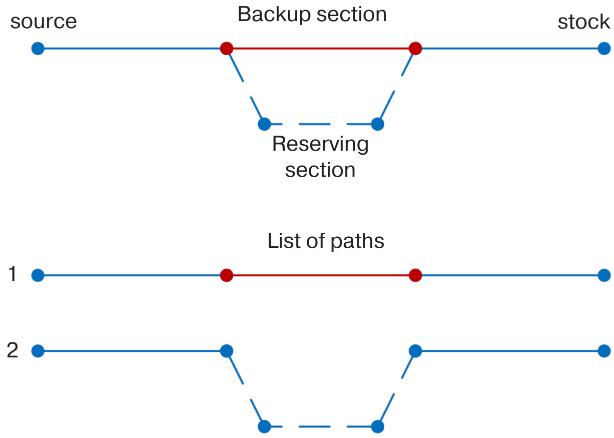

Fig. 2. Protective switching architecture for one protected and one backup section and list of paths

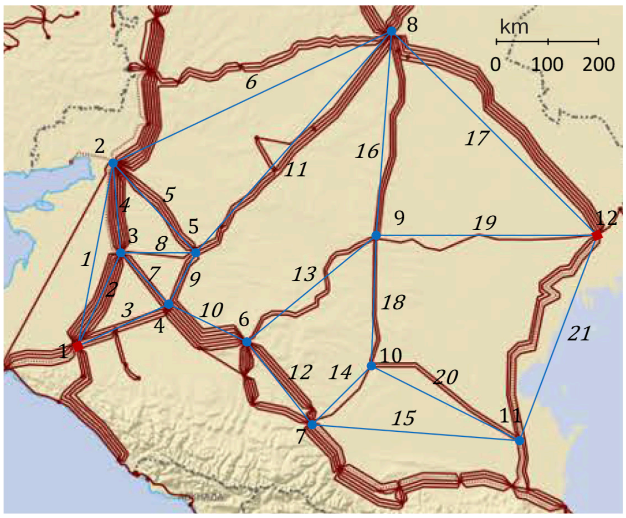

Fig. 3. Cable structure of the main network in the south of Russia

There is assumed to be at least one cross-connector or I/O multiplexer on the node, working for all valid communication directions. It has an average MTBF of 10^5 h and mean recovery time of 6 h [9]. So the availability factor of any unit is

$$p_{\text{vertex}}=1-\frac{6}{10^5}=0.99994.$$

Availability factor p_1 of individual links is calculated for fiber-optic transmission systems based on the length

[11] https://bbmaps.itu.int/bbmaps/. Accessed February 26, 2024.

[12] GOST R 53111–2008. National Standard of the Russian Federation. *Stability of functioning of the public communications network. Requirements and check methods*. Moscow: Standartinform; 2009. 16 p. (in Russ.).

Table 1. Reliability parameters of the communication lines

Line No.	Length d_l, km	Availability factor p_l	Line No.	Length d_l, km	Availability factor p_l	Line No.	Length d_l, km	Availability factor p_l
1	375	0.99755	8	150	0.99901	15	410	0.99729
2	200	0.99866	9	115	0.99923	16	400	0.99735
3	200	0.99866	10	110	0.99926	17	565	0.9963
4	175	0.99886	11	575	0.99624	18	265	0.99827
5	250	0.99836	12	225	0.99851	19	430	0.99717
6	600	0.99604	13	325	0.99785	20	325	0.99785
7	140	0.99908	14	165	0.99892	21	440	0.99711

calculated from the geographic coordinates of the cities between which the link is deployed.

Calculated on the basis of (1) parameters of the communication lines are given in the Table 1.

All types of protected sections for protective switching mechanisms for one protected section and one standby section (1 + 1 or 1 : 1 schemes) are considered. The results of calculations obtained by computer modeling in accordance with the multivariable inversion method [15] are given in Table 2.

Table 2. Network reliability parameters without backup and with protective switching

Section	Availability factor
Line	0.99966
Unit	0.99984
Segment	0.99284
Route	0.99981
Ring	0.99985
p-cycle	0.99986
Without backup	0.99266

The use of protection switching mechanisms for a single required transmission route (Table 2) shows a significant increase in reliability. The exception is protection switching on segments. This is primarily due to the specific nature of the topology of the considered network. Thus, the most reliable route 1–4–6–9–9–12 contains three backup segments 1–4–6, 4–6–9 and 6–9–12, each of which has a reserving path intersecting with the reserving paths of neighboring segments, significantly reducing the protective properties of the route.

CONCLUSIONS

The proposed method of analyzing the reliability of telecommunication networks supporting protective switching mechanisms divides elements of the main and backup routes into three groups. The first includes permanent unchangeable parts of the paths, the second—backup, and the third—reserving sections. Such representation allows the effects of duplication of elements in different routes to be taken into account. As a consequence, this eliminates errors in estimating the availability factor when compared with methods using the assumption of independence of information transmission paths.

Based on the example of a mainline network by computer modeling, the study shows that the use of protective switching mechanisms for one required transmission route demonstrates a significant increase in reliability. The exception is protective switching on segments. This is primarily due to the specific topology of the considered network which prevents the formation of segments completely independent of other paths.

Authors' contributions

K.A. Batenkov—the idea of the study, consultations on conducting all stages of the study.

A.B. Fokin—developing the approach to the analysis of the structural reliability of communication networks with protective switching mechanisms, computer modeling.

REFERENCES

1. Netes V.A. Service level agreement and dependability. *Nadezhnost' = Dependability*. 2017;17(4):27–30 (in Russ.). http://doi.org/10.21683/1729-2646-2017-17-4-27-30
2. Batenkov K.A., Batenkov A.A. Analysis and synthesis of communication network structures by deterministic stability indicators. *Trudy SPIIRAN = SPIIRAS Proceedings*. 2018;3(58):128–159 (in Russ.). https://doi.org/10.15622/sp.58.6
3. Batenkov A.A., Batenkov K.A., Fokin A.B. Analysis of the probability of connectivity of a telecommunications network based on the reduction of several non-connectivity events to a union of independent events. *Informatsionno-upravlyayushchie sistemy = Information and Control Systems*. 2021;6(115):53–63 (in Russ.). https://doi.org/10.31799/1684-8853-2021-6-53-63
4. Netes V.A. Virtualization, cloud services and reliability. *Vestnik svyazi = Vestnik Communications*. 2016;8:7–9 (in Russ.).
5. Batenkov K.A. Accurate and Boundary Estimate of Communication Network Connectivity Probability Based on Model State Complete Enumeration Method. *Trudy SPIIRAN = SPIIRAS Proceedings*. 2019;18(5):1093–1118 (in Russ.). https://doi.org/10.15622/sp.2019.18.5.1093-1118
6. Anfyorov M.A. Algorithm for finding subcritical paths on network diagrams. *Russ. Technol. J.* 2023;11(1):60–69 (in Russ.). https://doi.org/10.32362/2500-316X-2023-11-1-60-69
7. Batenkov A.A., Batenkov K.A., Fokin A.B. Forming the telecommunication networks' cross-sections to analyze the latter stability with different connectivity measures. *Informatika i avtomatizatsiya = Informatics and Automation*. 2021;20(2):371–406 (in Russ.). https://doi.org/10.15622/ia.2021.20.2.5
8. Wosinska L., Chen J., Larsen C.P. Fiber Access Networks: Reliability Analysis and Swedish Broadband Market. *IEICE Trans. Commun*. 2009;E92–B(10):3006–3014. https://doi.org/10.1587/transcom.E92.B.3006
9. Vasseur J.-P., Pickavet M., Demeester P. *Network Recovery. Protection and Restoration of Optical, SONET-SDH, IP, and MPLS*. San Francisco, CA: Elsevier; 2004. 542 p.
10. Lashgari M., Tonini F., Capacchione M., Woosinka L., Rigamonti G., Monti P. Techno-economics of Fiber vs. Microwave for Mobile Nransport Network Deployments. *J. Opt. Comm. and Netw.* 2023;15(7):C74–C87. https://doi.org/10.1364/JOCN.482865
11. Yusuf M.N., Bakar K.b.A., Isyaku B., Saheed A.L. Review of Path Selection Algorithms with Link Quality and Critical Switch Aware for Heterogeneous Traffic in SDN. *Int. J. Electr. Computer Eng. Syst.* 2023;14(3):345–370. https://doi.org/10.32985/ijeces.14.3.12
12. Isyaku B., Bakar K.B.A., Nagmeldin W., Abdelmaboud A., Saeed F., Ghaleb F.A. Reliable Failure Restoration with Bayesian Congestion Aware for Software Defined Networks. *CSSE*. 2023;46(3):3729–3748. https://doi.org/10.32604/csse.2023.034509
13. Bosisio A., Berizzi A., Lupis D., Morotti A., Iannarelli G., Greco B. A Tabu-search-based Algorithm for Distribution Network Restoration to Improve Reliability and Resiliency. *J. Modern Power Systems and Clean Energy*. 2023;11(1):302–311. https://doi.org/10.35833/MPCE.2022.000150
14. Sergeeva T.P., Tetekin N.N. Reliability Enhancemrnt Methods for SDN Networks. *T-Comm*. 2014;6:53–55 (in Russ.).
15. Batenkov A.A., Batenkov K.A., Fokin A.B. Network connectivity probability analysis based on its states inversion. *Vestnik Tomskogo gosudarstvennogo universiteta. Upravlenie, vychislitelnaja tehnika i informatika = Tomsk State University Journal of Control and Computer Science.* 2022;59:91–98 (in Russ.). https://doi.org/10.17223/19988605/59/10

СПИСОК ЛИТЕРАТУРЫ

1. Нетес В.А. Соглашение об уровне обслуживания и надежность. *Надежность*. 2017;17(4):27–30. http://doi.org/10.21683/1729-2646-2017-17-4-27-30
2. Батенков К.А., Батенков А.А. Анализ и синтез структур сетей связи по детерминированным показателям устойчивости. *Труды СПИИРАН*. 2018;3(58):128–159. https://doi.org/10.15622/sp.58.6
3. Батенков А.А., Батенков К.А., Фокин А.Б. Вероятность связности телекоммуникационной сети на основе приведения нескольких событий несвязности к объединению независимых событий. *Информационно-управляющие системы*. 2021;6(115):53–63. https://doi.org/10.31799/1684-8853-2021-6-53-63
4. Нетес В.А. Виртуализация, облачные услуги и надежность. *Вестник связи*. 2016;8:7–9.
5. Батенков К.А. Точные и граничные оценки вероятностей связности сетей связи на основе метода полного перебора типовых состояний. *Труды СПИИРАН*. 2019;18(5):1093–1118. https://doi.org/10.15622/sp.2019.18.5.1093-1118
6. Анфёров М.А. Алгоритм поиска подкритических путей на сетевых графиках. *Russ. Technol. J.* 2023;11(1):60–69. https://doi.org/10.32362/2500-316X-2023-11-1-60-69
7. Батенков А.А., Батенков К.А., Фокин А.Б. Формирование сечений телекоммуникационных сетей для анализа их устойчивости с различными мерами связности. *Информатика и автоматизация*. 2021;20(2):371–406. https://doi.org/10.15622/ia.2021.20.2.5
8. Wosinska L., Chen J., Larsen C.P. Fiber Access Networks: Reliability Analysis and Swedish Broadband Market. *IEICE Trans. Commun*. 2009;E92–B(10):3006–3014. https://doi.org/10.1587/transcom.E92.B.3006
9. Vasseur J.-P., Pickavet M., Demeester P. *Network Recovery. Protection and Restoration of Optical, SONET-SDH, IP, and MPLS*. San Francisco, CA: Elsevier; 2004. 542 p.

10. Lashgari M., Tonini F., Capacchione M., Woosinka L., Rigamonti G., Monti P. Techno-economics of Fiber vs. Microwave for Mobile Nransport Network Deployments. *J. Opt. Comm. and Netw.* 2023;15(7):C74–C87. https://doi.org/10.1364/JOCN.482865
11. Yusuf M.N., Bakar K.b.A., Isyaku B., Saheed A.L. Review of Path Selection Algorithms with Link Quality and Critical Switch Aware for Heterogeneous Traffic in SDN. *Int. J. Electr. Computer Eng. Syst.* 2023;14(3):345–370. https://doi.org/10.32985/ijeces.14.3.12
12. Isyaku B., Bakar K.B.A., Nagmeldin W., Abdelmaboud A., Saeed F., Ghaleb F.A. Reliable Failure Restoration with Bayesian Congestion Aware for Software Defined Networks. *CSSE*. 2023;46(3):3729–3748. https://doi.org/10.32604/csse.2023.034509
13. Bosisio A., Berizzi A., Lupis D., Morotti A., Iannarelli G., Greco B. A Tabu-search-based Algorithm for Distribution Network Restoration to Improve Reliability and Resiliency. *J. Modern Power Systems and Clean Energy*. 2023;11(1):302–311. https://doi.org/10.35833/MPCE.2022.000150
14. Сергеева Т.П., Тетёкин Н.Н. Методы повышения надежности в сетях SDN. *T-Comm.* 2014;6:53–55.
15. Батенков А.А., Батенков К.А., Фокин А.Б. Анализ вероятности связности телекоммуникационной сети на основе инверсий ее состояний. *Вестник Томского государственного университета. Управление, вычислительная техника и информатика*. 2022;59:91–98. https://doi.org/10.17223/19988605/59/10

About the authors

Kirill A. Batenkov, Dr. Sci. (Eng.), Docent, Professor, Department of Applied Mathematics, Institute of Information Technologies, MIREA – Russian Technological University (78, Vernadskogo pr., Moscow, 119454 Russia). E-mail: pustur@yandex.ru. Scopus Author ID 35777325300, RSCI SPIN-code 8570-6327, https://orcid.org/0000-0001-6083-1242

Aleksandr B. Fokin, Employee, Russian Federation Security Guard Service Federal Academy (FSO Academy of Russia) (35, Priborostroitelnaya ul., Orel, 302015 Russia). Email: tatarin57ru@mail.ru. Scopus Author ID 57218934996, RSCI SPIN-code 7727-1166, https://orcid.org/0000-0002-2187-7325

Об авторах

Батенков Кирилл Александрович, д.т.н., доцент, профессор кафедры прикладной математики, Институт информационных технологий ФГБОУ ВО «МИРЭА – Российский технологический университет» (119454, Россия, Москва, пр-т Вернадского, д. 78). E-mail: pustur@yandex.ru. Scopus Author ID 35777325300, SPIN-код РИНЦ 8570-6327, https://orcid.org/0000-0001-6083-1242

Фокин Александр Борисович, сотрудник, ФГКВОУ ВО «Академия Федеральной службы охраны Российской Федерации» (302015, Россия, Орёл, ул. Приборостроительная, д. 35). E-mail: tatarin57ru@mail.ru. Scopus Author ID 57218934996, SPIN-код РИНЦ 7727-1166, https://orcid.org/0000-0002-2187-7325

Translated from Russian into English by Lyudmila O. Bychkova
Edited for English language and spelling by Dr. David Mossop

Russian Technological Journal. 2024;12(2):48–56 ISSN 2500-316X (Online)

Modern radio engineering and telecommunication systems
Современные радиотехнические и телекоммуникационные системы

UDC 621.396.969.3
https://doi.org/10.32362/2500-316X-2024-12-2-48-56

RESEARCH ARTICLE

Mathematical modeling of microwave channels of a semi-active radar homing head

Nikolay M. Legkiy @,
Ivan V. Unchenko

MIREA – Russian Technological University, Moscow, 119454 Russia
@ Corresponding author, e-mail: legki@mirea.ru

Abstract
Objectives. Radar homing heads of guided missiles form a large group of radars which differ from other radars due to their specific purpose. The advantages of a semi-active radar homing head (SARH) include the ability to have a powerful irradiator at the command post and, as a result, a powerful reflected signal from the target. This results in an increase in the range of its detection and guidance. The absence of an emitter simplifies the missile's onboard control equipment, reduces its weight and dimensions, thereby improving its maneuverability and increasing the guidance accuracy, resulting in the greatest distribution of this type of SARH. However, in order to determine the exact Doppler shift of the target signal as part of SARH, a reference signal with a frequency coinciding with the illumination transmitter signal must be supplied to the receiving path. This study aims to synthesize and analyze the SARH receiver circuit with improved accuracy characteristics.
Methods. The following methods are used: statistical radio engineering; optimal signal reception theories; and computer modeling in CAD *AWR Design Environment*.
Results. A mathematical model of the SARH receiver was obtained and analyzed. The proposed receiver model allows the spectral characteristics of signals to be calculated at any point of the microwave paths, as well as signal characteristics at the input of the head channel, at the output of the first conversion mixer, at the output of the first intermediate frequency selector, and at the output of the receiving path. The calculated values of the main characteristics of high-frequency channels are also given.
Conclusions. The resulting model allows the frequency dependencies of main parameters of the receiving path, such as the gain factor, noise factor, decibel compression points, and third-order intermodulation intercept points to be estimated. The values obtained during the simulation are maximally close to existing systems, since the models of real-life and mass-used microcircuits thu created are used as the main elements when designing high-frequency paths. The model can be used to study methods of improving technical indicators, as well as to develop new principles and schemes for developing radioelectronic complexes, for example, when designing a receiving path using advanced radio photonics.

Keywords: semi-active radar homing head, microwave receiver, receiver characteristics, modeling

• **Submitted:** 26.04.2023 • **Revised:** 09.08.2023 • **Accepted:** 15.02.2024

For citation: Legkiy N.M., Unchenko I.V. Mathematical modeling of microwave channels of a semi-active radar homing head. *Russ. Technol. J.* 2024;12(2):48–56. https://doi.org/10.32362/2500-316X-2024-12-2-48-56

Financial disclosure: The authors have no a financial or property interest in any material or method mentioned.

The authors declare no conflicts of interest.

НАУЧНАЯ СТАТЬЯ

Математическое моделирование сверхвысокочастотных каналов полуактивной радиолокационной головки самонаведения

Н.М. Легкий @,
И.В. Унченко

МИРЭА – Российский технологический университет, Москва, 119454 Россия
@ Автор для переписки, e-mail: legki@mirea.ru

Резюме
Цели. Радиолокационные головки самонаведения (РГСН) управляемых ракет – это большая группа радиолокаторов, которые в виду особенностей назначения отличаются от других радиолокаторов. Преимуществом полуактивной РГСН является возможность иметь мощный облучатель на командном пункте и, как следствие, мощный отраженный сигнал от цели, что в результате приводит к увеличению дальности ее обнаружения и точности наведения на цель. Отсутствие аппаратуры излучения упрощает бортовую аппаратуру управления ракеты, уменьшает ее вес и габариты и, следовательно, улучшаются ее маневренные свойства, что обуславливает наибольшее распространение данного типа РГСН. Для точного определения доплеровского смещения сигнала цели в приемный тракт полуактивной РГСН должен поступать эталонный сигнал, частота которого совпадает с частотой сигнала передатчика подсвета. Цель работы – оптимизация бортовой аппаратуры и подтверждение предлагаемого подхода с помощью моделирования.
Методы. В работе использованы методы статистической радиотехники, теории оптимального приема сигналов и компьютерное моделирование в системе автоматизированного проектирования *AWR Design Environment*.
Результаты. Получена и проанализирована математическая модель приемника РГСН. Предложенная модель приемника позволяет произвести расчет спектральных характеристик сигналов в любой точке СВЧ-трактов, характеристик сигналов на входе основного канала, на выходе смесителя первого преобразования, на выходе селектора первой промежуточной частоты и на выходе приемного тракта. Приведены расчетные значения основных характеристик высокочастотных каналов.
Выводы. Полученная модель позволяет оценивать частотные зависимости основных параметров приемного тракта, таких как коэффициент передачи, коэффициент шума, точки децибельной компрессии, точки пересечения интермодуляций третьего порядка. Полученные при моделировании значения максимально приближены к характеристикам существующих систем, т.к. в качестве основных элементов высокочастотных трактов использовались созданные модели реально существующих и массово используемых микросхем. Модель может использоваться для исследования путей совершенствования технических показателей, разработки новых принципов и схем построения радиоэлектронных комплексов, например, при построении приемного тракта с использованием перспективных средств радиофотоники.

Ключевые слова: полуактивная радиолокационная головка самонаведения, СВЧ-приемник, характеристики приемника, моделирование

• **Поступила:** 26.04.2023 • **Доработана:** 09.08.2023 • **Принята к опубликованию:** 15.02.2024

Для цитирования: Легкий Н.М., Унченко И.В. Математическое моделирование сверхвысокочастотных каналов полуактивной радиолокационной головки самонаведения. *Russ. Technol. J.* 2024;12(2):48–56. https://doi.org/10.32362/2500-316X-2024-12-2-48-56

Прозрачность финансовой деятельности: Авторы не имеют финансовой заинтересованности в представленных материалах или методах.

Авторы заявляют об отсутствии конфликта интересов.

INTRODUCTION

Radar homing heads (RH) of guided missiles form a large group of radars which differ from other radars due to their specific purpose [1–3]. A distinction is made between active (ARH) and semi-active radar homing heads (SARH). Each type has its own advantages and disadvantages. In the case of active homing, a missile using RH irradiates the target and receives part of the reflected energy by means of a single antenna, active [4], or digital [5] phased antenna array. The information (energy) received is processed by RH and output as control signals to the missile autopilot.

The advantage of SARH is its ability to create a powerful irradiator at the command post and, consequently, a powerful reflected signal from the target. This results in increased detection range and targeting accuracy. The absence of a microwave signal generator simplifies the onboard control equipment of the missile, and also reduces its weight and dimensions, hence improving its maneuverability. As a result, SARH is widely used.

FUNCTIONAL DIAGRAM AND MATHEMATICAL DESCRIPTION OF SARH

A variety of modeling packages and technologies are used to work out most efficient solutions of SARH modules [6–9].

The basic concept behind semi-active homing heads is that since almost all detection and tracking systems contain ground-based radar systems, duplication of this equipment on the missile itself in some cases is redundant. In order to synchronize the SARH hardware, the ground-based radar signal can be used as a reference signal. In order to determine the Doppler shift of the target signal as part of SARH, a reference signal with a frequency coinciding with that of the illumination transmitter signal should be fed into the receiving path. The solution to this problem is the use of a direct signal (reference signal) received by a special antenna, propagating from the transmitter of the ground radar station towards SARH. In order to receive this signal, a special reference receiver is added to SARH to amplify the signals received by the reference signal antenna oriented to the rear hemisphere of the missile, i.e., towards the illumination station. The amplified reference signal is used for heterodyne synchronization in SARH or directly as a heterodyne signal in the receiver [10].

The functional diagram of the SARH receiver is shown in Fig. 1 [6]. The illumination station radiates a signal with frequency f_0. The frequency $f_{\text{ref.ch.}}$ of the signal received by the reference channel is shifted downward due to the Doppler effect when the missile moves away from the illumination station, as follows:

$$f_{\text{ref.ch.}} = f_0 - \frac{V_\text{r}}{\lambda}, \tag{1}$$

where f_0 is the illumination station signal frequency, V_r is the missile radial velocity, λ is the reference signal wavelength.

The frequency of the target signal received by the reference channel is shifted upward due to the oncoming motion of the missile and target, as follows:

$$f_{\text{head ch.}} = f_0 + \frac{V_\text{r}}{\lambda} + \frac{V_\text{t}}{\lambda}, \tag{2}$$

where $f_{\text{head ch.}}$ is the frequency of the signal as reflected from the target received by the head (main) channel; V_t is the target velocity.

Both the signal reflected from the target and the reference signal are converted to the first intermediate frequency using the common first heterodyne signal f_{h1}, as follows:

- first intermediate frequency of the reference channel

$$f_{\text{ref.ch.1}} = f_0 - \frac{V_\text{r}}{\lambda} - f_{\text{h1}}, \tag{3}$$

- first intermediate frequency of the head channel

$$f_{\text{head ch.1}} = f_0 + \frac{V_\text{r}}{\lambda} + \frac{V_\text{t}}{\lambda} - f_{\text{h1}}. \tag{4}$$

The reference signal $f_{\text{ref.ch.1}}$ cannot be directly used as a heterodyne signal in the further processing

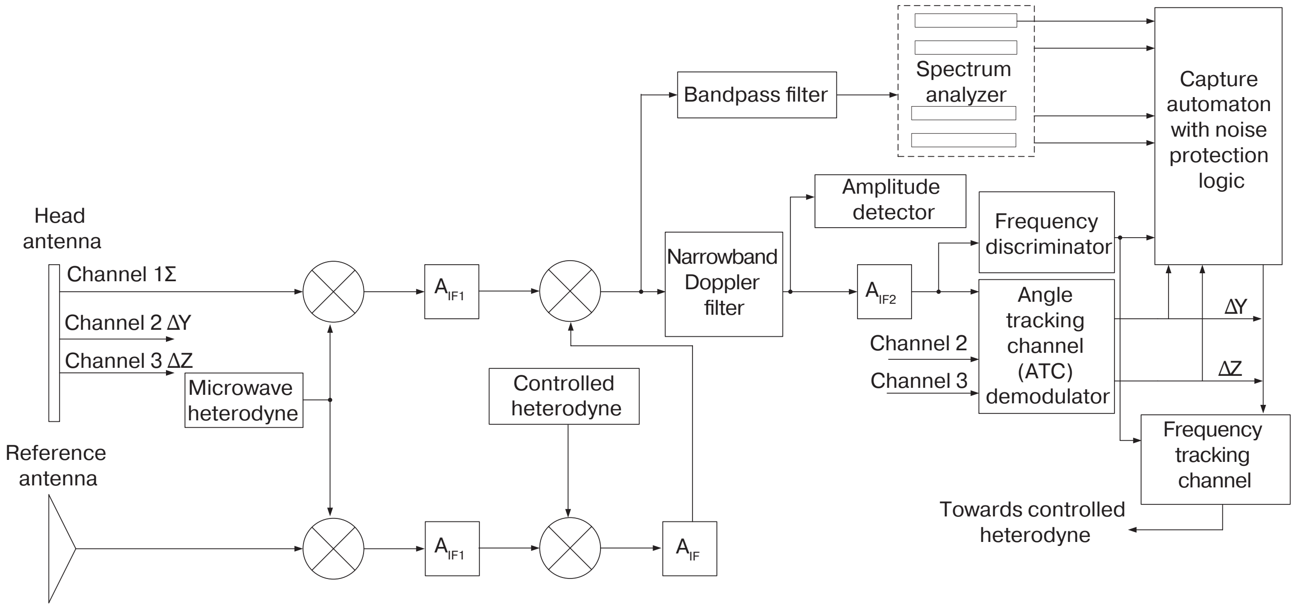

Fig. 1. Functional diagram of the SARH receiver. ATC is the angular tracking channel; A_{IF}, A_{IF1}, and A_{IF2} are intermediate frequency amplifiers

of the head channel signal, since in this case, the signal conversion occurs at low frequencies, where for circuitry reasons processing is difficult. In order to prevent this, the reference signal is shifted to the second intermediate frequency using an additional controlled heterodyne. The frequency of the controlled heterodyne signal may be written as follows:

$$f_{c.h.} = f_{IF2} + f_{DF}, \quad (5)$$

where f_{IF2} is a fixed value equal to the second intermediate frequency of the head channel; and f_{DF} is the predicted value of the Doppler frequency of the target signal received from the target channel or as a result of target tracking.

The second intermediate frequency of the reference channel is equal to the following:

$$f_{ref.ch.2} = f_0 - \frac{V_r}{\lambda} - f_{h1} + f_{IF2} + f_{DF}. \quad (6)$$

Signal $f_{ref.ch.2}$ is used as a heterodyne signal in further conversion of head channel signals in the so-called convolution mixer, and since frequency $f_{ref.ch.2}$ is higher than $f_{head\ ch.1}$, the frequency of the second signal is subtracted from the first, as follows:

$$f_{head\ ch.2} = f_{ref.ch.2} - f_{head\ ch.1} = \\ = f_{IF2} + f_{DF} - \frac{2(V_r - V_t)}{\lambda}. \quad (7)$$

Here $f_{head\ ch.2}$ is the signal frequency of the second intermediate frequency of the head channel, while the actual Doppler shift of the target signal may be written as follows:

$$\frac{2(V_r - V_t)}{\lambda} = f_d. \quad (8)$$

Since term f_d represents the actual Doppler shift of the target signal, the frequency of the signal after conversion is shifted relative to f_{IF2} by the difference between the predicted and actual Doppler frequency values. When they are equal, it falls exactly on f_{IF2}. When processing the target signal, this allows use of the narrowband Doppler filter tuned to the fixed value of frequency f_{IF2}, irrespective of the Doppler shift of the target signal. The principle of operation and SARH functional diagrams are described in more detail in [6].

MATHEMATICAL MODELING OF SARH MICROWAVE CHANNELS

In order to calculate the characteristics of SARH microwave channels, closest to the real ones, the characteristics of real existing microcircuits and systems of radar stations are used for modeling [11–17].

Applying the *Visual System Simulator* (*VSS*) module of the *AWR Design Environment*[1] system for computer-aided design and modeling of high-frequency (HF) systems and devices enables the work at the design stage to be automated, and the main characteristics of microwave channels to be calculated. The model of SARH microwave channels developed in the *VSS* environment is shown in Fig. 2.

The first functional block in the SARH receiving path is the input power limiter. It reduces the signal level

[1] https://pcbsoftware.com/product/awr/. Accessed September 13, 2023.

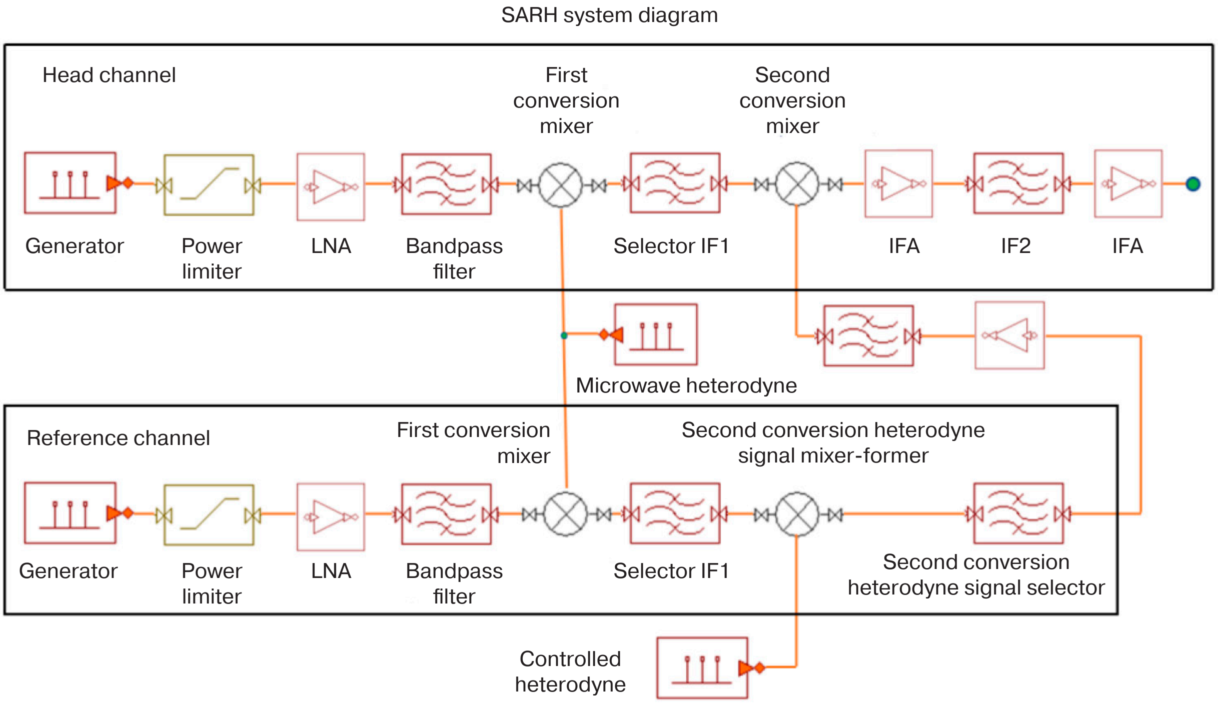

Fig. 2. Model of SARH microwave channels

entering the low-noise amplifier (LNA) to a safe level. The TGL2208-SM[2] chip is used as a power limiter. In order to achieve the required transmission coefficient, a multi-stage construction scheme of the receiving path is used. Each stage amplifies the incoming signal in accordance with its gain factor G and has its own noise level characterized by noise factor F.

The formula for determining the noise factor of the stage amplifier is given in [14] and has the following form:

$$NF = NF_1 + \frac{NF_2 - 1}{G_1} + \ldots + \frac{NF_n - 1}{G_{n-1}}, \quad (9)$$

where NF is the noise factor, F_1 is the noise factor of the first stage, F_n is the noise factor of the nth stage, G_1 is the gain factor of the first stage, and G_n is the gain factor of the nth stage.

The formula shows that the largest contribution to the total noise factor is made by the noise of the first stage. Furthermore, the higher the gain factor of the first stage, the lower the total noise factor.

Since the mixers where the frequency conversion occurs are quite noise intensive, the very first gain stage (LNA) is performed before the frequency conversion, i.e., at the carrier frequency. During modeling, the parameters of the QPA2609[3] chip are used as LNA.

The intermediate frequency amplifier (IFA) provides for maximum amplification of the received signal. The IFA brings the signal level to the value necessary for normal operation of the signal processing equipment, thus providing the necessary sensitivity for the receiver. The PMA3-83LN+[4] chip is used as IFA.

The mixer is used to gain the received carrier frequency signal to the intermediate frequency. The HMC773ALC3B[5] chip is selected as the mixer.

During modeling, the calculation of the main characteristics of microwave channels is carried out under normal climatic conditions. This includes the frequency dependencies of the gain factor ($S21$), noise factor (NF), decibel compression points (OP1dB), and third-order intermodulation cross points (OIP3).

The following frequencies are specified, in order to calculate the main parameters of the model: the operating frequency of the illumination station F_{il} (8 GHz); the frequency of the signal reflected from the target F_{refl}; the frequency of the first (reference) microwave heterodyne F_{h1}; and the frequency and bandwidth of signal processing (1 GHz). Signals F_{il} and F_{refl} are formed by library models of signal sources TONE and are fed to the input of the reference and main channel, respectively. Here they are reduced (if necessary) to a safe level by the first element of

[2] https://www.qorvo.com/products/p/TGL2208-SM. Accessed September 13, 2023.

[3] https://www.qorvo.com/products/p/QPA2609. Accessed September 13, 2023.

[4] https://www.minicircuits.com/pdfs/PMA3-83LN+.pdf. Accessed September 13, 2023.

[5] https://www.micro-semiconductor.com/datasheet/46-HMC773ALC3B.pdf. Accessed September 13, 2023.

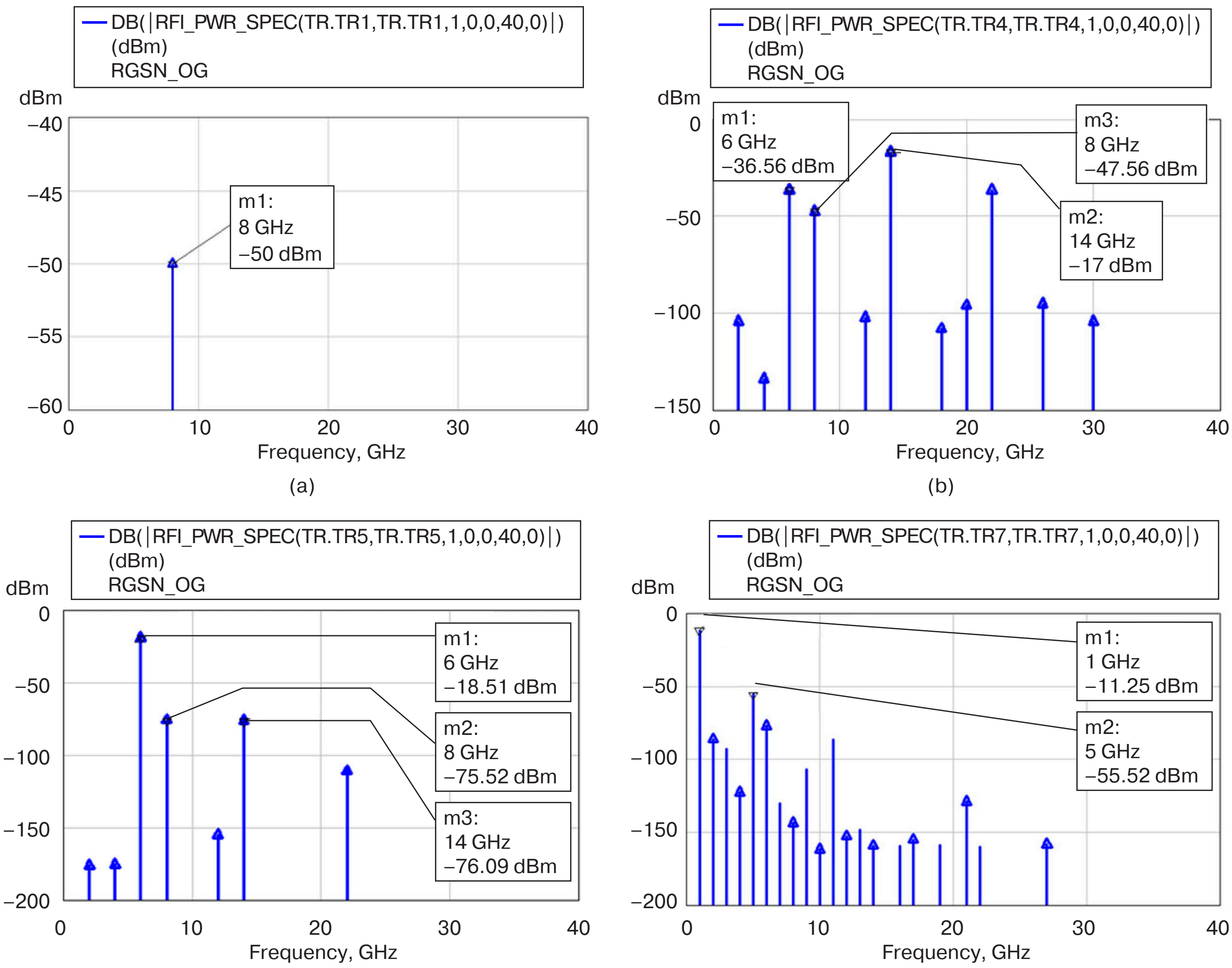

Fig. 3. Signal spectra: (a) at the input of the head channel, (b) at the output of the first conversion mixer, (c) at the output of the first intermediate frequency selector, (d) at the output of the receiving path

the receiving path that is TGL2208-SM power limiter. The safe level signals are fed to the QPA2609 LNA input and then to the input of the bandpass filter which separates the signals of the receiver working range. Signals are fed from the range filter output to the first conversion mixers where they are mixed with the microwave heterodyne signal F_{h1}. Then they are transferred to the spectrum of the first intermediate frequency signals $F_{IF\ up}$ and $F_{IF\ low}$ in the upper head (original) channel and in the lower reference (providing) channel, respectively. The operating frequency is selected by the first intermediate frequency selector, the bandwidth of which is changed in accordance with the specified equations depending on the illumination station operating frequency F_{il}.

The signal $F_{IF\ low}$, amplified in IFA, is transferred by the mixer-former to the signal frequency spectrum of the second heterodyne F_{h2} using the controlled heterodyne. The operating frequency is selected by the signal selector of the second heterodyne, while the signal level is increased to the required level in the IFA chain. Signal F_{h2} is fed to the heterodyne input of the second conversion mixer, to which signal $F_{IF\ up}$ is also fed, and then transferred to the signal processing frequency.

The resulting model allows the spectral characteristics of signals at any point of microwave paths to be calculated. The spectra of signals at the head channel input, at the first conversion mixer output, at the first intermediate frequency selector output, and at the receiving path output are shown in Fig. 3. The calculated values for main characteristics of HF channels are presented in Fig. 4.

By analyzing the graphs shown in Figs. 3 and 4, it can be concluded that the head channel receiving path in the configuration shown in Fig. 2 has a gain factor of at least 38 dB with an output decibel compression point level of at least 13 dBm.

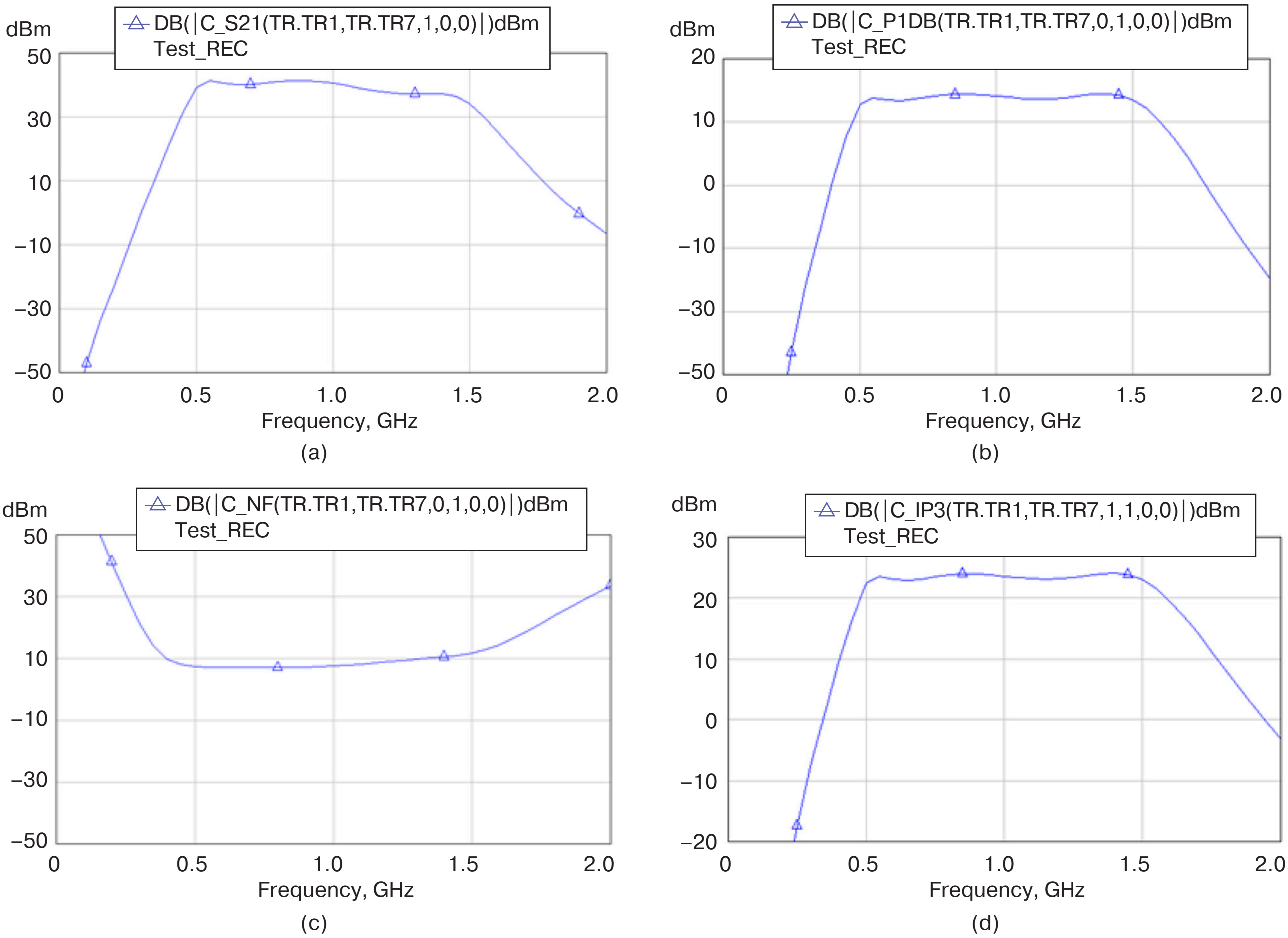

Fig. 4. Calculated values for the main HF channel characteristics:
(a) head channel gain factor, (b) head channel OP1dB, (c) noise factor *NF*, and (d) OIP3

CONCLUSIONS

The resulting model allows the frequency dependencies of the receiving path main parameters, such as gain factor, noise factor, decibel compression points, and third-order intermodulation cross points to be estimated. The simulation values are maximally close to those of existing systems due to using models of real widespread microcircuits as the main elements in constructing HF paths. The model can be used to study ways of improving the technical performance, as well as in the development of new principles and construction schemes for radioelectronic complexes (in particular, SARH), e.g., in constructing the receiving path using promising means of radio photonics.

Authors' contribution. All authors equally contributed to the research work.

REFERENCES

1. Degtyareva E.E., Lokacheva Yu.A., Sudin A.P., Petushkevich N.A., Nedosekova E.A. Homing Radar. In: *European Research. Collection of articles of the 22nd International Scientific and Practical Conference*. 2019. P. 19–21 (in Russ.).
2. Gorbachev M., Svistov V., Ulyanova E. The specifics of functioning of the active homing head exposed to ground surface clutter. *Vestnik Koncerna VKO "Almaz – Antey" = Journal of "Almaz – Antey" Air and Space Defence Corporation*. 2021;4:25–35.
3. Pavlov V., Belousov O., Dorokhova T., Belyaev M., Trapeznikov E. Algorithm for controlling objects implementing a semi-passive guidance technique. *J. Phys.: Conf. Ser*. 2021;1901(1):012018. http://doi.org/10.1088/1742-6596/1901/1/012018
4. Legky N.M., Unchenko I.V. Formation of the directional diagram in phased antenna array. *Russ. Technol. J*. 2019;7(2):29–38 (in Russ.). https://doi.org/10.32362/2500-316X-2019-7-2-29-38
5. Chistyakov V.A. Monopulse radio direction finder using digital antenna array. *Trudy MAI*. 2020;115:7 (in Russ.). https://doi.org/10.34759/trd-2020-115-07

6. Elizarov V.S., Chepkasov A.V. Simulation of radar signal reflection at half-nature modelling of the active homing head. *Antenny = Antennas*. 2013;1(188):94–97 (in Russ.).
7. Veksin S.I. *Tsifrvaya obrabotka signalov v doplerovskikh golovkakh samonavedeniya* (*Digital signal processing in Doppler homing heads*). Moscow: Bauman Press; 2018. 324 p. (in Russ.).
8. Porkin A.G. Modeling of transceiver modules AFAR the homing missiles. *Alleya nauki = Alley-Science*. 2017;2(15):196–199 (in Russ.).
9. Konovaltsev E.V., Linnik A.P. Justification of the minimum sample size with small numbers of observations to assess the characteristics of aircraft weapons equipped with radar homing heads. *Vozdushno-kosmicheskie sily. Teoriya i praktika = Aerospace Forces. Theory and practice*. 2022;23:43–49 (in Russ.).
10. Ilchuk A.R., Merkulov V.I., Panas A.I., Chernov V.S., Shcherbakov S.V. Analysis of the current state and development prospects of radar systems for guided weapons of air objects destruction. *Radioelektronika. Nanosistemy. Informatsionnye tekhnologii = Radioelectronics. Nanosystems. Information Technologies* (*RENSIT*). 2021;13(3):227–244 (in Russ.). https://doi.org/10.17725/rensit.2021.13.227
11. Muratov I.V. Mathematical model of direction-finding characteristic of seeker. *Elektromagnitnye volny i elektronnye sistemy = Electromagnetic Waves and Electronic Systems*. 2013;11:34–38 (in Russ.).
12. Dvoiris L.I., Ivanov V.A., Galev K.V. Simulation model of signals and interference for testing detection systems. *Radiotekhnika = Radioengineering*. 2020;84(2-4):14–19 (in Russ.).
13. Volkov V.V., Gordyaskina T.V. Research of analog radio technical communication channel in the MATHCAD software package. In: *Great Rivers – 2020. Proceedings of the 22nd International Scientific and Industrial Forum*. 2020. P. 94 (in Russ.).
14. Dunsmore J.P. *Nastol'naya kniga inzhenera. Izmereniya parametrov SVCh-ustroistv s ispol'zovaniem peredovykh metodik vektornogo analiza tsepei* (*The Engineer's Handbook. Microwave measurements using advanced vector network analysis techniques*): transl. from Engl. Moscow: Tekhnosfera; 2019. 736 p. (in Russ.).
[Dunsmore J.P. *Handbook of Microwave Component Measurements with Advanced VNA Techniques*. Wiley; 2014. 735 p.]
15. Ivannikov A.P., Ivannikov D.A. Broadband signal generation and processing method in antenna array radars. *Radiotekhnicheskie i telekommunikatsionnye sistemy = Radio Engineering and Telecommunications Systems*. 2018;3(31):17–25 (in Russ.).
16. Unchenko I.V., Emelyanov A.A Photonics-based modular multistate digital coherent system. *Russ. Technol. J*. 2022;10(4):27–37 (in Russ.). https://doi.org/10.32362/2500-316X-2022-10-4-27-37
17. Shumov A.V., Nefedov S.I., Bikmetov A.R. The concept of building a radar station based on the Microwave photonics components. *Nauka i Obrazovanie = Science & Education. Bauman Moscow State Technical University.* 2016;5:41–65 (in Russ.).

СПИСОК ЛИТЕРАТУРЫ

1. Дегтярева Е.Е., Локачева Ю.А., Судин А.П., Петушкевич Н.А., Недосекова Е.А. Радиолокационная головка самонаведения. В сборнике: *European Research: Сборник статей XXII Международной научно-практической конференции*. 2019. С. 19–21.
2. Горбачев М.А., Свистов В.В., Ульянова Е.А. Особенности работы активной ГСН при воздействии отражений от земной поверхности. *Вестник Концерна ВКО «Алмаз – Антей»*. 2021;4:25–35.
3. Pavlov V., Belousov O., Dorokhova T., Belyaev M., Trapeznikov E. Algorithm for controlling objects implementing a semi-passive guidance technique. *J. Phys.: Conf. Ser*. 2021;1901(1):012018. http://doi.org/10.1088/1742-6596/1901/1/012018
4. Легкий Н.М., Унченко И.В. Формирование диаграммы направленности в фазированных антенных решетках. *Russ. Technol. J*. 2019;7(2):29–38. https://doi.org/10.32362/2500-316X-2019-7-2-29-38
5. Чистяков В.А. Моноимпульсный радиопеленгатор с использованием цифровой антенной решетки. *Труды МАИ*. 2020;115:7. https://doi.org/10.34759/trd-2020-115-07
6. Елизаров В.С., Чепкасов А.В. Имитация отраженного радиолокационного сигнала при полунатурном моделировании активной головки самонаведения. *Антенны*. 2013;1(188): 94–97.
7. Вексин С.И. *Цифрвая обработка сигналов в доплеровских головках самонаведения*. М.: Издательство МГТУ им. Н.Э. Баумана; 2018. 324 с.
8. Поркин А.Г. Моделирование приемо-передающих модулей АФАР в головке самонаведения ракет. *Аллея науки*. 2017;2(15):196–199.
9. Коновальцев Э.В., Линник А.П. Обоснование минимального объема выборки при малых количествах наблюдений для оценки характеристик авиационных средств поражения, оснащенных радиолокационными головками самонаведения. *Воздушно-космические силы. Теория и практика.* 2022;23:43–49.
10. Ильчук А.Р., Меркулов В.И., Панас А.И., Чернов В.С., Щербаков С.В. Анализ современного состояния и перспектив развития радиолокационных систем для управляемых средств поражения воздушных объектов. *Радиоэлектроника. Наносистемы. Информационные технологии* (*РЭНСИТ*). 2021;13(3):227–244. https://doi.org/10.17725/rensit.2021.13.227
11. Муратов И.В. Математическая модель пеленгационной характеристики следящего координатора цели. *Электромагнитные волны и электронные системы*. 2013;11:34–38.
12. Двойрис Л.И., Иванов В.А., Галев К.В. Имитационная модель сигналов и помех для тестирования систем обнаружения. *Радиотехника*. 2020;84(2–4):14–19.

13. Волков В.В., Гордяскина Т.В. Исследование аналогового радиотехнического канала связи в программном пакете MATHCAD. В сборнике: *Великие реки – 2020: Труды 22-го международного научно-промышленного форума*. 2020. С. 94.
14. Дансмор Д.П. *Настольная книга инженера. Измерения параметров СВЧ-устройств с использованием передовых методик векторного анализа цепей*: пер. с англ. М.: Техносфера; 2019. 736 с.
15. Иванников А.П., Иванников Д.А. Способ формирования и обработки широкополосных сигналов в радиолокаторах с антенными решетками. *Радиотехнические и телекоммуникационные системы*. 2018;3(31):17–25.
16. Унченко И.В., Емельянов А.А. Модульная многопозиционная когерентная цифровая радиофотонная система. *Russ. Technol. J.* 2022;10(4):27–37. https://doi.org/10.32362/2500-316X-2022-10-4-27-37
17. Шумов А.В., Нефедов С.И., Бикметов А.Р. Концепция построения радиолокационной станции на основе элементов радиофотоники. *Наука и Образование. Научное издание МГТУ им. Н.Э. Баумана.* 2016;5:41–65.

About the authors

Nikolay M. Legkiy, Dr. Sci. (Eng.), Docent, Head of the Department of Engineering Ecology of the Technosphere, Institute of Radio Electronics and Informatics, MIREA – Russian Technological University (78, Vernadskogo pr., Moscow, 119454 Russia). E-mail: legki@mirea.ru. Scopus Author ID 56178415900, ResearcherID GWQ-9074-2022, RSCI SPIN-code 6636-6401, http://orcid.org/0000-0003-1242-5113

Ivan V. Unchenko, Teacher, Department of Engineering Ecology of the Technosphere, Institute of Radio Electronics and Informatics, MIREA – Russian Technological University (78, Vernadskogo pr., Moscow, 119454 Russia). E-mail: unchenko@mirea.ru. RSCI SPIN-code 8819-1136, https://orcid.org/0000-0002-6048-3476

Об авторах

Легкий Николай Михайлович, д.т.н., доцент, заведующий кафедрой инженерной экологии техносферы, Институт радиоэлектроники и информатики ФГБОУ ВО «МИРЭА – Российский технологический университет» (119454, Россия, Москва, пр-т Вернадского, д. 78). E-mail: legki@mirea.ru. Scopus Author ID 56178415900, ResearcherID GWQ-9074-2022, SPIN-код РИНЦ 6636-6401, http://orcid.org/0000-0003-1242-5113

Унченко Иван Владимирович, преподаватель, кафедра инженерной экологии техносферы, Институт радиоэлектроники и информатики ФГБОУ ВО «МИРЭА – Российский технологический университет» (119454, Россия, Москва, пр-т Вернадского, д. 78). E-mail: unchenko@mirea.ru. SPIN-код РИНЦ 8819-1136, https://orcid.org/0000-0002-6048-3476

Translated from Russian into English by Kirill V. Nazarov
Edited for English language and spelling by Dr. David Mossop

Micro- and nanoelectronics. Condensed matter physics

Микро- и наноэлектроника. Физика конденсированного состояния

UDC 538.958
https://doi.org/10.32362/2500-316X-2024-12-2-57-66

RESEARCH ARTICLE

Magnetorefractive effect in metallic Co/Pt nanostructures

Alexey N. Yurasov @,
Diana A. Sayfullina,
Tatiana N. Bakhvalova

MIREA – Russian Technological University, Moscow, 119454 Russia
@ Corresponding author, e-mail: alexey_yurasov@mail.ru

Abstract
Objectives. To carry out a theoretical investigation of the features of magnetorefractive effect for metal-to-metal nanostructures. This study uses the example of multilayer Co/Pt nanostructures (ferromagnetic metal–paramagnetic metal) with a different ratio of ferromagnetic and paramagnetic phases in the visible and near-infrared (IR) spectral regions.
Methods. The dependence was expressed explicitly using the basic formulas for permittivity, refraction and extinction coefficients, and optical conductivity. This then confirms the common nature of these two effects. The magnetorefractive effect for s-polarization of light was calculated using Fresnel formulas for a three-layer structure. This took into account the thickness of the samples and the influence of the substrate. Effective medium methods were used to calculate the dielectric permittivity of materials. Since the average range of cobalt concentrations was being studied, the Bruggeman approximation was used to establish the effective permittivity of nanostructures. The reflection coefficient at normal incidence was calculated for all nanostructures.
Results. Since the permittivity of inhomogeneous samples was replaced by a common effective parameter depending on the permittivity of each component, we were able to apply the Drude–Lorentz theory for conductors in a high-frequency alternating field and then estimate the parameters of the electronic structure of the samples being studied. Plasma and relaxation frequencies were calculated for each sample. This made it possible for the number of free electrons to be estimated and scattering in nanostructures to be investigated.
Conclusions. It was shown that Langmuir shielding can be observed in the given energy range in the IR region of the spectrum. The calculated values correlate well with the experimental data.

Keywords: magnetorefractive effect, giant magnetoresistance, ferromagnet, nanostructures

• **Submitted:** 09.07.2023 • **Revised:** 06.10.2023 • **Accepted:** 12.02.2024

For citation: Yurasov A.N., Sayfullina D.A., Bakhvalova T.N. Magnetorefractive effect in metallic Co/Pt nanostructures. *Russ. Technol. J.* 2024;12(2):57–66. https://doi.org/10.32362/2500-316X-2024-12-2-57-66

Financial disclosure: The authors have no a financial or property interest in any material or method mentioned.

The authors declare no conflicts of interest.

НАУЧНАЯ СТАТЬЯ

Магниторефрактивный эффект в металлических наноструктурах Co/Pt

А.Н. Юрасов @,
Д.А. Сайфулина,
Т.Н. Бахвалова

МИРЭА – Российский технологический университет, Москва, 119454 Россия
@ Автор для переписки, e-mail: alexey_yurasov@mail.ru

Резюме

Цели. Теоретически исследовать особенности магниторефрактивного эффекта для наноструктур типа металл – металл на примере многослойных наноструктур Co/Pt (ферромагнитный металл – парамагнитный металл) с разным соотношением ферромагнитной и парамагнитной фаз в видимой и ближней инфракрасной (ИК) областях спектра.

Методы. С помощью основных формул для диэлектрической проницаемости, оптической проводимости, коэффициентов рефракции и экстинкции, выявлена и выражена в явном виде связь магниторефрактивного эффекта с эффектом гигантского магнитосопротивления (магниторезистивным эффектом), что подтверждает общую природу этих двух эффектов. С помощью формул Френеля для трехслойной структуры рассчитан магниторефрактивный эффект для s-поляризации света с учетом толщины образцов и влияния подложки. Для расчета диэлектрической проницаемости материалов применялись методы эффективной среды. Так как исследовался средний диапазон концентраций кобальта, то для нахождения эффективных диэлектрических проницаемостей наноструктур применялось приближение Бруггемана. Для всех наноструктур рассчитывался коэффициент отражения при нормальном падении.

Результаты. Благодаря тому, что диэлектрическая проницаемость неоднородных образцов была заменена общим эффективным параметром, зависящим от диэлектрической проницаемости каждого компонента, мы смогли применить теорию Друде – Лоренца для проводников в высокочастотном переменном поле и оценить параметры электронной структуры исследуемых образцов. Были рассчитаны значения плазменной и релаксационной частот для каждого образца. Это позволило оценить число свободных электронов и исследовать рассеяние в наноструктурах.

Выводы. Было показано, что в исследуемом диапазоне энергий в ИК-области спектра наблюдается ленгмюровская экранировка. Рассчитанные значения хорошо соотносятся с экспериментальными данными.

Ключевые слова: магниторефрактивный эффект, гигантское магнитосопротивление, ферромагнетик, наноструктуры

• **Поступила:** 09.07.2023 • **Доработана:** 06.10.2023 • **Принята к опубликованию:** 12.02.2024

Для цитирования: Юрасов А.Н., Сайфулина Д.А., Бахвалова Т.Н. Магниторефрактивный эффект в металлических наноструктурах Co/Pt. *Russ. Technol. J.* 2024;12(2):57–66. https://doi.org/10.32362/2500-316X-2024-12-2-57-66

Прозрачность финансовой деятельности: Авторы не имеют финансовой заинтересованности в представленных материалах или методах.

Авторы заявляют об отсутствии конфликта интересов.

INTRODUCTION

Heterogeneous metallic magnetic materials exhibit a giant magnetoresistance effect (GMR), associated with a change in the conductivity of the nanostructure, and depending on the mutual location of the magnetic moment vectors of the ferromagnetic regions. Such a change in the properties of matter must inevitably have an optical response correlated with the GMR. Such an effect, called the magnetorefractive effect (MRE), can indeed be observed in metallic nanostructures and consists of a change in the reflection, transmission, and absorption coefficients of an electromagnetic wave under the influence of a magnetic field [1–4]. This is based on spin-dependent scattering, as well as on the GMR effect. As a rule, magneto-optical effects are related to a change in the non-diagonal component of the dielectric permittivity tensor (DPT) under the action of a magnetic field, However, the MRE is an exception in this respect, since it is not a direct consequence of the effect of a magnetic field on a substance. It is not directly caused by the spin-orbit interaction, but is even in magnetization and is associated primarily with the diagonal part of the DPT and magnetoresistance [5, 6].

METHODOLOGY AND STUDIED STRUCTURES

Co/Pt nanostructures [7–9] with a different volume concentration of cobalt were chosen for the MRE study. Platinum in pure form is a classical paramagnetic with a high level of stability of properties and temperature stability. It also possesses environmental inertness, corrosion resistance and good optical and conducting properties. In turn, cobalt is one of the most important ferromagnetics with significant spontaneous magnetization and a relatively high Curie temperature. This element finds broad practical application due to its high magneto-optical activity. Nanostructures based on cobalt and platinum have a good combination of mechanical strength, conductivity and magneto-optical properties. In addition, their fabrication process is relatively simple. As the amount of cobalt in the nanostructure increases, there is a transition from the paramagnetic state to the ferromagnetic state, the so-called concentration phase transition. This is accompanied by an increase in the conductivity of the structure. The type of magnetic ordering is usually determined using the Stoner criterion [10].

This work considers Co/Pt nanostructures with a volume concentration of cobalt from 0.3 to 0.6 in the energy range of 0.54–3.3 eV of incident electromagnetic waves. These nanostructures can be considered as quasi-uniform. It is thus reasonable to use the effective medium theory, in order to calculate their dielectric permittivity. Thus, knowing the dielectric permittivities of cobalt and platinum, the effective medium methods can be used to calculate their total effective dielectric permittivity for all bulk concentrations. Since concentrations close to the mean are being considered, it is best to use the Bruggeman approximation (effective medium approximation) for the calculations. This model does not take into account dimensional effects and the influence of interfaces. So, the formulas [11] required modification, in order to improve the accuracy of calculations. The obtained dependencies of the real and imaginary parts of the dielectric permittivity are shown in Fig. 1.

These graphs clearly show that in the infrared (IR) region of the spectrum, the functions of the real and imaginary components of the dielectric permittivity resemble a hyperbolic dependence on frequency (Drudean character of the dependence). Within the framework of this model, the resulting samples with effective dielectric permittivity can be considered homogeneous. Moreover, they can also be considered in terms of the Drude–Lorentz conduction theory. This means that the electrons in the samples are considered a classical gas of non-interacting particles moving freely in the ion lattice with some average velocity. In this case, the frequency of collisions with the lattice and the mass of electrons do not depend on their velocity, and the collisions themselves are absolutely elastic. As can be seen from the graph in Fig. 1, this model works best in the IR region of the spectrum.

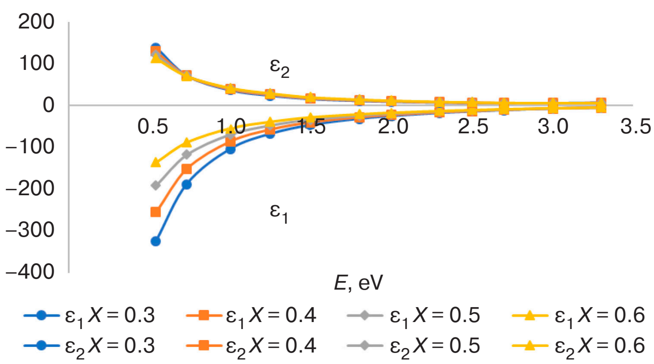

Fig. 1. Spectral dependencies of the real (ε_1) and imaginary (ε_2) parts of the complex dielectric permittivity for different volume concentrations of cobalt *X*. *E* is electromagnetic wave energy, eV

In this case dielectric permittivity is equal to:

$$\varepsilon(\omega)=\varepsilon_1-i\varepsilon_2=1-\frac{\omega_p^2}{\omega^2+i\omega\gamma_{rel}}=1-\frac{\omega_p^2}{\omega}\cdot\frac{(\omega-i\gamma_{rel})}{\omega^2+\gamma_{rel}^2}=$$
$$=1-\frac{\omega_p^2}{\omega^2+\gamma_{rel}^2}+i\frac{\gamma_{rel}}{\omega}\cdot\frac{\omega_p^2}{\omega^2+\gamma_{rel}^2}, \quad (1)$$

where ω_p is the plasma frequency, and γ_{rel} is the relaxation frequency. These are parameters of conduction electrons characterizing the number of free electrons and their scattering.

Knowing the real part of the effective dielectric permittivity, using formula (2), the parameters of conduction electrons can be estimated. These are the effective values of the plasma ω_p and relaxation γ_{rel} frequencies, as well as the relaxation time τ_{rel} (a value inverse to the relaxation frequency) [12].

$$\frac{1}{1-\varepsilon_1} = \left(\frac{\omega}{\omega_p}\right)^2 + \left(\frac{\gamma_{rel}}{\omega_p}\right)^2. \quad (2)$$

The results of the calculations of plasma and relaxation frequencies and relaxation times are summarized in the table below.

For clarity, the dependence of the plasma frequency (in eV) on the cobalt concentration X is plotted in Fig. 2.

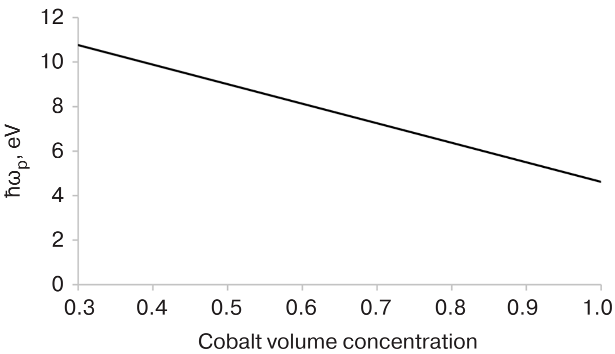

Fig. 2. Dependence of the plasma frequency $\hbar\omega_p$ ($\hbar$ is the reduced Planck constant) on the cobalt volume concentration X

The calculated value of the plasma frequency of pure cobalt $\hbar\omega_p \approx 4.46$ eV is larger than the real value of 3.69 eV. This may be due to the unaccounted influence of interzone transitions and the different contribution to the plasma frequency of electrons with spin up and spin down. The plasma frequency of pure platinum is about twice that of the plasma frequency of cobalt. This means that when the concentration of cobalt in the nanostructure increases, the plasma frequency decreases [13]. Consequently, the number of free electrons in the effective medium also decreases. The plasma frequency from concentration varies uniformly without sharp jumps. Thus, phase transition begins at lower concentrations of cobalt, meaning that all the nanostructures under consideration have ferromagnetic order.

The electromagnetic wave range being studied herein lies between the relaxation frequency and the plasma frequency $\gamma_{rel} < \omega < \omega_p$. Langmuir shielding can be observed in this region. Since the radiation frequency is larger than the relaxation (collision) frequency, the field has time to change many times during the relaxation time equal to $1/\gamma_{rel.}$. The electrons tend to compensate for the effects of the electromagnetic wave, in such a way that the field barely penetrates, although the level of attenuation is very small. Due to the reflected wave, the reflection coefficient R is close to unity. However, near the plasma frequency it decreases since the depth of Langmuir shielding begins to depend on the frequency (Fig. 3).

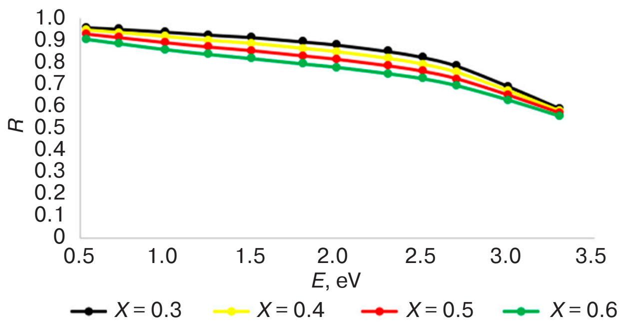

Fig. 3. Spectral dependencies of the reflection coefficient at normal incidence for different cobalt concentrations

The higher the cobalt concentration, the lower the reflection coefficient. In the ultraviolet (UV) region of the spectrum, the optical conductivity of the metallic nanostructure decreases significantly. This in turn affects the refraction coefficients n and extinction k, and hence the reflection coefficient R. In addition to the fact that the values of n and k are decreasing, the ratio between them also changes. In the near-IR and visible regions of the spectrum, $k \gg n$, but also when approaching the UV region, their values gradually equalize.

Table. Results of plasma frequency and relaxation time calculations

X	$\left(\frac{1}{\omega_p}\right)^2, \frac{1}{s^2}$	$\omega_p \cdot 10^{16}, \frac{1}{s}$	$\left(\frac{\gamma_{rel}}{\omega_p}\right)^2, \frac{1}{s^2}$	$\gamma_{rel} \cdot 10^{16}, \frac{1}{s}$	$\tau_{rel} \cdot 10^{-16}$, s
0.3	$0.39 \cdot 10^{-32}$	1.60	0.001	0.04	27.87
0.4	$0.45 \cdot 10^{-32}$	1.49	0.001	0.05	21.19
0.5	$0.52 \cdot 10^{-32}$	1.38	0.002	0.06	16.57
0.6	$0.61 \cdot 10^{-32}$	1.28	0.004	0.07	13.00

The real and imaginary parts of dielectric permittivity are equal to:

$$\varepsilon_1(\omega) = n^2 - k^2, \qquad (3)$$

$$\varepsilon_2(\omega) = 2nk. \qquad (4)$$

Optical conductivity σ_{opt} is equal to:

$$\sigma_{opt}(\omega) = \frac{Ne^2}{m\gamma_{rel}\left(1+\left(\frac{\omega}{\gamma_{rel}}\right)^2\right)^2} = \frac{1}{\rho}, \qquad (5)$$

where m is the mass of an electron, N is the number of electrons, e is the charge of an electron, ρ is the electrical resistance.

The imaginary part of the diagonal component Im ε of the DPT is related to the optical conductivity of the metal σ_{opt}:

$$\sigma_{opt}(\omega) = \frac{\omega}{4\pi}\operatorname{Im}\varepsilon(\omega) = \frac{\omega}{2\pi}nk. \qquad (6)$$

When an alloy with GMR is magnetized, the optical conductivity changes in accordance with the change in magnetoresistance. The change in optical conductivity can be expressed through the magnetoresistive effect [14]:

$$\sigma_{opt}(\omega) = \frac{1}{\rho_0} - \frac{1}{\rho_H} = \frac{\Delta\rho}{\rho_0^2\left(1-\frac{\Delta\rho}{\rho_0}\right)} = \frac{\frac{\Delta\rho}{\rho_0}}{\left(1-\frac{\Delta\rho}{\rho_0}\right)}\sigma, \qquad (7)$$

where $\Delta\sigma_{opt}$ is the magnetic conductivity, ρ_H is the electrical resistance in a magnetic field, ρ_0 is the electrical resistance without a magnetic field, and $\Delta\rho/\rho_0$ is the magnetoresistance of the material.

Using formulas (3), (4), and (6) in a magnetic field, by replacing the refraction and extinction coefficients by $n_H = n + \Delta n$ and $k_H = k + \Delta k$, we can calculate Δn and Δk through $\Delta\sigma_{opt}$. In this case, the product $\Delta n \cdot \Delta k$ can be neglected as a value of the second order of smallness.

$$\Delta n = \frac{2\pi\Delta\sigma}{\omega}\left(\frac{n+k}{n^2+k^2}\right), \qquad (8)$$

$$\Delta k = \frac{2\pi\Delta\sigma}{\omega}\left(\frac{n-k}{n^2+k^2}\right). \qquad (9)$$

Thus, considering formulas (7)–(9), the MRE can be estimated using optical parameters and magnetoresistive effect parameter [11].

MRE on reflection at normal incidence is calculated using the following formula:

$$\frac{\Delta R}{R} = \frac{R_0 - R_H}{R_0}, \qquad (10)$$

where R_H and R_0 are the light reflection coefficients of the sample in the magnetic field and without the field, respectively.

MAIN RESULTS AND DISCUSSION

In Fig. 4, the spectral dependencies of the MRE parameter at different cobalt concentrations for the magnetoresistive effect $\frac{\Delta\rho}{\rho} = 1\%, 5\%, 10\%$ are plotted.

MRE has a negative value. This means that the reflection coefficient of the nanostructure increases in the magnetic field. The effect is more noticeable the larger the magnetoresistive effect and the higher the cobalt concentration. This means that the MRE is very sensitive to changes in the microstructure, which affects its conductivity. The MRE parameter takes the highest value in the low frequency region close to the relaxation frequency [15–18].

Now let us calculate the MRE parameter at an arbitrary angle of incidence using the 30° angle as an example, using the Fresnel equations for s-polarization. Let us represent the nanostructures under consideration as films deposited on a silicon substrate. Then the samples can be considered as three-layer air-Co/Pt-Si structures.

This model will be closer to real samples on a silicon substrate. The reflection coefficient of the s-component for the whole three-layer structure jki is equal to [17]:

$$R_s = \left|\frac{r_{jk} + F_k^2 r_{ki}}{1 + F_k^2 r_{jk} r_{ki}}\right|^2, \qquad (11)$$

where $F_k = e^{\frac{-2\pi g_k d_k}{\lambda}}$ is the phase multiplier in the kth layer, $g_i = \sqrt{n_j^2 - n_i^2 \sin^2\varphi}$ is the parameter for convenient calculation of reflection coefficients at the interfaces, $r_{jk} = \frac{g_j n_j^2 - g_k n_k^2}{g_j n_j^2 + g_k n_k^2}$ is the partial reflection and transmission coefficient at the interface of j–k media, φ is the angle of incidence of light from the first medium, and d_k is the thickness of the corresponding medium.

In Fig. 5, the spectral dependencies of the MRE parameter with regard to the angle of incidence, substrate influence and thickness at different cobalt concentrations for the magnetoresistive effect are plotted: $\frac{\Delta\rho}{\rho} = 1\%, 5\%, 10\%$.

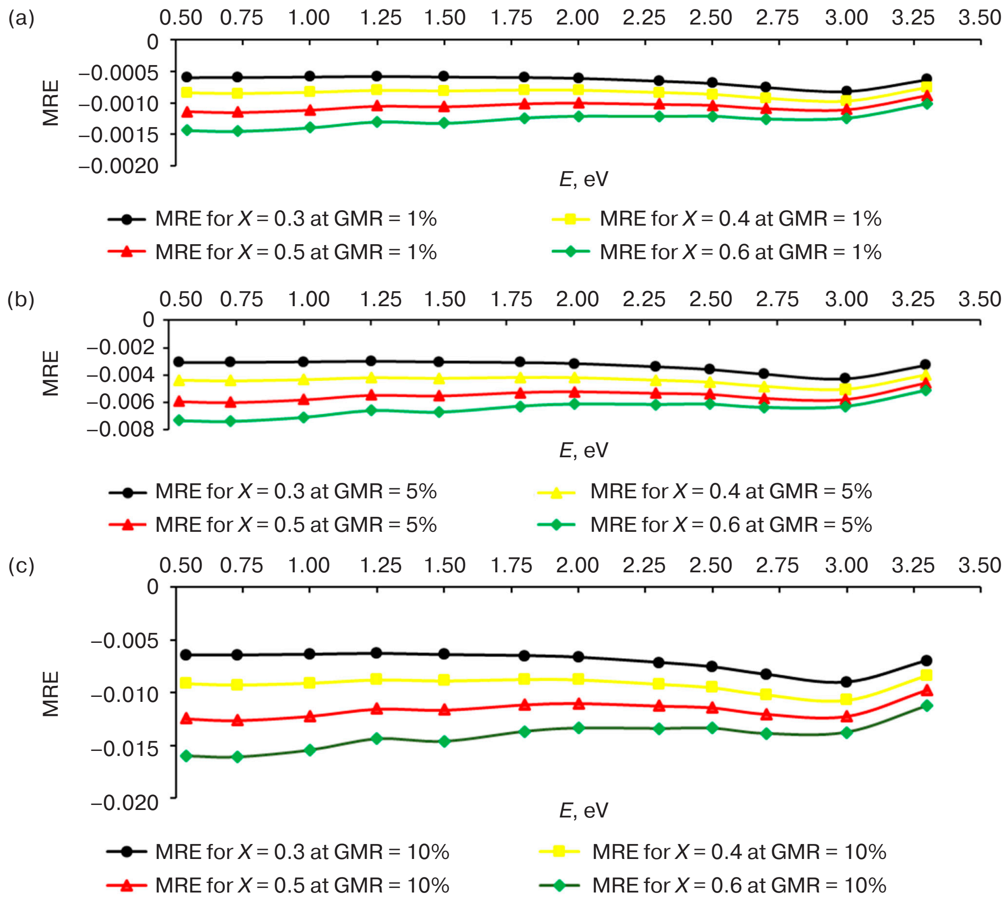

Fig. 4. MRE spectral dependencies for different cobalt concentrations at different GMR values: (a) 1%, (b) 5%, (c) 10%

Experimental data of the MRE parameter for the Si/Ta(2)/$Co_{50}Pt_{50}$(4.6)/Ta(2) nanostructure, where Ta is the buffer layer (Fig. 6), are plotted for comparison in the graphs (Fig. 5). The experimental curve lies roughly between the plots for $X = 0.5$ and $X = 0.6$ at GMR = 5%. It is worth considering that the thickness of the kth layer has a noticeable effect on the MRE parameter, since it is under the exponent function. As can be seen from the graph in Fig. 5, the MRE parameter in the IR region of the spectrum increases sharply up to some maximum value. It then gradually decreases. The greater the cobalt concentration, the more strongly this maximum point

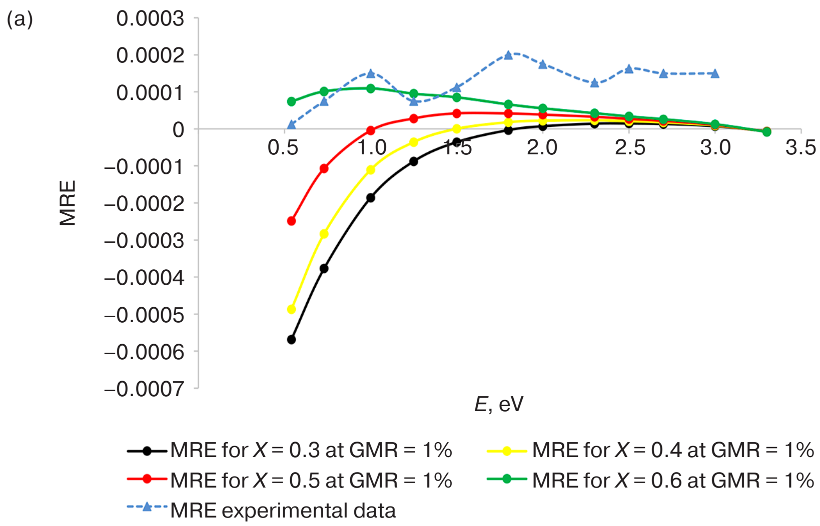

Fig. 5 (***start***). MRE spectral dependencies for different cobalt concentrations at different GMR values for s-polarization and 30° angle of incidence calculated by Fresnel formulas and experimental data for s-polarization, 30° angle of incidence: (a) GMR = 1%, (b) GMR = 5%, (c) GMR = 10%

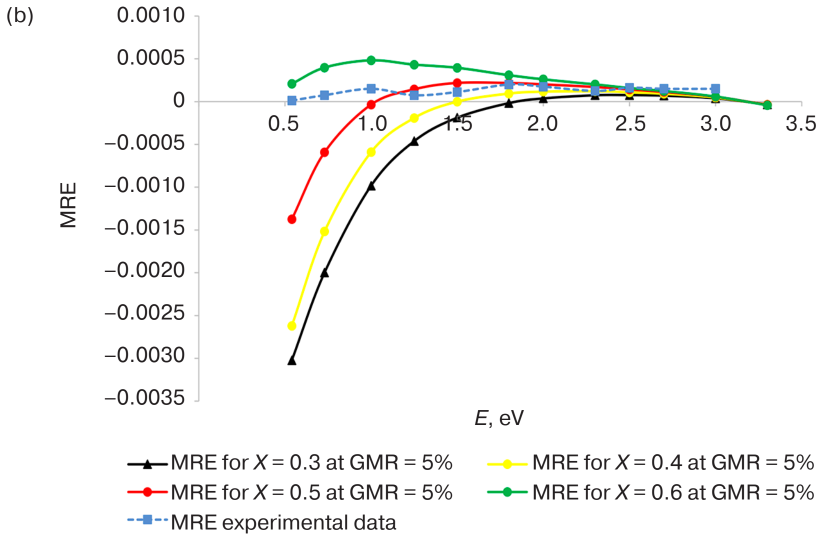

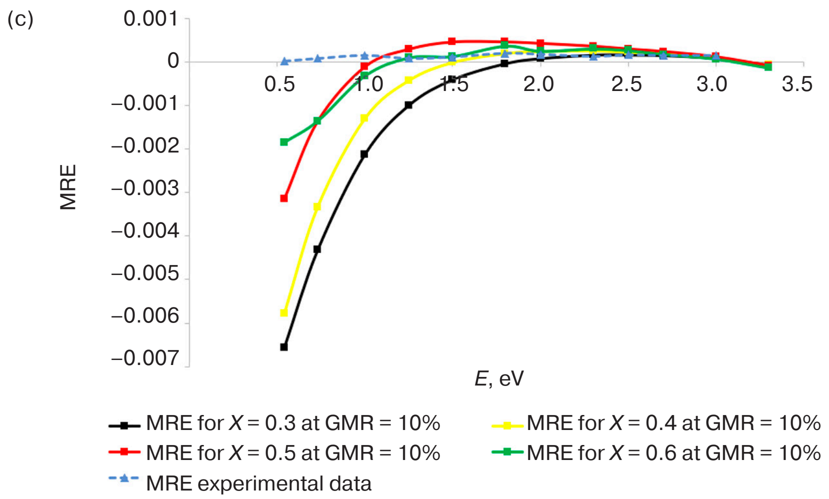

Fig. 5 (***end***)**.** MRE spectral dependencies for different cobalt concentrations at different GMR values for s-polarization and 30° angle of incidence calculated by Fresnel formulas and experimental data for s-polarization, 30° angle of incidence: (a) GMR = 1%, (b) GMR = 5%, (c) GMR = 10%

is shifted towards the IR range. At the same time, the greater the concentration of cobalt and HMS, the more pronounced the oscillations of the MRE parameter. The sign of the effect parameter changes. This means that after some value of the emission frequency, the reflection coefficient in the magnetic field decreases. At GMR 10%, the MRE parameter for cobalt concentration 0.5 at some frequencies slightly exceeds the MRE parameter for concentration 0.6.

At high frequencies, the concentration of cobalt has practically no effect on the MRE, which itself is very small. This correlates well with the data in Fig. 1. The values of the real and imaginary components of the dielectric permittivity for all samples also converge at high frequencies. At an electromagnetic wave energy of about 2 eV, there is no special difference between samples with $X = 0.3$ and 0.6. This does not coincide with the experimental data, since the experimental curve at high frequencies on the contrary increases. This is

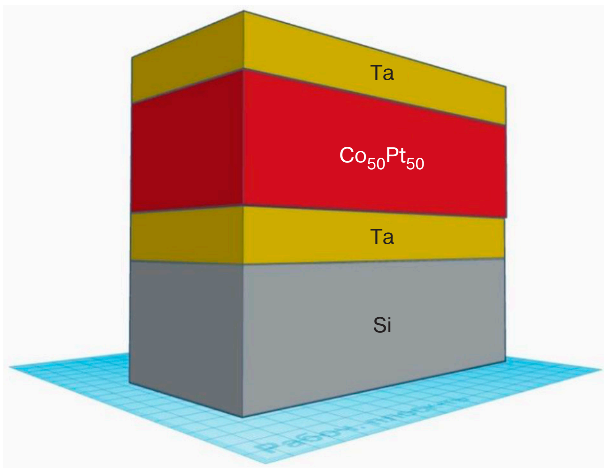

Fig. 6. Schematic representation of heterogeneous layered Si/Ta(2)/$Co_{50}Pt_{50}$(4.6)/Ta(2) nanostructure

because the model considered herein does not describe the effects at high frequencies. All calculations are based on the dielectric permittivity of the nanostructure. Thus, when refining the model, it will be necessary to calculate more accurately the dielectric permittivity of the considered nanostructures at high frequencies [18].

It can be concluded that the model under consideration is best suited for calculating spectra in the IR region. However, it does not take into account the influence of interzone transitions and size effects. The MRE strongly depends on the GMR. The higher the cobalt concentration, the more noticeable this dependence is. This means that it is very sensitive to the microstructure of the sample. The graph in Fig. 5c, it shows the oscillatory character of the dependence of the MRE parameter for the nanostructure with $X = 0.6$. Moreover, unlike the previous graphs, it shows the intersection of the curves with $X = 0.5$ and 0.6 in the IR region of the spectrum. At some frequencies the curve 0.5 is higher than the curve 0.6.

CONCLUSIONS

This study investigates plasma frequencies, reflection coefficients, and MRE spectra on reflection at normal incidence. The MRE spectra for Co/Pt nanostructures with different cobalt concentrations at an angle of incidence of 30° for s-polarization were calculated. The data obtained for a 30° incidence angle was compared with the experimental data, and a good level of agreement was established. A complete correlation between the MRE and magnetoresistance was explicitly shown. The effect is more noticeable the larger the magnetoresistivity and the higher the cobalt concentration. This means that the MRE is very sensitive to microstructure changes affecting its conductivity. The highest value of the MRE parameter is in the low frequency region, close to the relaxation frequency.

ACKNOWLEDGMENTS

The work was implemented in the scientific structural subdivision "Laboratory of New Functional Materials" of RTU MIREA under the grant FSFZ-2022-0007 of the Ministry of Education and Science of the Russian Federation and with the support of the Ministry of Education and Science of the Russian Federation (State task for universities No. FGFZ-2023-0005).

Authors' contributions

A.N. Yurasov—setting the aims and objectives of the study, discussing and summarizing the results, and drawing conclusions.

D.A. Sayfullina—calculation of the magnetorefractive effect and plotting.

T.N. Bakhvalova—developing the theory of the magnetorefractive effect.

REFERENCES

1. Granovsky A., Sukhorukov Yu., Gan'shina E., Telegin A. Magnetorefractive effect in magnetoresistive materials. In: *Magnetophotonics: From Theory to Applications.* Berlin Heidelberg: Springer; 2013. P. 107–133. http://doi.org/10.1007/978-3-642-35509-7_5
2. Shkurdoda Yu.O., Dekhtyaruk L.V., Basov A.G., Chornous A.M., Shabelnyk Yu.M., Kharchenko A.P., Shabelnyk T.M. The giant magnetoresistance effect in Co/Cu/Co three-layer films. *J. Magn. Magn. Mater*. 2019;477:88–91. https://doi.org/10.1016/j.jmmm.2019.01.040
3. Dekhtyaruk L.V., Kharchenko A.P., Klymenko Yu.O., Shkurdoda Yu.O., Shabelnyk Yu.M., Bezdidko O.V., Chornous A.M. Negative and Positive Effect of Giant Magnetoresistance in The Magnetically Ordered Sandwich. In: *2020 IEEE 10th International Conference Nanomaterials: Applications & Properties* (*NAP*). 2020. P. 01NMM13-1–01NMM13-3. https://doi.org/10.1109/NAP51477.2020.9309694
4. Kelley C.S., Naughton J., Benson E., Bradley R.C., Lazarov V.K., Thompson S.M., Matthew J.A. Investigating the magnetic field-dependent conductivity in magnetite thin films by modelling the magnetorefractive effect. *J. Phys.: Condens. Matter*. 2014;26(3):036002. http://doi.org/10.1088/0953-8984/26/3/036002
5. Lysina E.A., Yurasov A.N. Magneto-optical effects in $CoSiO_2$ nanocomposite. In: *Informatika i tekhnologii. Innovatsionnyye tekhnologii v promyshlennosti i informatike* (*MNTK FTI 2017*) (*Informatics and Technologies. Innovative Technologies in Industry and Informatics*). Moscow: MIREA; 2017. P. 622–628 (in Russ.).
6. Lobov I.D., Kirillova M.M., Makhnev A.A., et al. Magnetooptical, optical, and magnetotransport properties of Co/Cu superlattices with ultrathin cobalt layers. *Phys. Solid State.* 2017;59(1):53–62. https://doi.org/10.1134/S1063783417010206 [Original Russian Text: Lobov I. D. Kirillova M.M., Makhnev A.A., Romashev L.N., Korolev A.V., Milyaev M.A., Proglyado V.V., Bannikova N.S., Ustinov V.V. Magnetooptical, optical, and magnetotransport properties of Co/Cu superlattices with ultrathin cobalt layers. *Fizika Tverdogo Tela*. 2017;59(1):54–62 (in Russ.). https://doi.org/10.21883/FTT.2017.01.43950.161]
7. Oh J., Humbard L., Humbert V., Sklenar J., Mason N. Angular evolution of thickness-related unidirectional magnetoresistance in Co/Pt multilayers. *AIP Advances*. 2019;9(4):045016. https://doi.org/10.1063/1.5079894
8. Kawaguchi M., Towa D., Lau Y.-C., Takahashi S., Hayashi M. Anomalous spin Hall magnetoresistance in Pt/Co bilayers. *Appl. Phys. Lett*. 2018;112(20):202405. https://doi.org/10.1063/1.5021510

9. Heigl M., Wendler R., Haugg S.D., Albrecht M. Magnetic properties of Co/Ni-based multilayers with Pd and Pt insertion layers. *J. Appl. Phys*. 2020;127(23):233902. https://doi.org/10.1063/5.0010112
10. Povzner A.A., Volkov A.G., Filanovich A.N. Electronic structure and magnetic susceptibility of nearly magnetic metals (palladium and platinum). *Phys. Solid State*. 2010;52(10):2012–2018. https://doi.org/10.1134/S1063783410100021
[Original Russian Text: Povzner A.A., Volkov A.G., Filanovich A.N. Electronic structure and magnetic susceptibility of nearly magnetic metals (palladium and platinum). *Fizika Tverdogo Tela*. 2010;52(10):1879–1884 (in Russ.).]
11. Yurasov A.N., Telegin A.V., Bannikova N.S., et al. Features of Magnetorefractive Effect in a $[CoFe/Cu]_n$ Multilayer Metallic Nanostructure. *Phys. Solid State.* 2018;60(2):281–287. https://doi.org/10.1134/S1063783418020300
[Original Russian Text: Yurasov A.N., Telegin A.V., Bannikova N.S., Milyaev M.A., Sukhorukov Yu.P. Features of Magnetorefractive Effect in a $[CoFe/Cu]_n$ Multilayer Metallic Nanostructure. *Fizika Tverdogo Tela*. 2018;60(2):276–282 (in Russ.). https://doi.org/10.21883/FTT.2018.02.45381.201]
12. Lobov I.D., Kirillova M.M., Romashev L.N., et al. Magnetorefractive effect and giant magnetoresistance in Fe(t_x)/Cr superlattices. *Phys. Solid State.* 2009;51(12):2480–2485. https://doi.org/10.1134/S1063783409120099
[Original Russian Text: Lobov I.D., Kirillova M.M., Romashev L.N., Milyaev M.A., Ustinov V.V. Magnetorefractive effect and giant magnetoresistance in Fe(t_x)/Cr superlattices. *Fizika Tverdogo Tela*. 2009;51(12):2337–2341 (in Russ.).]
13. Pogodaeva M.K., Levchenko S.V., Drachev V.P., Gabitov I.R. Optical properties of metals from the first principles. *Photon Express*. 2021;6(174):294–295 (in Russ.).
14. Ustinov V.V., Sukhorukov Yu.P., Milyaev M.A., et al. Magnetotransmission and magnetoreflection in multilayer FeCr nanostructures. *J. Exp. Theor. Phys*. 2009;108(2):260–266. https://doi.org/10.1134/S1063776109020083
[Original Russian Text: Ustinov V.V., Sukhorukov Yu.P., Milyaev M.A., Granovskii A.B., Yurasov A.N., Gan'shina E.A., Telegin A.V. Magnetotransmission and magnetoreflection in multilayer FeCr nanostructures. *Zhurnal Eksperimental'noi i Teoreticheskoi Fiziki*. 2009;135(2):293–300 (in Russ.).]
15. Jacquet J.C., Valet T. A new magnetooptical effect discovered on magnetic multilayers: The magnetorefractive effect. *MRS Online Proceedings Library* (*OPL*). 1995;384:477–490. https://www.doi.org/10.1557/PROC-384-477
16. Kravets V.G. Correlation between the magnetoresistance, IR magnetoreflectance, and spin-dependent characteristics of multilayer magnetic films. *Phys. Res. Int*. 2012;2012(5):323279. https://www.doi.org/10.1155/2012/323279
17. Maevskii V.M. Theory of magneto-optical effects in multilayer systems with arbitrary orientation of magnetization. *Fizika metallov i metallovedenie = Physics of Metals and Metallography)*. 1985;59:213–216 (in Russ.).
18. Yurasov A.N. Magnetorefractive effect in nanostructures. *Pribory = Instruments*. 2022;4(262):22–25 (in Russ.).

СПИСОК ЛИТЕРАТУРЫ

1. Granovsky A., Sukhorukov Yu., Gan'shina E., Telegin A. Magnetorefractive effect in magnetoresistive materials. In: *Magnetophotonics: From Theory to Applications.* Berlin Heidelberg: Springer; 2013. P. 107–133. http://doi.org/10.1007/978-3-642-35509-7_5
2. Shkurdoda Yu.O., Dekhtyaruk L.V., Basov A.G., Chornous A.M., Shabelnyk Yu.M., Kharchenko A.P., Shabelnyk T.M. The giant magnetoresistance effect in Co/Cu/Co three-layer films. *J. Magn. Magn. Mater*. 2019;477:88–91. https://doi.org/10.1016/j.jmmm.2019.01.040
3. Dekhtyaruk L.V., Kharchenko A.P., Klymenko Yu.O., Shkurdoda Yu.O., Shabelnyk Yu.M., Bezdidko O.V., Chornous A.M. Negative and Positive Effect of Giant Magnetoresistance in The Magnetically Ordered Sandwich. In: *2020 IEEE 10th International Conference Nanomaterials: Applications & Properties* (*NAP*). 2020. P. 01NMM13-1–01NMM13-3. https://doi.org/10.1109/NAP51477.2020.9309694
4. Kelley C.S., Naughton J., Benson E., Bradley R.C., Lazarov V.K., Thompson S.M., Matthew J.A. Investigating the magnetic field-dependent conductivity in magnetite thin films by modelling the magnetorefractive effect. *J. Phys.: Condens. Matter*. 2014;26(3):036002. http://doi.org/10.1088/0953-8984/26/3/036002
5. Лысина Е.А., Юрасов А.Н. Магнитооптические эффекты в нанокомпозите $CoSiO_2$. *Информатика и технологии. Инновационные технологии в промышленности и информатике* (*МНТК ФТИ – 2017*). М.: МИРЭА; 2017. С. 622–628.
6. Лобов И.Д., Кириллова М.М., Махнев А.А., Ромашев Л.Н., Королев А.В., Миляев М.А., Проглядо В.В., Банникова Н.С., Устинов В.В. Магнитооптические, оптические и магнитотранспортные свойства сверхрешеток Co/Cu с ультратонкими слоями кобальта. *Физика твердого тела*. 2017;59(1):54–62. https://doi.org/10.21883/FTT.2017.01.43950.161
7. Oh J., Humbard L., Humbert V., Sklenar J., Mason N. Angular evolution of thickness-related unidirectional magnetoresistance in Co/Pt multilayers. *AIP Advances*. 2019;9(4):045016. https://doi.org/10.1063/1.5079894
8. Kawaguchi M., Towa D., Lau Y.-C., Takahashi S., Hayashi M. Anomalous spin Hall magnetoresistance in Pt/Co bilayers. *Appl. Phys. Lett*. 2018;112(20):202405. https://doi.org/10.1063/1.5021510
9. Heigl M., Wendler R., Haugg S.D., Albrecht M. Magnetic properties of Co/Ni-based multilayers with Pd and Pt insertion layers. *J. Appl. Phys*. 2020;127(23):233902. https://doi.org/10.1063/5.0010112
10. Повзнер А.А., Волков А.Г., Филанович А.Н. Электронная структура и магнитная восприимчивость почти магнитных металлов (на примере палладия и платины). *Физика твердого тела*. 2010;52(10):1879–1884.
11. Юрасов А.Н., Телегин А.В, Банникова Н.С., Миляев М.А., Сухоруков Ю.П. Особенности магниторефрактивного эффекта в многослойной металлической наноструктуре $[CoFe/Cu]_n$. *Физика твердого тела*. 2018;60(2):276–282. https://doi.org/10.21883/FTT.2018.02.45381.201

12. Лобов И.Д., Кириллова М.М., Ромашев Л.Н., Миляев М.А., Устинов В.В. Магниторефрактивный эффект и гигантское магнитосопротивление в сверхрешетках Fe(t_x)/Cr. *Физика твердого тела*. 2009;51(12):2337–2341.
13. Погодаева М.К., Левченко С.В., Драчев В.П., Габитов И.Р. Оптические свойства металлов из первых принципов. *Фотон-экспресс*. 2021;6(174):294–295. https://doi.org/10.24412/2308-6920-2021-6-294-295
14. Устинов В.В., Сухоруков Ю.П., Миляев М.А., Грановский А.Б., Юрасов А.Н., Ганьшина Е.А., Телегин А.В. Магнитопропускание и магнитоотражение в многослойных наноструктурах FeCr. *Журнал экспериментальной и теоретической физики*. 2009;135(2):293–300.
15. Jacquet J.C., Valet T. A new magnetooptical effect discovered on magnetic multilayers: The magnetorefractive effect. *MRS Online Proceedings Library* (*OPL*). 1995;384:477–490. https://www.doi.org/10.1557/PROC-384-477
16. Kravets V.G. Correlation between the magnetoresistance, IR magnetoreflectance, and spin-dependent characteristics of multilayer magnetic films. *Phys. Res. Int*. 2012;2012(5):323279. https://www.doi.org/10.1155/2012/323279
17. Маевский В.М. Теория магнетооптических эффектов в многослойных системах с произвольной ориентацией намагниченности. *Физика металлов и металловедение*. 1985;59:213–216.
18. Юрасов А.Н. Магниторефрактивный эффект в наноструктурах. *Приборы*. 2022;4(262):22–25.

About the authors

Alexey N. Yurasov, Dr. Sci. (Phys.-Math.), Professor, Department of Nanoelectronics, Institute for Advanced Technologies and Industrial Programming, MIREA – Russian Technological University (78, Vernadskogo pr., Moscow, 119454 Russia). E-mail: alexey_yurasov@mail.ru. ResearcherID M-3113-2016, Scopus Authors ID 6602974416, RSCI SPIN-code 4259-8885, https://orcid.org/0000-0002-9104-3529

Diana A. Sayfulina, Student, Institute for Advanced Technologies and Industrial Programming, MIREA – Russian Technological University (78, Vernadskogo pr., Moscow, 119454 Russia). E-mail: diana-sayfulina@mail.ru. ResearcherID IQU-6785-2023, RSCI SPIN-code 4397-9205, https://orcid.org/0009-0006-2905-9753

Tatiana N. Bakhvalova, Teacher, Department of Nanoelectronics, Institute for Advanced Technologies and Industrial Programming, MIREA – Russian Technological University (78, Vernadskogo pr., Moscow, 119454 Russia). E-mail: bahvalova@mirea.ru. ResearcherID ITW-2747-2023, Scopus Author ID 35145196400, https://orcid.org/0000-0001-7595-785X

Об авторах

Юрасов Алексей Николаевич, д.ф.-м.н., профессор, профессор кафедры наноэлектроники, Институт перспективных технологий и индустриального программирования ФГБОУ ВО «МИРЭА – Российский технологический университет» (119454, Россия, Москва, пр-т Вернадского, д. 78). E-mail: alexey_yurasov@mail.ru. ResearcherID M-3113-2016, Scopus Authors ID 6602974416, SPIN-код РИНЦ 4259-8885, https://orcid.org/0000-0002-9104-3529

Сайфулина Диана Алексеевна, студент, Институт перспективных технологий и индустриального программирования ФГБОУ ВО «МИРЭА – Российский технологический университет» (119454, Россия, Москва, пр-т Вернадского, д. 78). E-mail: diana-sayfulina@mail.ru. ResearcherID IQU-6785-2023, SPIN-код РИНЦ 4397-9205, https://orcid.org/0009-0006-2905-9753

Бахвалова Татьяна Николаевна, преподаватель, кафедра наноэлектроники, Институт перспективных технологий и индустриального программирования ФГБОУ ВО «МИРЭА – Российский технологический университет» (119454, Россия, Москва, пр-т Вернадского, д. 78). E-mail: bahvalova@mirea.ru. ResearcherID ITW-2747-2023, Scopus Author ID 35145196400, https://orcid.org/0000-0001-7595-785X

Translated from Russian into English by Lyudmila O. Bychkova
Edited for English language and spelling by Dr. David Mossop

Russian Technological Journal. 2024;12(2):67–76 ISSN 2500-316X (Online)

UDC 519.95:621.3
https://doi.org/10.32362/2500-316X-2024-12-2-67-76

RESEARCH ARTICLE

Study of the probabilistic and temporal characteristics of wireless networks using the CSMA/CA access method

Alexander S. Leontyev,
Dmitry V. Zhmatov @

MIREA – Russian Technological University, Moscow, 119454 Russia
@ *Corresponding author, e-mail: zhmatov@mirea.ru*

Abstract
Objectives. The aim of this study is to develop analytical methods to evaluate the probabilistic and temporal characteristics and performance of wireless networks using the CSMA/CA access method. These methods enable the process of selecting rational operating modes to be automated and the impact of collisions in networks implementing the 802.11 protocols to be reduced.
Methods. The methods employed herein include reliability theory, theory of random processes, queuing theory, and the Laplace–Stieltjes transform.
Results. A problem statement is presented and developed, along with an analytical method for evaluating the probabilistic and temporal characteristics and performance of wireless networks using the CSMA/CA access method. This method considers time constraints on information transmission, thus expanding the applicability of previously proposed analytical approaches for studying Ethernet local area networks. The analysis of networks that use the CSMA/CA access method was carried out. An original mathematical model was developed that allows evaluating various characteristics of packet transmission processes in wireless networks under time constraints on the transmission. These characteristics include latency, packet transfer time, node load, and network performance. A software package was developed to simplify the analysis and evaluation of various operation modes of wireless networks using the CSMA/CA access method.
Conclusions. We demonstrate the need for developing nested analytical models describing packet transmission processes in wireless networks under time constraints on link-layer transmission. This implies the development of more complex models for more exact description of packet transmission processes in such networks. The software package developed herein enables the various options for the functioning of the network to be studied and analytical calculations to be performed. Calculations were carried out, in order to assess the probabilistic and temporal characteristics of packet transmission processes and the wireless network performance. The research involved varying the number of workstations and the intensity of packet flows entering the network nodes under the time constraint on packet transmission. The application of the developed mathematical models will be useful in creating and optimizing wireless networks such as Wi-Fi networks, networks based on the IEEE 802.11 standard, and other data transmission systems using the CSMA/CA access method. Such models and the analysis based on them will be useful in optimizing network performance, adjusting parameters, as well as selecting the capacity and configuration of wireless networks.

Keywords: analytical method, mathematical model, wireless networks, jam packets, CSMA/CA, 802.11 standard, temporal characteristics

• **Submitted:** 29.06.2023 • **Revised:** 10.10.2023 • **Accepted:** 12.02.2024

For citation: Leontyev A.S., Zhmatov D.V. Study of the probabilistic and temporal characteristics of wireless networks using the CSMA/CA access method. *Russ. Technol. J.* 2024;12(2):67–76. https://doi.org/10.32362/2500-316X-2024-12-2-67-76

Financial disclosure: The authors have no a financial or property interest in any material or method mentioned.

The authors declare no conflicts of interest.

НАУЧНАЯ СТАТЬЯ

Исследование вероятностно-временных характеристик беспроводных сетей с методом доступа CSMA/CA

А.С. Леонтьев,
Д.В. Жматов @

МИРЭА – Российский технологический университет, Москва, 119454 Россия
@ Автор для переписки, e-mail: zhmatov@mirea.ru

Резюме
Цели. Целью статьи является разработка аналитических методов оценки вероятностно-временных характеристик и производительности беспроводных сетей с методом доступа CSMA/CA, позволяющих автоматизировать процессы выбора рациональных режимов работы и снизить влияние наложений в сетях, реализующих протоколы 802.11.
Методы. Использованы методы теории надежности, теории случайных процессов и теории массового обслуживания, преобразование Лапласа – Стилтьеса.
Результаты. Разработан аналитический метод оценки вероятностно-временных характеристик и производительности беспроводных сетей с методом доступа CSMA/CA с учетом ограничений на время передачи информации. Метод расширяет область применимости аналитических подходов, предложенных ранее для исследования локальных сетей Ethernet. Проведен анализ сетей, которые используют метод доступа CSMA/CA. Разработана оригинальная математическая модель, позволяющая оценить различные характеристики процессов передачи пакетов в беспроводных сетях при ограничениях на время передачи. Эти характеристики включают время ожидания, время передачи пакетов, загрузку узлов и производительность сети. Для упрощения анализа и оценки различных режимов работы беспроводных сетей с методом доступа CSMA/CA был разработан программный комплекс.
Выводы. Показана необходимость первоочередной разработки вложенных аналитических моделей, описывающих процессы передачи пакетов в беспроводных сетях при ограничениях на время передачи информации на канальном уровне. Это означает, что для более точного описания процессов передачи пакетов в таких сетях требуется создание более сложных моделей. Разработанный программный комплекс позволяет изучать различные варианты функционирования сети и проводить аналитические расчеты. Были проведены расчеты для оценки вероятностно-временных характеристик процессов передачи пакетов и производительности беспроводной сети. Исследования включали изменение количества рабочих станций и интенсивности потоков пакетов, поступающих в узлы сети, при ограничении времени передачи пакетов. Применение разработанных математических моделей может быть полезным при создании и оптимизации беспроводных сетей, таких как Wi-Fi-сети, сети связи на основе стандарта IEEE 802.11 и другие системы передачи данных с использованием метода доступа CSMA/CA. Такие модели и анализ на их основе различных режимов функционирования беспроводных сетей могут помочь в оптимизации производительности сетей, настройке параметров, а также при выборе емкости и конфигурации беспроводных сетей.

Ключевые слова: аналитический метод, математическая модель, беспроводные сети, jam-пакеты, CSMA/CA, стандарт 802.11, временные характеристики

• **Поступила:** 29.06.2023 • **Доработана:** 10.10.2023 • **Принята к опубликованию:** 12.02.2024

Для цитирования: Леонтьев А.С., Жматов Д.В. Исследование вероятностно-временных характеристик беспроводных сетей с методом доступа CSMA/CA. *Russ. Technol. J.* 2024;12(2):67–76. https://doi.org/10.32362/2500-316X-2024-12-2-67-76

Прозрачность финансовой деятельности: Авторы не имеют финансовой заинтересованности в представленных материалах или методах.

Авторы заявляют об отсутствии конфликта интересов.

INTRODUCTION

The search for new ways of improving the performance of wireless local area network (WLAN) is driven by the dramatic increase in the number of Wi-Fi enabled devices, as well as by the intense growing demand.

In order to achieve a high quality of streaming, WLAN uses a common physical medium to exchange data between active devices. An important challenge in WLAN is to control access to the physical medium. In the most common Wi-Fi networks, the medium access station uses carrier sensing multiple access with collision avoidance (CSMA/CA). The use of a portion of the network bandwidth for CSMA/CA implementation reduces network bandwidth for subscriber traffic, thus negatively impacting wireless network performance.

The methods used to access the physical medium of wireless networks play an important role in the operation of the medium access control (MAC) sublayer. Access to the WLAN physical medium is governed by the IEEE 802.11 standard[1]. The most widely used MAC address is based on the CSMA/CA scheme. The scheme provides competitive access to the physical medium.

In early IEEE 802.11 versions, the CSMA/CA mechanism is implemented as a distributed coordination function which provides equal access to all nodes in the network.

In addition, in AP-centric networks, the IEEE 802.11 standard implements a point coordination function which provides centralized access to the physical medium. The distributed coordination function does not maintain the quality of service (QoS).

In general terms, higher priority frames have more chance of being transmitted, while the channel load is reduced. There have been many studies aimed at improving the performance of the MAC sublayer using different techniques and approaches. While most of them focus on ensuring the transmission of different types of traffic, the impact of different ratios of traffic types on network performance has not yet been studied. Knowing this would enable the development of specialized algorithms for improving the information transmission in wireless networks.

The MAC sublayer is oriented towards specific ratios of traffic types in each particular application.

The development of mathematical methods to estimate node load, transmission medium, time characteristics, and performance of local and wireless networks allows the design process [1, 2] to be automated, thus resulting in improved network efficiency. Modern network technologies and protocols are described in [3, 4].

The main research techniques of multimachine computing systems and local networks include methods based on the reliability theory [5–7], queuing theory, and simulation modeling [8–15]. Known analytical research techniques do not consider directive constraints on the packet transmission time in wireless networks. For the CSMA/CA access method, certain ratios of the "transmission rate/frame size" and "network size/frame size" parameters need to be maintained.

This paper presents an original analytical model for evaluating the probabilistic and temporal characteristics and performance of wireless networks with CSMA/CA access method under directive constraints on the information transmission time. It thus develops the well-known analytical research techniques for Ethernet networks [16].

1. CHARACTERIZING THE CSMA/CA ACCESS METHOD

The probability of data transmission error is much higher in a wireless medium rather than in a wired medium. The transmitted signal strength is much higher than that of the received signal. The operating range of transmitters is limited in this case, so not all the computers on the Wi-Fi network are able to receive the transmitted data. This results in a number of problems. The most prominent of these are hidden and

[1] IEEE 802.11 is a set of communication standards for communication in the wireless local area networking frequency bands of 2.4, 3.6, and 5 GHz.

exposed terminal problems [11, 12]. In the Ethernet network, the carrier senses multiple access using the collision detection or CSMA/CD access method, since conflicts are relatively cheap. They are detected almost immediately, and computers stop the transmission at once [4]. In Wi-Fi wireless networks, the carrier senses multiple access using the conflict avoidance or CSMA/CA access method, since collisions are very expensive [9, 10]. In [11, 12], modern data transmission technologies and prospects for their development are considered.

The CSMA/CA access method is most often used in wireless networks in which operation at the physical layer is described by the ISO/OSI (International Organization for Standardization / Open Systems Interconnection) model and 802.11 standard. In particular, the IEEE 802.11x, 802.11ac, 802.11ax, and 802.11be communication standards are used in high-speed Wi-Fi networks [16]. The CSMA/CA method demonstrates a high level of efficiency in compact wireless networks with a small number of nodes.

With an increasing number of workstations and workload, a dramatic decrease in the efficiency of the wireless network can be observed. These two factors inevitably increase the number of conflicts and result in more time spent on resolving them. Unlike methods for studying cable or fiber-optic local area networks [16], analytical methods used in studying probabilistic and temporal characteristics of wireless networks are not sufficiently developed. When developing models based on simulation techniques [13, 14] it can be cumbersome and time-consuming to achieve reliable results in the entire research area of CSMA/CA-enabled transport medium and network node load. This is because the number of conflicts is highly dependent on the load. In addition, this model is nested with respect to models used to estimate the probabilistic and temporal characteristics of information processes in the distributed computing system. Thus, calculations require its multiple use, dramatically increasing the time required for study.

Networks which implement 802.11 protocols require analytical methods for evaluating probabilistic and temporal characteristics to be developed. They also require the implementation of wireless networks with CSMA/CA access method, thus allowing the processes of selecting rational operating modes to be automated and the impact of collisions to be reduced. These factors represent both relevant and indisputable novelty.

2. PROBLEM STATEMENT

Given:

1. The transmitting medium of wireless network is ether.
2. Access to the transmitting medium is CSMA/CA.
3. The number of nodes in the wireless network is N.
4. Placement of nodes. The main characteristic: the distance between the nodes in the network is L_{ik}, m, (i and k are node numbers).
5. Bandwidth is c, Mbit/s.
6. Signal propagation speed is V_c, m/s.
7. Delay in the jampack retransmission when conflicts are detected is τ, s.
8. Jampack size is L_{jam}, bit.
9. Delay in receiving confirmation for the transmitted jampack is Δt_{jam}, s.
10. Info pack length is L_{pack}, bits.
11. Directive time of the info pack transmission is $T_{dir}^{(1)}$, s.
12. Streams of packs coming to the wireless network nodes is λ_k, pack/s $(k = \overline{1, N})$.
13. Interframe interval is Δt, s.

To be defined:

1. $T_k^{(1)}$ is the delivery time of info packs $(k = \overline{1, N})$.
2. Q_k is probability of the info pack on-time delivery $(k = \overline{1, N})$.
3. λ_{sum} is network performance.
4. Load of nodes and transmission medium of wireless network.

The wireless network performance is defined as the total intensity of the on-time served stream.

3. MATHEMATICAL MODEL OF THE METHOD FOR EVALUATING WIRELESS NETWORK CHARACTERISTICS

The problem is resolved under the assumption of the Poisson nature of streams λ_k $(k = \overline{1, N})$, coming to the wireless network nodes for service.

When transmitting a jampack from the kth node, a conflict occurs if node i starts transmitting a jampack in the interval (0, T_{ik}], or node i starts transmitting a jampack in the interval [$-T_{ik}$, 0), as follows:

$$\{T_{ik} = L_{ik} / V_c,\ i = \overline{1, N},\ i \neq k\}.$$

The probability that node i will not start transmission in the interval $2T_{ik}$ with a Poisson stream of packets arriving at the nodes of the network is determined by ratio $e^{-\lambda_i 2T_{ik}}$.

Then the probability that the transmission of a jampack from the kth node will not cause conflicts with jampacks transmitted from other nodes in the network can be evaluated using the following formula:

$$g_k = \prod_{i=1, i \neq k}^{N} e^{-\lambda_i 2T_{ik}},\ k = \overline{1, N}. \tag{1}$$

Let $P_k^*(s) = \int_0^\infty e^{-st} dP_k(t)$ be the Laplace–Stieltjes transform of the distribution function $P_k(t)$ of the packet transmission time from the kth node allowing for emerging conflicts, and let s be a complex parameter. $P_k^*(s)$ is defined by the following expression:

$$P_k^*(s) = \sum_{n=1}^{\infty} \left\{ P_n (X^*(s))^{n-1} \cdot (V_k^*(s))^{n-1} F^*(s) \right\}, \quad (2)$$

where $P_n = (1-g_k)^{n-1} g_k$ is the probability that the packet will be transmitted in exactly n attempts (when transmitting jampack, conflicts will occur n – 1 times); $F^*(s) = \int_0^\infty e^{-st} dF(t)$, $F(t)$ is the dependence of the transmission time of a data pack with jampack without overlay. $X^*(s) = \int_0^\infty e^{-st} dX(t)$, $X(t)$ is the distribution function of random delay in the jampack retransmission, in the event of conflict (overlay of jampacks from different nodes of the network); while $V_k^*(s) = \int_0^\infty e^{-st} dV_k(t)$, $V_k(t)$ is the dependence of the jampack transmission time and delay in confirmation transmission on the transmitted jampack from the kth node in case of conflict.

Then

$$P_k^*(s) = \sum_{n=1}^{\infty} (1-g_k)^{n-1} g_k (X^*(s))^{n-1} \times \times (V_k^*(s))^{n-1} F^*(s) = g_k F^*(s) \frac{1}{1-(1-g_k) X^*(s) V_k^*(s)} \quad (3)$$

Considering the properties of the Laplace–Stieltjes transform [16], expressions for moments $P_k^{(1)}$ and $P_k^{(2)}$ of distribution function $P_k(t)$ are easily obtained using differentiating expression (3) by s.

The methods for calculating the moments of distribution function $V_k(t)$ and $X(t)$ together with the necessary calculation formulas to evaluate the load of the transmission medium and network nodes are presented in [16].

The moments of distribution function $G_k(t)$ of the service time for a packet arriving at the kth node of the network are determined by the following formula:

$$G_k^{(1)} = P_k^{(1)} + W_k^{(1)}, \ G_k^{(2)} = P_k^{(2)} + 2P_k^{(1)} W_k^{(1)} + W_k^{(2)}, \quad (4)$$

wherein $W_k^{(1)}$ and $W_k^{(2)}$ are the moments of distribution function $W_k(t)$ of the waiting time for starting the packet transmission when it arrives at the free kth node of the wireless network [16].

Considering the Poisson character of packet streams arriving to the network nodes, the average waiting time of packets in the queue for service in the kth node $W_{\exp k}^{(1)}$ is determined by the Pollaczek–Khinchine formula [10], as follows:

$$W_{\exp k}^{(1)} = \frac{1}{2} \cdot \frac{\lambda_k G_k^{(2)}}{1 - \lambda_k G_k^{(1)}}. \quad (5)$$

The average packet service time $T_k^{(1)}$ allowing for the waiting time for starting the transmission in the network nodes is determined by the following expression:

$$T_k^{(1)} = W_{\exp k}^{(1)} + G_k^{(1)}. \quad (6)$$

As in [16], the probabilities of the on-time delivery of packets Q_k, arriving at the kth node of the wireless network are also defined by the following relations:

$$Q_k = \frac{h(1-\lambda_k G_k^{(1)})}{h - \lambda_k + \lambda_k G_k^*(h)} G_k^*(h), \ k = \overline{1,N}, \quad (7)$$

where $h = 1/T_{\text{dir}}^{(1)}$, $T_{\text{dir}}(t) = 1 - e^{-ht}$, $T_{\text{dir}}^{(1)}$ is the directive packet transmission time in the network.

$$G_k^*(h) = \frac{1}{\left(\frac{h}{y_k}+1\right)^{x_k}}, \quad x_k = \frac{(G_k^{(1)})^2}{G_k^{(2)} - (G_k^{(1)})^2}, \quad y_k = \frac{G_k^{(1)}}{G_k^{(2)} - (G_k^{(1)})^2}. \quad (8)$$

Relations (8) can be easily established by approximating the distribution function $G_k(t)$ at two moments $G_k^{(1)}$ and $G_k^{(2)}$ by means of gamma distribution, while also considering the assumption that the constraint on the directive packet service time in the network $T_{\text{dir}}(t)$ is a random variable distributed according to the exponential law. The corresponding transformations are presented in [16].

The total intensity of the on-time served stream (network performance) is calculated by the following formula:

$$\lambda_{\text{sum}} = \sum_{k=1}^{N} \lambda_k Q_k, \quad (9)$$

where Q_k is determined by relation (7).

The method thus developed for evaluating the efficiency of wireless networks with the CSMA/CA access method forms the basis for implementing the computer-aided design systems for multi-purpose wireless networks. These include Wi-Fi and long-distance wireless networks using narrow-area antennas and CSMA/CA access method for communication.

4. MODELING THE WIRELESS NETWORK EFFICIENCY EVALUATION

A software package entitled "*The analytical modeling system for information transmission processes in networks*" has been developed for the general purposes of implementing the analytical model considered here. The aim is to evaluate the efficiency of networks with CSMA/CA access method in C++ language in the *Boland C++ Builder* object-oriented programming environment,

Initial data is entered from the display screen in the dialog mode according to the forms specified. Without leaving the modeling system, the operator is able to adjust the initial data and save the corresponding calculation results in text and graphic files.

The on-screen form for entering the initial data and outputting simulation results is shown in Fig. 1.

The software package enables the network bandwidth to be calculated for any given size of the wireless network with CSMA/CA and different placement of network nodes. The type of node placement can be random or deterministic. In deterministic placement, nodes can be located at the same distance from neighboring nodes (equidistant placement) or at different distances (non-equidistant placement). The packet transmission time constraint must be defined when entering initial data. The probability of delivering packets in less time than the directive one depends significantly on the constraint defined for the packet delivery time. The performance defined as the total on-time transmitted packet stream in the wireless network also depends significantly on the given packet delivery time constraints. Characteristics such as node and transmission medium load, as well as probabilistic and temporal characteristics (waiting time in queues, packet transmission time) do not depend on the constraints imposed on the transmission time. However, they certainly depend significantly on the transmission medium bandwidth, the number of nodes and their placement, the network size, the intensity of packet streams arriving at the wireless network nodes for service, the length of info packs, and time delays resulting from jampacks overlay. During modeling, the speed of signal propagation in the transmission medium is assumed to be equivalent to the speed of light.

The packet transmission in the wireless network with CSMA/CA is simulated, in order to demonstrate calculations of probability-time characteristics of packet delivery processes and wireless network performance using the developed analytical method. For modeling purposes, the following initial data was selected:

- the size of the wireless network with CSMA/CA is 500 m;
- the type of node distribution in the network is random;
- the number of nodes in the network $N = 100$;
- bandwidth is 100 Mbps;
- signal propagation speed is $3 \cdot 10^8$ m/s;
- maximum packet retransmission delay is 10 µs;
- jampack length is 32 bits;
- directive time is 0.005 s;
- info pack length is 1 Kbit;
- packet arrival rate is the same in all nodes.

It should be noted that the developed software package also enables modeling to be performed at different packet arrival rate at network nodes for service.

The calculation results for probabilistic and temporal characteristics, performance, load of nodes and transmission medium with the defined initial data at load change (change of intensity of packet streams arriving at the network nodes for service) are presented in Fig. 2–6.

Packet delivery time in a wireless network depends on the time of waiting for transmission in the queue at network nodes, as well as the time of packet transmission allowing for emerging conflicts. Therefore, the parameters of information processing in a wireless network should be selected in such a way that no bottlenecks, i.e., overloads of individual nodes and the transmission medium might occur within the entire range of changes in the intensity of the packet streams being processed in the system. In a balanced system, the load of the transmission medium and the load of the nodes when the load increases should be close to each other. As the network length decreases and the number of nodes decreases for a given transmission medium capacity, the length of the transmitted packets should increase in order to balance the network when the load increases.

When increasing the network size and the number of nodes at a given network bandwidth, in order to balance the network within the entire range of load changes, the length of transmitted information packets must be reduced. This will enable optimal performance under transmission time constraints, due to a reduced probability of conflicts.

Specific recommendations on selecting parameters and modes of operation for the wireless network can be obtained by conducting multivariate analytical calculations. This can be done by using the software package implementing the analytical method used for studying wireless networks with CSMA/CA access to the transmission medium.

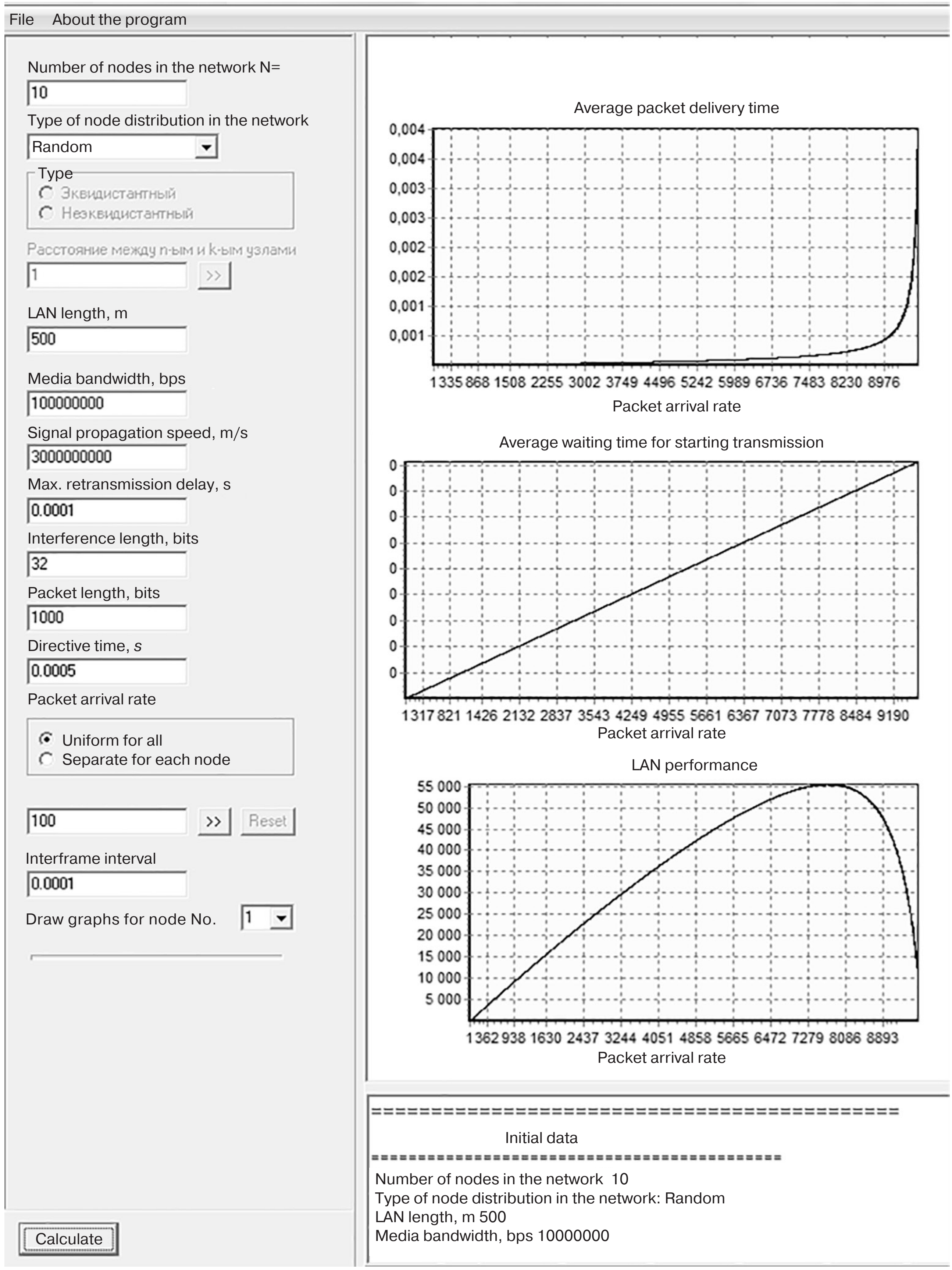

Fig. 1. The screen form for input/output of simulation results

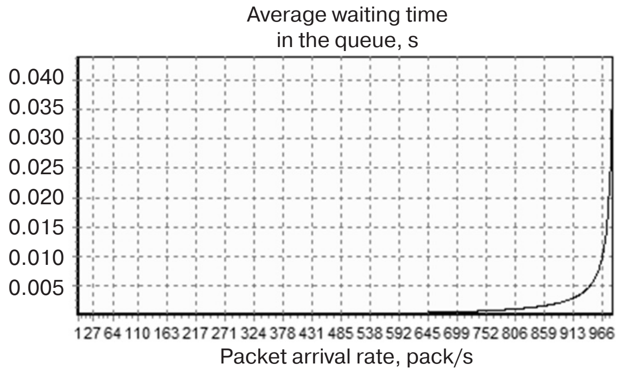

Fig. 2. Dependence of the average waiting time for packet transmission in nodes (s) on the packet arrival rate at the wireless network nodes and equal packet arrival rate at the network nodes

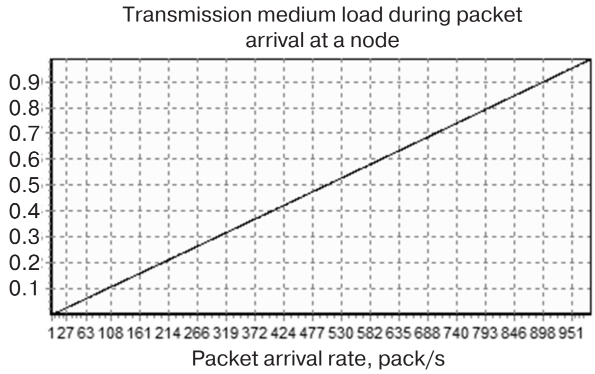

Fig. 5. Dependence of the transmission medium load during packet arrival at the node on the packet arrival rate at the wireless network nodes at random node placement (N = 100), and equal packets arrival rate at network nodes

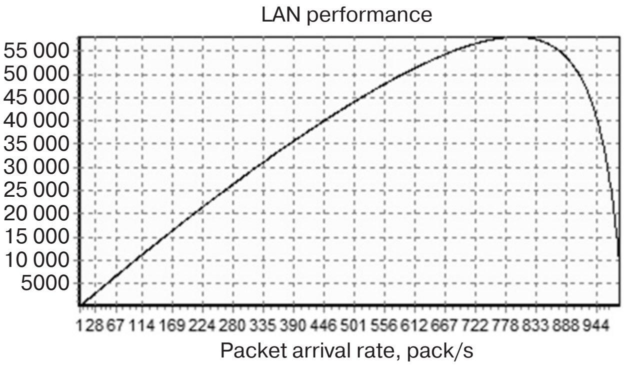

Fig. 3. Dependence of network performance on the packet arrival rate at the wireless network nodes at random node placement (N = 100), equal packet arrival rate at network nodes, and constraints on the packet delivery time

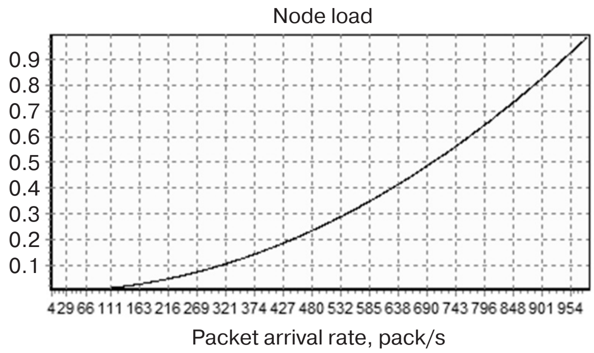

Fig. 6. Dependence of network node load on the packet arrival rate at wireless network nodes at random node placement (N = 100) and equal packet arrival rate at the network nodes

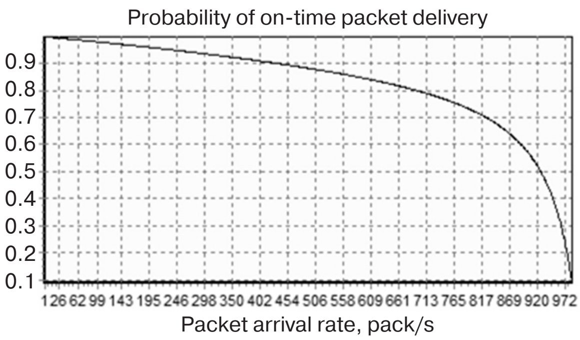

Fig. 4. Dependence of the probability of on-time packet delivery on the packet arrival rate of the wireless network nodes under random node placement (N = 100), equal packet arrival rate at network nodes, and packet delivery time constraint

CONCLUSIONS

In this paper, the following main results were obtained.

Models used to analyze the probability-time characteristics of information processing in distributed information-computing systems were classified.

The paper also demonstrated the necessity of priority development of nested analytical models describing the processes of packet transmission under limitations on the time of information transmission in networks at the channel level.

Analytical formulas for evaluating time characteristics of packet transmission, node load, transmission medium load, and performance of wireless networks with CSMA/CA access method were established. Their operation is described by the IEEE 802.11 communication standard.

The software package is based on the developed analytical method. Use of the software allows the performance of wireless network and probabilistic and temporal characteristics of packet transmission at different transmission medium bandwidths and network sizes to be evaluated. It also provides an opportunity for multivariate analysis of different operating modes of wireless networks with CSMA/CA access method to be performed.

The description of the theoretical principles of the proposed analytical method for evaluating probabilistic and temporal characteristics and performance under the time constraint on information transmission in wireless networks with CSMA/CA is universal. It is used in the development of practical works in such disciplines as "Architecture of computing systems" and "Methods and means of protection of computer information" at the MIREA – Russian Technological University.

Authors' contribution. All authors equally contributed to the research work.

REFERENCES

1. Tanenbaum E.S., Wetherall D. *Computer Networks*: transl. from Engl. St. Petersburg: Piter; 2018. 960 p. (in Russ.).
   [Tanenbaum E.S., Wetherall D. *Computer Networks*. Prentice Hall; 2011. 962 p.]
2. Kuzmenko N.G. *Komp'yuternye seti i setevye tekhnologii* (*Computer Networks and Networking Technologies*). Moscow: Nauka i Tekhnika; 2015. 368 p. (in Russ.).
3. Epanishnikov A.M. *Lokal'nye vychislitel'nye seti* (*Local Area Networks*). Moscow: Dialog-MIFI; 2014. 224 p. (in Russ.).
4. Smirnova E.V. *Tekhnologii sovremennykh setei Ethernet. Metody kommutatsii i upravleniya potokami dannykh* (*Modern Ethernet Network Technologies. Methods of Data Switching and Flow Control*). Moscow: BKhV-Peterburg; 2012. 272 p. (in Russ.).
5. Akimova G.P., Solovyev A.V., Tarkhanov I.A. Modelling the Reliability of Distributed Information Systems. *Informatsionnye tekhnologii i vychislitel'nye sistemy* (*ITiVS*) = *J. Inform. Technol. & Computing Syst.* 2019;3:79–86 (in Russ.). https://doi.org/10.14357/20718632190307
6. Pavsky V.A., Pavsky K.V. Mathematical Model for Calculating Reliability Indicators of Scalable Computer Systems Considering Switching Time. *Izvestiya YuFU. Tekhnicheskie nauki* = *Izvestiya SFedU. Engineering Sciences*. 2020;2(212): 134–145 (in Russ.). https://doi.org/10.18522/2311-3103-2020-2-134-145
7. Leontyev A.S. Multilevel Analytical and Analytical-Simulation Models for Evaluating the Probabilistic and Temporal Characteristics of Multimachine Computing Complexes with Regard to Reliability. *Mezhdunarodnyi nauchno-issledovatel'skii zhurnal* = *International Research Journal*. 2023;5(131) (in Russ.). https://doi.org/10.23670/IRJ.2023.131.8
8. Leontyev A.S., Timoshkin M.S. Research of the error of multilevel analytical and analytic-simulation models for evaluation of the probabilistic-time characteristics of multi-machine computing complexes with reliability included. *Naukosfera.* 2023;3(1):143–156 (in Russ.). https://doi.org/10.5281/zenodo.7736570
9. Alshaev I.A., Lavrukhin V.A. Wi-Fi Networks Designand Optimization. *Informatsionnye tekhnologii i telekommunikatsii* = *Information Technologies and Telecommunications.* 2016;4(1):87–95 (in Russ.).
10. Denisenko V. Wireless Local Area Networks. Part 2. *Sovremennye Tekhnologii Avtomatizatsii* = *STA.* 2009;2:96–101 (in Russ.).
11. Held G. *Tekhnologii peredachi dannykh* (*Data Transmission Technologies*): transl. from Engl. St. Petersburg: Piter, BHV; 2003. 720 p. (in Russ.).
    [Held G. *Understanding Data Communications*. Boston: Addison-Wesley; 2002. 788 p.]
12. Sharafullina A.Yu., Galyamov R.R., Zaripova R.S. Technical Principles of Creating a Wireless Local Network Wi-Fi. *T-Comm: Telekommunikatsiya i transport* = *T-Comm.* 2021;15(7):28–33 (in Russ.).
13. Zvonareva G.A., Buzunov D.S. Using Simulation Modeling to Estimate Time Characteristics of a Distributed Computing System. *Otkrytoe obrazovanie* = *Open Education*. 2022;26(5):32–39 (in Russ.). https://doi.org/10.21686/1818-4243-2022-5-32-39
14. Brodskii Yu.I. *Raspredelennoe imitatsionnoe modelirovanie slozhnykh system* (*Distributed Simulation Modeling of Complex Systems*). Moscow: Vychislitel'nyi tsentr im. A.A. Dorodnitsyna RAN; 2010. 156 p. (in Russ.).
15. Zhmatov D.V. Impulse Disturbance Filtration at Digital Substations. In: *Proceedings of 14th International Conference Management of Large-Scale System Development* (*MLSD*). 2021. https://doi.org/10.1109/MLSD52249.2021.9600257
16. Leontyev A.S. Development of Analytical Methods, Models, and Techniques for Local Area Networks Analysis. In: *Theoretical Issues of Software Engineering: Interuniversity Collection of Scientific Papers*. Moscow: MIREA; 2001. P. 70–94 (in Russ.).

СПИСОК ЛИТЕРАТУРЫ

1. Таненбаум Э.С., Уэзеролл Д. *Компьютерные сети*: пер. с англ. СПб.: Питер; 2018. 960 с.
2. Кузьменко Н.Г. *Компьютерные сети и сетевые технологии*. М.: Наука и техника; 2015. 368 с.
3. Епанишников А.М. *Локальные вычислительные сети*. М.: Диалог-МИФИ; 2014. 224 с.
4. Смирнова Е.В. *Технологии современных сетей Ethernet. Методы коммутации и управления потоками данных*. М.: БХВ-Петербург; 2012. 272 с.
5. Акимова Г.П., Соловьев А.В., Тарханов И.А. Моделирование надежности распределенных вычислительных систем. *Информационные технологии и вычислительные системы* (*ИТиВС*). 2019;3:79–86. https://doi.org/10.14357/20718632190307
6. Павский В.А., Павский К.В. Математическая модель для расчета показателей надежности масштабируемых вычислительных систем с учетом времени переключения. *Известия ЮФУ. Технические науки*. 2020;2(212):134–145. https://doi.org/10.18522/2311-3103-2020-2-134-145
7. Леонтьев А.С. Многоуровневые аналитические и аналитико-имитационные модели оценки вероятностно-временных характеристик многомашинных вычислительных комплексов с учетом надежности. *Международный научно-исследовательский журнал.* 2023;5(131). https://doi.org/10.23670/IRJ.2023.131.8
8. Леонтьев А.С., Тимошкин М.С. Исследование погрешности многоуровневых аналитических и аналитико-имитационных моделей оценки вероятностно-временных характеристик многомашинных вычислительных комплексов с учетом надежности. *Научный журнал «Наукосфера»*. 2023;3(1):143–156. https://doi.org/10.5281/zenodo.7736570
9. Альшаев И.А., Лаврухин В.А. О проектировании и оптимизации сетей Wi-Fi. *Информационные технологии и телекоммуникации*. 2016;4(1):87–95.
10. Денисенко В. Беспроводные локальные сети. Часть 2. *Современные технологии автоматизации* (*СТА*). 2009;2: 96–101.
11. Хелд Г. *Технологии передачи данных*: пер. с англ. СПб.: Питер, BHV; 2003. 720 с.
12. Шарафуллина А.Ю., Галямов Р.Р., Зарипова Р.С. Технические принципы создания беспроводной локальной сети Wi-Fi. *T-Comm: Телекоммуникация и транспорт*. 2021;15(7):28–33.
13. Звонарева Г.А., Бузунов Д.С. Использование имитационного моделирования для оценки временных характеристик распределенной вычислительной системы. *Открытое образование*. 2022;26(5):32–39. https://doi.org/10.21686/1818-4243-2022-5-32-39
14. Бродский Ю.И. *Распределенное имитационное моделирование сложных систем*. М.: Вычислительный центр им. А.А. Дородницына РАН; 2010. 156 с.
15. Zhmatov D.V. Impulse Disturbance Filtration at Digital Substations. In: *Proceedings of 14th International Conference Management of Large-Scale System Development* (*MLSD*). 2021. https://doi.org/10.1109/MLSD52249.2021.9600257
16. Леонтьев А.С. Разработка аналитических методов, моделей и методик анализа локальных вычислительных сетей. *Теоретические вопросы программного обеспечения: Межвузовский сборник научных трудов*. М.: МИРЭА; 2001. С. 70–94.

About the authors

Alexander S. Leontyev, Cand. Sci. (Eng.), Senior Researcher, Associate Professor, Department of Mathematical Support and Standardization, Institute of Information Technologies, MIREA – Russian Technological University (78, Vernadskogo pr., Moscow, 119454 Russia). E-mail: leontev@mirea.ru. RSCI SPIN-code 5798-9721, https://orcid.org/0000-0003-3673-2468

Dmitry V. Zhmatov, Cand. Sci. (Eng.), Docent, Associate Professor, Department of Mathematical Support and Standardization, Institute of Information Technologies, MIREA – Russian Technological University (78, Vernadskogo pr., Moscow, 119454 Russia). E-mail: zhmatov@mirea.ru. Scopus Author ID 56825948100, RSCI SPIN-code 2641-6783, https://orcid.org/0000-0002-7192-2446

Об авторах

Леонтьев Александр Савельевич, к.т.н., старший научный сотрудник, доцент кафедры математического обеспечения и стандартизации информационных технологий, Институт информационных технологий ФГБОУ ВО «МИРЭА – Российский технологический университет» (119454, Россия, Москва, пр-т Вернадского, д. 78). E-mail: leontev@mirea.ru. SPIN-код РИНЦ 5798-9721, https://orcid.org/0000-0003-3673-2468

Жматов Дмитрий Владимирович, к.т.н., доцент, доцент кафедры математического обеспечения и стандартизации информационных технологий, Институт информационных технологий ФГБОУ ВО «МИРЭА – Российский технологический университет» (119454, Россия, Москва, пр-т Вернадского, д. 78). E-mail: zhmatov@mirea.ru. Scopus Author ID 56825948100, SPIN-код РИНЦ 2641-6783, https://orcid.org/0000-0002-7192-2446

Translated from Russian into English by Kirill V. Nazarov
Edited for English language and spelling by Dr. David Mossop

Russian Technological Journal. 2024;12(2):77–89 ISSN 2500-316X (Online)

UDC 531.391
https://doi.org/10.32362/2500-316X-2024-12-2-77-89

RESEARCH ARTICLE

A mathematical model of the gravitational potential of the planet taking into account tidal deformations

Albina V. Shatina @,
Alexandra S. Borets

MIREA – Russian Technological University, Moscow, 119454 Russia
@ Corresponding author, e-mail: shatina_av@mail.ru

Abstract

Objectives. This paper investigates the gravitational potential of a viscoelastic planet moving in the gravitational field of a massive attracting center (star), a satellite and one or more other planets moving in Keplerian elliptical orbits relative to the attracting center. Celestial bodies other than a viscoelastic planet are modeled by material points. Within the framework of the linear model of the theory of viscoelasticity, the problem of finding the vector of elastic displacement has been resolved. Traditionally, a solid body model is used to determine the Earth's gravitational field, while tidal deformations are taken into account in the form of small corrections to the coefficients of the geopotential model. In this work, the viscoelastic ball model is used to take into account tidal effects. The relevance of the research topic is associated with high-precision forecasting of the movement of artificial satellites of the Earth, high-precision measurement of the Earth's gravitational field.

Methods. In this study the asymptotic and analytical methods developed by V.G. Vilke are used for mechanical systems containing viscoelastic elements of high rigidity, as well as methods of classical mechanics, mathematical analysis. The graphs were plotted using the *Octave* mathematical package.

Results. After resolving the quasi-static problem of elasticity theory by calculating triple integrals over a spherical area, a formula for the gravitational potential of a deformable planet was obtained. In addition, the gravitational potential of the Earth was also calculated taking into account solid-state tidal effects from the Moon, Sun, and Venus at an external point. Graphs were constructed to show the dependence of the Earth's gravitational potential on time.

Conclusions. The theoretical and numerical results established herein show that the main contribution to the gravitational potential of the Earth is made by the Moon and the Sun. The influence of other planets in the solar system is small. The value of the gravitational potential at the outer point of the Earth, taking into account tidal effects, depends both on the position of the point in the moving coordinate system and on the relative position of celestial bodies.

Keywords: gravitational potential, viscoelastic planet, tides, orbit, orbit elements, mathematical modeling

• **Submitted:** 25.07.2023 • **Revised:** 25.09.2023 • **Accepted:** 13.02.2024

For citation: Shatina A.V., Borets A.S. A mathematical model of the gravitational potential of the planet taking into account tidal deformations. *Russ. Technol. J.* 2024;12(2):77–89. https://doi.org/10.32362/2500-316X-2024-12-2-77-89

Financial disclosure: The authors have no a financial or property interest in any material or method mentioned.

The authors declare no conflicts of interest.

НАУЧНАЯ СТАТЬЯ

Математическая модель гравитационного потенциала планеты с учетом приливных деформаций

А.В. Шатина @,
А.С. Борец

МИРЭА – Российский технологический университет, Москва, 119454 Россия
@ *Автор для переписки, e-mail: shatina_av@mail.ru*

Резюме
Цели. В работе исследуется гравитационный потенциал вязкоупругой планеты, совершающей движение в гравитационном поле массивного притягивающего центра (звезды), спутника и еще одной или нескольких планет, движущихся по кеплеровским эллиптическим орбитам относительно притягивающего центра. Отличные от вязкоупругой планеты небесные тела моделируются материальными точками. В рамках линейной модели теории вязкоупругости решается задача нахождения вектора упругого смещения. Традиционно для определения гравитационного поля Земли используется модель твердого тела, а учет приливных деформаций отражается в виде малых поправок к коэффициентам модели геопотенциала. В данной работе для учета приливных эффектов используется модель вязкоупругого шара. Актуальность темы исследования связана с высокоточным прогнозированием движения искусственных спутников Земли, высокоточным измерением гравитационного поля Земли.
Методы. Используются асимптотические и аналитические методы, разработанные В.Г. Вильке для механических систем, содержащих вязкоупругие элементы большой жесткости, методы классической механики, математического анализа. Построение графиков выполнено с помощью математического пакета *Octave*.
Результаты. На основе решения квазистатической задачи теории упругости путем вычисления тройных интегралов по шаровой области получена формула для гравитационного потенциала деформируемой планеты, а также вычислен гравитационный потенциал Земли с учетом твердотельных приливных эффектов от Луны, Солнца и Венеры во внешней точке. Построены графики, показывающие зависимость гравитационного потенциала Земли от времени.
Выводы. Из полученных теоретических и численных результатов следует, что основной вклад в гравитационный потенциал Земли вносят Луна и Солнце. Влияние других планет Солнечной системы мало. Значение гравитационного потенциала во внешней точке Земли с учетом приливных эффектов зависит как от положения точки в подвижной системе координат, так и от взаимного расположения небесных тел.

Ключевые слова: гравитационный потенциал, вязкоупругая планета, приливы, орбита, элементы орбиты, математическое моделирование

• **Поступила:** 25.07.2023 • **Доработана:** 25.09.2023 • **Принята к опубликованию:** 13.02.2024

Для цитирования: Шатина А.В., Борец А.С. Математическая модель гравитационного потенциала планеты с учетом приливных деформаций. *Russ. Technol. J.* 2024;12(2):77–89. https://doi.org/10.32362/2500-316X-2024-12-2-77-89

Прозрачность финансовой деятельности: Авторы не имеют финансовой заинтересованности в представленных материалах или методах.

Авторы заявляют об отсутствии конфликта интересов.

INTRODUCTION

One of the most important objectives at the present time is to determine the shape of the Earth's geoid (equipotential surface of the Earth's gravity field). This is required for the topographic exploration in various scales, determination of coordinates of turning points of land plots during cadastral registration, engineering exploration, geodetic support of construction, among other reasons. In order to define the exact surface of a geoid at any point of the planet, a set of measurements need to be performed to establish the surface of the geoid or at a specific point on the Earth's surface, taking into account the nature of mass distribution. However, this is practically unfeasible.

In order to solve this task, the GRACE (a joint satellite mission of NASA and the German Aerospace Center, 2002) and GOCE (European Space Agency, 2009) spacecraft were sent into Earth orbit. These satellites have provided important data for gravimetry and higher geodesy. In particular, an improved geoid model has been constructed, which is superior in accuracy to all previous ones. Nevertheless, taking into account the so-called tidal effects, including elastic deformations of the entire globe under the influence of the gravitational force of the Moon and the Sun, all the results obtained for measuring the shape of the Earth's geoid present an average picture and are to a certain extent inaccurate.

In order to resolve the fundamental problem of determining the actual form of the Earth's geoid, considering all tidal effects, the Soviet scientist M.S. Molodensky proposed in 1950 [1, 2] that a quasigeoid should be used instead of the geoid. This is a surface close to it and does not require knowledge of the internal structure of the Earth's crust. When comparing quasigeoid and geoid, it has to be taken into account that in the case of high mountains the divergence will be approximately 2–4 m. In the case of lowland plains this divergence will be 0.02–0.12 m, and on the water surface there will be no divergence. The surface of the quasigeoid is defined by the values of the gravitational potential.

Article [3] presents an overview of the methods used to study the classical theory of tides. The traditional idea of the slowing down of the Earth's rotation under the action of tidal friction was expressed by I. Kant in 1755. The first fundamental studies on the influence of tides on the motion of planets and satellites belong to J.G. Darwin [4]. After the start of outer space exploration in the 1960s, as well as with the emergence of atomic time standards, interest in the tidal theory was revived [5].

At the present time, in accordance with the International Earth Rotation and Reference Systems Service (2010) [6] agreements, tidal deformations are recorded as small corrections to the geopotential model coefficients.

Tides in planets and their natural satellites play a crucial role in their dynamics. They are the cause of the transition to a 1:1 spin-orbit resonance [4, 5, 7]. It is also believed that tidal forces drive exoplanets into higher-order spin-orbit resonances with their parent stars [8].

Lunar-solar tides affect the change in the angular velocity of the Earth's rotation [9–11], weather and climate changes [12], and also influence volcanic activity [13]. The relevance of the research topic is related to high-precision forecasting of the motion of artificial satellites [14–17].

The aim of this study is to derive a formula for the gravitational potential of a planet modeled by a spherical viscoelastic body moving in the gravitational field of an attracting body, a natural satellite, and another planet. In order to achieve this, a motion separation method is used for mechanical systems containing viscoelastic bodies of large stiffness [18]. This work is a continuation and development of the results obtained in [19, 20].

1. TASK STATEMENT

In order to study the gravitational potential of a deformable planet, a mechanical system consisting of a stationary attracting center (material point O with mass m_1), a viscoelastic planet-satellite linkage, and another planet will be considered. The satellite and the second planet will be modeled as material points F and P with masses m_2 and m_3, respectively, and the planet being studied will be modeled as a homogeneous viscoelastic body with the shape of a ball of radius r_0 in the absence of deformations. The mass of the viscoelastic planet is m, and the density is ρ.

Let $OXYZ$ be an inertial coordinate system the origin of which coincides with the attracting center. Let $Dx_1x_2x_3$ be a mobile coordinate system associated with the viscoelastic planet with origin at its center of mass D; and C the barycenter of the viscoelastic planet–satellite system. The König axis systems $CX'Y'Z'$ and $DX''Y''Z''$ will also be introduced (Fig. 1).

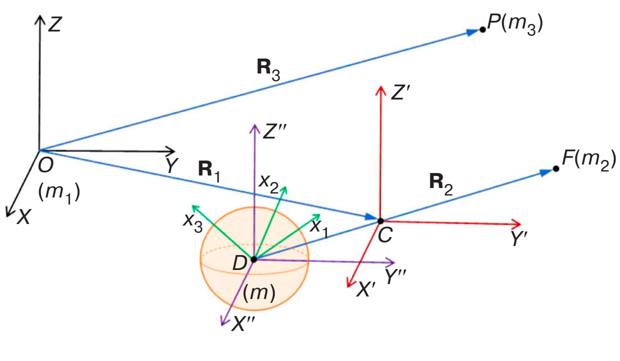

Fig. 1. Task statement

Let us assume that $\mathbf{R}_1 = \overline{OC}$ and $\mathbf{R}_2 = \overline{DF}$, $\mathbf{R}_3 = \overline{OP}$. According to the task statement

$$m_2 \ll m \ll m_1, \ |\mathbf{R}_2| \ll |\mathbf{R}_1|. \tag{1.1}$$

Deformations of a viscoelastic planet at the point M with the radius vector $\mathbf{r}$ are described by the elastic displacement vector $\mathbf{u}(\mathbf{r}, t)$. In the moving coordinate system $Dx_1x_2x_3$

$$\mathbf{u} = (u_1, u_2, u_3),\ \mathbf{r} = (x_1, x_2, x_3).$$

Radius vector of the point M in $OXYZ$ coordinate system has the following form:

$$\zeta(\mathbf{r},t) = \overline{OD} + \mathbf{\Gamma}\left(\mathbf{r} + \mathbf{u}(\mathbf{r},t)\right), \tag{1.2}$$

where $\mathbf{\Gamma}$ is the transition matrix from the moving coordinate system $Dx_1x_2x_3$ to the coordinate system $DX''Y''Z''$.

In order to determine the center of mass of the deformed planet (radius vector $\overline{OD}$) and the associated coordinate system $Dx_1x_2x_3$, the conditions [7] must be satisfied:

$$\overline{OD} = \frac{1}{m}\int_V \zeta(\mathbf{r},t)\rho\, dx,\ \int_V \mathbf{u}\, dx = 0,$$
$$\int_V \operatorname{rot}\mathbf{u}\, dx = 0,\ dx = dx_1 dx_2 dx_3, \tag{1.3}$$

where integration is performed over the ball of the radius r_0: $V = \{\mathbf{r} \in \mathbb{E}^3, |\mathbf{r}| \le r_0\}$, $\mathbb{E}^3$ is the Euclidean space.

Considering the conditions (1.3), the radius vectors $\overline{OD}$, $\overline{OF}$ of the points D and F are expressed through the vectors $\mathbf{R}_1$, $\mathbf{R}_2$ as follows:

$$\overline{OD} = \mathbf{R}_1 - \frac{m_2}{m + m_2}\mathbf{R}_2,\ \overline{OF} = \mathbf{R}_1 + \frac{m}{m + m_2}\mathbf{R}_2. \tag{1.4}$$

The potential energy of gravitational fields of the given mechanical system is represented in the following form:

$$\Pi = -\frac{fm_1m_3}{|\overline{OP}|} - \frac{fm_1m_2}{|\overline{OF}|} - \frac{fm_2m_3}{|\overline{FP}|} - \int_V \frac{fm_1\rho dx}{|\zeta(\mathbf{r},t)|} -$$
$$-\int_V \frac{fm_2\rho dx}{|\zeta(\mathbf{r},t) - \overline{OF}|} - \int_V \frac{fm_3\rho dx}{|\zeta(\mathbf{r},t) - \overline{OP}|},$$

where f is the universal gravitational constant.

The viscoelastic properties of the planet are described by the following parameters: Young's modulus E, Poisson's ratio ν and viscous friction coefficient χ ($\chi > 0$). Potential energy of the elastic deformations $\mathcal{E}$ and dissipative functional D are given according to the linear model [7, 18]:

$$\mathcal{E} = \int_V \mathcal{E}[\mathbf{u}]dx,\ \mathcal{E}[\mathbf{u}] = \alpha_1\left(\mathrm{I}_E^2 - \alpha_2 \mathrm{II}_E\right),$$
$$\alpha_1 = \frac{E(1-\nu)}{2(1+\nu)(1-2\nu)},\ \alpha_2 = \frac{2(1-2\nu)}{1-\nu},$$
$$\alpha_1 > 0,\ 0 < \alpha_2 < 3,$$
$$\mathrm{I}_E = \sum_{i=1}^{3} e_{ii},\ \mathrm{II}_E = \sum_{i<j}\left(e_{ii}e_{jj} - e_{ij}^2\right), \tag{1.5}$$
$$e_{ij} = \frac{1}{2}\left(\frac{\partial u_i}{\partial x_j} + \frac{\partial u_j}{\partial x_i}\right),$$
$$D = \int_V D[\dot{\mathbf{u}}]dx,\ D[\dot{\mathbf{u}}] = \chi\mathcal{E}[\dot{\mathbf{u}}].$$

We will assume that the points D, C, F, P move in the plane OXY, and $\mathbf{R}_1$, $\mathbf{R}_2$, $\mathbf{R}_3$ are the given vector functions of time. In addition, we assume that the angular velocity vector $\boldsymbol{\omega}$ of the coordinate system $Dx_1x_2x_3$ is constant relatively to $DX''Y''Z''$. This vector is defined by the equation

$$\boldsymbol{\omega} \times \mathbf{a} = \mathbf{\Gamma}^{-1}\dot{\mathbf{\Gamma}}\mathbf{a},$$

where $\mathbf{a}$ is a random vector.

2. ELASTIC DISPLACEMENT VECTOR

According to the D'Alembert–Lagrange variational principle, there exists an equality [18, 21]:

$$\int_V (\ddot{\zeta}, \delta\zeta)\rho dx + \delta\Pi + \int_V \left(\nabla\mathcal{E}[\mathbf{u}] + \nabla D[\dot{\mathbf{u}}] + \boldsymbol{\lambda}_1, \delta\mathbf{u}\right)dx +$$
$$+ \boldsymbol{\lambda}_2 \int_V \operatorname{rot}\delta\mathbf{u}\, dx = 0 \qquad \forall\delta\mathbf{u} \in \left(W_2^1(V)\right)^3. \tag{2.1}$$

Lagrange multipliers $\boldsymbol{\lambda}_1$, $\boldsymbol{\lambda}_2$ in (2.1) satisfy conditions (1.3); $\left(W_2^1(V)\right)^3$ is the Sobolev space.

According to (1.2) and (1.4)

$$\zeta = \mathbf{R}_1 - \frac{m_2}{m + m_2}\mathbf{R}_2 + \mathbf{\Gamma}(\mathbf{r} + \mathbf{u}).$$

Then

$$\dot{\zeta} = \dot{\mathbf{R}}_1 - \frac{m_2}{m + m_2}\dot{\mathbf{R}}_2 + \mathbf{\Gamma}\left[\boldsymbol{\omega} \times (\mathbf{r} + \mathbf{u}) + \dot{\mathbf{u}}\right],$$

$$\ddot{\zeta} = \ddot{\mathbf{R}}_1 - \frac{m_2}{m+m_2}\ddot{\mathbf{R}}_2 + $$
$$+ \mathbf{\Gamma}\left\{\boldsymbol{\omega}\times\left[\boldsymbol{\omega}\times(\mathbf{r}+\mathbf{u})\right] + \dot{\boldsymbol{\omega}}\times(\mathbf{r}+\mathbf{u}) + 2\boldsymbol{\omega}\times\dot{\mathbf{u}} + \ddot{\mathbf{u}}\right\},$$

$$\delta\zeta = \mathbf{\Gamma}\delta\mathbf{u}. \tag{2.2}$$

Equality (2.2) assumes that the orbital and rotational motions of the mechanical system are specified, so the variations $\mathbf{R}_1$, $\mathbf{R}_2$, $\mathbf{\Gamma}$ are equal to zero.

Further:

$$\delta\Pi = \int_V \left(\frac{fm_1\zeta}{|\zeta|^3}, \delta\zeta\right)\rho dx + \int_V \left(\frac{fm_2\left(\zeta - \overline{OF}\right)}{\left|\zeta - \overline{OF}\right|^3}, \delta\zeta\right)\rho dx + $$
$$+ \int_V \left(\frac{fm_3\left(\zeta - \overline{OP}\right)}{\left|\zeta - \overline{OP}\right|^3}, \delta\zeta\right)\rho dx. \tag{2.3}$$

Here

$$\zeta - \overline{OF} = -\mathbf{R}_2 + \mathbf{\Gamma}(\mathbf{r}+\mathbf{u}),$$

$$\zeta - \overline{OP} = \mathbf{R}_1 - \frac{m_2}{m+m_2}\mathbf{R}_2 - \mathbf{R}_3 + \mathbf{\Gamma}(\mathbf{r}+\mathbf{u}).$$

Explanation for finding the variation (2.3) of the functional Π: let $\mathbf{a} = (a_1, a_2, a_3)$, then

$$\delta\frac{1}{|\mathbf{a}|} = \delta\frac{1}{\sqrt{a_1^2+a_2^2+a_3^2}} = -\frac{1}{2}\left(a_1^2+a_2^2+a_3^2\right)^{-3/2} \times$$
$$\times\, \delta\left(a_1^2+a_2^2+a_3^2\right) = -\frac{\delta\left(a_1^2+a_2^2+a_3^2\right)}{2\left(\sqrt{a_1^2+a_2^2+a_3^2}\right)^3} =$$
$$= -\frac{2a_1\delta a_1 + 2a_2\delta a_2 + 2a_3\delta a_3}{2|\mathbf{a}|^3} = -\frac{(\mathbf{a}, \delta\mathbf{a})}{|\mathbf{a}|^3}.$$

Considering (2.2):

$$\delta\Pi = \int_V \left(\frac{\mathbf{\Gamma}^{-1}\zeta}{|\zeta|^3}, \delta\mathbf{u}\right) fm_1\rho dx + $$
$$+ \int_V \left(\frac{\mathbf{\Gamma}^{-1}\left(\zeta - \overline{OF}\right)}{\left|\zeta - \overline{OF}\right|^3}, \delta\mathbf{u}\right) fm_2\rho dx + $$
$$+ \int_V \left(\frac{\mathbf{\Gamma}^{-1}\left(\zeta - \overline{OP}\right)}{\left|\zeta - \overline{OP}\right|^3}, \delta\mathbf{u}\right) fm_3\rho dx, \tag{2.4}$$

$$\int_V \left(\ddot{\zeta}, \delta\zeta\right)\rho\, dx = \int_V \left(\mathbf{\Gamma}^{-1}\ddot{\zeta}, \delta\mathbf{u}\right)\rho dx. \tag{2.5}$$

We can assume that the material stiffness of the deformable planet is high, i.e., $\hat{\varepsilon} = |\boldsymbol{\omega}|^2 \rho r_0^2 E^{-1} << 1$. Vectors $\mathbf{u}(\mathbf{r}, t)$, $\boldsymbol{\lambda}_1$ and $\boldsymbol{\lambda}_2$ can be retrieved as degree expansions $\varepsilon = E^{-1}$ [18]:

$$\mathbf{u}(\mathbf{r}, t) = \varepsilon\mathbf{u}_1(\mathbf{r}, t) + \varepsilon^2\mathbf{u}_2(\mathbf{r}, t) + \ldots ,$$

$$\boldsymbol{\lambda}_1(t) = \boldsymbol{\lambda}_{10}(t) + \varepsilon\boldsymbol{\lambda}_{11}(t) + \ldots ,\ \boldsymbol{\lambda}_2(t) = \boldsymbol{\lambda}_{20}(t) + \varepsilon\boldsymbol{\lambda}_{21}(t) + \ldots .$$

From Eq. (2.1), assuming (2.4), (2.5) for the vector function $\mathbf{u}_1$, we obtain the following equation:

$$\int_V \left(\mathbf{\Gamma}^{-1}\left(\ddot{\mathbf{R}}_1 - \frac{m_2}{m+m_2}\ddot{\mathbf{R}}_2\right) + \boldsymbol{\omega}\times[\boldsymbol{\omega}\times\mathbf{r}] + \right.$$
$$+ \frac{\left(\mathbf{\Gamma}^{-1}\overline{OD} + \mathbf{r}\right)}{\left|\mathbf{\Gamma}^{-1}\overline{OD} + \mathbf{r}\right|^3} fm_1 + \frac{\left(\mathbf{\Gamma}^{-1}\overline{FD} + \mathbf{r}\right)}{\left|\mathbf{\Gamma}^{-1}\overline{FD} + \mathbf{r}\right|^3} fm_2 + $$
$$\left. + \frac{\left(\mathbf{\Gamma}^{-1}\overline{PD} + \mathbf{r}\right)}{\left|\mathbf{\Gamma}^{-1}\overline{PD} + \mathbf{r}\right|^3} fm_3, \delta\mathbf{u}\right)\rho dx + \tag{2.6}$$
$$+ \int_V \varepsilon\left(\nabla\mathcal{E}[\mathbf{u}_1] + \nabla D[\dot{\mathbf{u}}_1] + \boldsymbol{\lambda}_{10}, \delta\mathbf{u}\right) dx + $$
$$+ \int_{\partial V} \left(\boldsymbol{\lambda}_{20}\times\mathbf{n}\right)\delta\mathbf{u}\, d\sigma = 0.$$

The last summand in (2.6) is derived from the Ostrogradsky–Gauss formula, as represented below:

$$\int_V \left(\boldsymbol{\lambda}_{20}, \mathrm{rot}\delta\mathbf{u}\right) dx = \int_{\partial V} \left(\delta\mathbf{u}\times\boldsymbol{\lambda}_{20}\right)\mathbf{n}\, d\sigma,$$

where ∂V is the boundary of area V, and $\mathbf{n}$ is the normal to ∂V.

Following [7, 18], we substitute into (2.6) sequentially $\delta\mathbf{u} = \delta\boldsymbol{\alpha}\times\mathbf{r}$ and $\delta\mathbf{u} = \boldsymbol{\alpha}$, $\boldsymbol{\alpha}\in\mathbb{E}^3$. As a result, we obtain the following:

$$\int_{\partial V} \left(\left(\boldsymbol{\lambda}_{20}\times\mathbf{n}\right), \left(\delta\boldsymbol{\alpha}\times\mathbf{r}\right)\right) d\sigma = \frac{8}{3}\pi r_0^3\left(\boldsymbol{\lambda}_{20}, \delta\boldsymbol{\alpha}\right) = 0$$

$$\forall\delta\boldsymbol{\alpha}\in\mathbb{E}^3 \Rightarrow \boldsymbol{\lambda}_{20} = 0,$$

$$\mathbf{\Gamma}^{-1}\left\{m\ddot{\mathbf{R}}_1 - \frac{mm_2}{m+m_2}\ddot{\mathbf{R}}_2 + \frac{fmm_1\overline{OD}}{\left|\overline{OD}\right|^3} + \right.$$
$$\left. + \frac{fmm_2\overline{FD}}{\left|\overline{FD}\right|^3} + \frac{fmm_3\overline{PD}}{\left|\overline{PD}\right|^3}\right\} + \frac{4}{3}\pi r_0^3\boldsymbol{\lambda}_{10} = 0 . \tag{2.7}$$

Also at the derivation of relation (2.7) the following equation was taken into account:

$$\int_V \frac{\mathbf{a}+\mathbf{r}}{|\mathbf{a}+\mathbf{r}|^3}\rho dx = \frac{m\mathbf{a}}{|\mathbf{a}|^3},$$

here vector **a** is independent of **r**.

Since the sizes of the deformed planet are much smaller than the distances between the mutually gravitating bodies, then

$$|\mathbf{r}| \ll |\overline{OD}|, \quad |\mathbf{r}| \ll |\overline{FD}|, \quad |\mathbf{r}| \ll |\overline{PD}|.$$

If $|\mathbf{r}| << |\mathbf{a}|$ then

$$\frac{\mathbf{a}+\mathbf{r}}{|\mathbf{a}+\mathbf{r}|^3} = \frac{\mathbf{a}+\mathbf{r}}{(\mathbf{a}+\mathbf{r},\mathbf{a}+\mathbf{r})^{3/2}} = \frac{\mathbf{a}+\mathbf{r}}{\left((\mathbf{a},\mathbf{a})+2(\mathbf{a},\mathbf{r})+(\mathbf{r},\mathbf{r})\right)^{3/2}} =$$

$$= \frac{\mathbf{a}+\mathbf{r}}{|\mathbf{a}|^3}\left\{1+\frac{2(\mathbf{a},\mathbf{r})}{|\mathbf{a}|^2}+\frac{(\mathbf{r},\mathbf{r})}{|\mathbf{a}|^2}\right\}^{-3/2} \approx$$

$$\approx \frac{\mathbf{a}+\mathbf{r}}{|\mathbf{a}|^3}\left\{1-\frac{3}{2}\cdot 2\frac{(\mathbf{a},\mathbf{r})}{|\mathbf{a}|^2}\right\} = \frac{\mathbf{a}}{|\mathbf{a}|^3} - \frac{3\mathbf{a}(\mathbf{a},\mathbf{r})}{|\mathbf{a}|^5} + \frac{\mathbf{r}}{|\mathbf{a}|^3}.$$

Then Eq. (2.6) will take the form:

$$\int_V \left(\mathbf{\Gamma}^{-1}\left(\ddot{\mathbf{R}}_1 - \frac{m_2}{m+m_2}\ddot{\mathbf{R}}_2\right) + \boldsymbol{\omega}\times[\boldsymbol{\omega}\times\mathbf{r}] + \right.$$
$$+ \sum_{j=1}^{3}\left\{\frac{fm_j\mathbf{q}_j}{|\mathbf{q}_j|^3} + \frac{fm_j}{|\mathbf{q}_j|^3}\cdot\left[\mathbf{r}-3(\xi_j,\mathbf{r})\xi_j\right]\right\} + \tag{2.8}$$
$$\left. +\frac{1}{\rho}\boldsymbol{\lambda}_{10}(t),\delta\mathbf{u}\right)\rho dx + \int_V \varepsilon\left(\nabla\mathcal{E}[\mathbf{u}_1+\chi\dot{\mathbf{u}}_1],\delta\mathbf{u}\right)dx = 0.$$

Here

$$\mathbf{q}_1 = \mathbf{\Gamma}^{-1}\overline{OD} = \mathbf{\Gamma}^{-1}\left(\mathbf{R}_1 - \frac{m_2}{m+m_2}\mathbf{R}_2\right),$$
$$\mathbf{q}_2 = \mathbf{\Gamma}^{-1}\overline{FD} = -\mathbf{\Gamma}^{-1}\mathbf{R}_2,$$
$$\mathbf{q}_3 = \mathbf{\Gamma}^{-1}\overline{PD} = \mathbf{\Gamma}^{-1}\left(\mathbf{R}_1 - \frac{m_2}{m+m_2}\mathbf{R}_2 - \mathbf{R}_3\right), \tag{2.9}$$
$$\xi_i = \frac{\mathbf{q}_i}{|\mathbf{q}_i|}, \quad i = 1, 2, 3.$$

Since $m = \frac{4}{3}\pi r_0^3\rho$, the following is derived from (2.7)

$$\boldsymbol{\lambda}_{10} = -\rho\left\{\mathbf{\Gamma}^{-1}\left(\ddot{\mathbf{R}}_1 - \frac{m_2}{m+m_2}\ddot{\mathbf{R}}_2\right) + \right.$$
$$\left. + \frac{fm_1\mathbf{q}_1}{|\mathbf{q}_1|^3} + \frac{fm_2\mathbf{q}_2}{|\mathbf{q}_2|^3} + \frac{fm_3\mathbf{q}_3}{|\mathbf{q}_3|^3}\right\}. \tag{2.10}$$

Assuming (2.10), we obtain from (2.8) the following task for determining $\mathbf{u}_1(\mathbf{r}, t)$:

$$\rho\left\{\boldsymbol{\omega}\times[\boldsymbol{\omega}\times\mathbf{r}] + \sum_{j=1}^{3}\frac{fm_j}{|\mathbf{q}_j|^3}\cdot\left[\mathbf{r}-3(\xi_j,\mathbf{r})\xi_j\right]\right\} + \tag{2.11}$$
$$+ \varepsilon\nabla\mathcal{E}[\mathbf{u}_1+\chi\dot{\mathbf{u}}_1] = 0,$$

$$\boldsymbol{\sigma}_n\Big|_{r=r_0} = 0. \tag{2.12}$$

Here

$$\varepsilon\nabla\mathcal{E} = -\frac{1}{2(1+\nu)}\left(\frac{1}{1-2\nu}\operatorname{grad}\operatorname{div}\mathbf{u} + \Delta\mathbf{u}\right),$$

$$\mathbf{u} = (u_1,u_2,u_3), \quad \mathbf{n} = (\gamma_1,\gamma_2,\gamma_3), \quad \boldsymbol{\sigma}_n = (\sigma_{n1},\sigma_{n2},\sigma_{n3}),$$

$$\sigma_{ni} = \frac{E\nu\gamma_i}{(1+\nu)(1-2\nu)}\operatorname{div}\mathbf{u} + \frac{E}{2(1+\nu)}\left(\frac{\partial\mathbf{u}}{\partial x_i} + \operatorname{grad}u_i,\mathbf{n}\right).$$

The solution of the task (2.11)–(2.12) has the following form [7, 22]:

$$\mathbf{u}_1(\mathbf{r}, t) = \mathbf{u}_{10}(\mathbf{r}, t) + \mathbf{u}_{11}(\mathbf{r}, t) +$$
$$+ \mathbf{u}_{12}(\mathbf{r}, t) + \mathbf{u}_{13}(\mathbf{r}, t), \tag{2.13}$$

where

$$\mathbf{u}_{10}(\mathbf{r},t) = \rho\left\{\frac{2}{3}\omega^2\left[d_1r^2 + d_2r_0^2\right]\mathbf{r} + \right.$$
$$+ b_1\left[\frac{1}{6}\omega^2r^2 - \frac{1}{2}(\boldsymbol{\omega},\mathbf{r})^2\right]\mathbf{r} + \tag{2.14}$$
$$\left. + \left[b_2r^2 + b_3r_0^2\right]\cdot\left[\frac{1}{3}\omega^2\mathbf{r} - (\boldsymbol{\omega},\mathbf{r})\boldsymbol{\omega}\right]\right\},$$
$$\omega = |\boldsymbol{\omega}|,$$

$$\mathbf{u}_{1k}(\mathbf{r},t) = -\frac{3\rho fm_k}{q_k^3}\left(1+\frac{3\chi\dot{q}_k}{q_k}\right)\left\{b_1\left[\frac{1}{6}r^2 - \frac{1}{2}(\xi_k,\mathbf{r})^2\right]\mathbf{r} + \right.$$
$$\left. + \left[b_2r^2 + b_3r_0^2\right]\cdot\left[\frac{1}{3}\mathbf{r} - (\xi_k,\mathbf{r})\xi_k\right]\right\} -$$
$$-\frac{3\chi\rho fm_k}{q_k^3}\{b_1(\dot{\xi}_k,\mathbf{r})(\xi_k,\mathbf{r})\mathbf{r} + \tag{2.15}$$
$$+ [b_2r^2 + b_3r_0^2][(\dot{\xi}_k,\mathbf{r})\xi_k + (\xi_k,\mathbf{r})\dot{\xi}_k]\},$$
$$q_k = |\mathbf{q}_k|, \; k = 1, 2, 3,$$

$$d_1 = -\frac{(1+\nu)(1-2\nu)}{10(1-\nu)}, \; d_2 = \frac{(1-2\nu)(3-\nu)}{10(1-\nu)},$$
$$b_1 = \frac{2(1+\nu)}{5\nu+7}, \; b_2 = -\frac{(1+\nu)(2+\nu)}{5\nu+7}, \tag{2.16}$$
$$b_3 = \frac{(1+\nu)(2\nu+3)}{5\nu+7}.$$

Elastic displacement vector **u** is related to vector function $\mathbf{u}_1$ by the following equation:

$$\mathbf{u}(\mathbf{r},t) = \frac{1}{E}\mathbf{u}_1(\mathbf{r},t). \quad (2.17)$$

In formula (2.13), the summand $\mathbf{u}_{10}$ is responsible for the flattening of the planet along the rotation axis. The functions $\mathbf{u}_{1k}$ ($k = 1, 2, 3$) describe the tidal deformations of the planet caused by the gravitational fields of the celestial bodies O, F and P.

3. GRAVITATIONAL POTENTIAL OF A VISCOELASTIC PLANET AT AN EXTERNAL POINT

Using the elastic displacement vector (2.17), the gravitational potential of the planet can be calculated by the formula:

$$\Pi(\mathbf{R},t) = -f\int_V \frac{\rho dx}{\left|\mathbf{\Gamma}(\mathbf{r}+\mathbf{u}(\mathbf{r},t))-\mathbf{R}\right|}. \quad (3.1)$$

Here $\mathbf{R} = \overline{DK}$ is the radius vector of the point K in which the potential is defined, **r** is the radius vector of the volume element dx with the density ρ. Vector **R** in formula (3.1) is given in the coordinate system $DX''Y''Z''$. The integral is calculated over the ball V of the radius r_0.

It is assumed that:

$$|\mathbf{R}| > r_0, \ |\mathbf{u}(\mathbf{r},t)| \ll |\mathbf{r}-\mathbf{\Gamma}^{-1}\mathbf{R}|. \quad (3.2)$$

According to the constructed model, the motion of points C, F, D, P occurs in the OXY plane. The coordinates of the vectors $\mathbf{R}_1$, $\mathbf{R}_2$, $\mathbf{R}_3$ in the inertial system $OXYZ$ are represented in the following form:

$$\mathbf{R}_i = R_i(\cos\psi_i, \sin\psi_i, 0), \ R_i = \frac{a_i(1-e_i^2)}{(1+e_i\cos\vartheta_i)},$$
$$\psi_i = g_i + \vartheta_i, \ i = 1, 2, 3,$$

a_i is the major semi-axis, e_i is the eccentricity, g_i is the pericenter longitude, ϑ_i is the true anomaly of the orbit of the end of vector $\mathbf{R}_i$. The values a_i, e_i, g_i are constant parameters of the task, and the true anomalies are time-dependent functions:

$$\dot{\vartheta}_i = \frac{(1+e_i\cos\vartheta_i)^2}{(1-e_i^2)^{3/2}}n_i, \ n_i = \frac{2\pi}{T_i}, \ i = 1, 2, 3. \quad (3.3)$$

The values T_i in formula (3.3) are the corresponding periods of circulation.

The transition matrix from the moving coordinate system $Dx_1x_2x_3$ to the system $DX''Y''Z''$ can be represented as a product:

$$\mathbf{\Gamma} = \mathbf{\Gamma}_3(\psi)\mathbf{\Gamma}_1(\theta)\mathbf{\Gamma}_3(\varphi),$$

$$\mathbf{\Gamma}_3(\alpha) = \begin{pmatrix} \cos\alpha & -\sin\alpha & 0 \\ \sin\alpha & \cos\alpha & 0 \\ 0 & 0 & 1 \end{pmatrix},$$

$$\mathbf{\Gamma}_1(\theta) = \begin{pmatrix} 1 & 0 & 0 \\ 0 & \cos\theta & -\sin\theta \\ 0 & \sin\theta & \cos\theta \end{pmatrix}.$$

Here ψ, θ, φ are the Euler angles [21]. The relationship between the coordinates of the angular velocity vector $\boldsymbol{\omega}$ of the planet p, q, s in the coordinate system $Dx_1x_2x_3$ and the Euler angles is expressed by means of the following kinematic Euler equations:

$$\begin{cases} p = \dot{\psi}\sin\theta\sin\varphi + \dot{\theta}\cos\varphi, \\ q = \dot{\psi}\sin\theta\cos\varphi - \dot{\theta}\sin\varphi, \\ s = \dot{\psi}\cos\theta + \dot{\varphi}. \end{cases} \quad (3.4)$$

By directing the axis Dx_3 along the vector $\boldsymbol{\omega}$, we obtain $\boldsymbol{\omega} = (0, 0, \omega)$. Therefore, the following can be derived from the (3.4) system: $\dot{\psi} = 0$, $\dot{\theta} = 0$, $\dot{\varphi} = \omega$, i.e., the angles ψ, θ are constant, and φ is a linear function of time. Without restriction of generality, we can assume that $\psi_0 = 0$. Therefore, the matrices $\mathbf{\Gamma}$ and $\mathbf{\Gamma}^{-1}$ are represented by the following equations:

$$\mathbf{\Gamma} = \mathbf{\Gamma}_1(\theta_0)\mathbf{\Gamma}_3(\varphi), \ \mathbf{\Gamma}^{-1} = \mathbf{\Gamma}_3(-\varphi)\mathbf{\Gamma}_1(-\theta_0),$$
$$\psi = \psi_0(\psi_0 = 0), \ \theta = \theta_0, \ \varphi = \omega t + \varphi(0).$$

Let us set the radius vector of the external point K in the moving coordinate system $Dx_1x_2x_3$, using spherical coordinates R, λ, μ ($R = |\overline{DK}|$, λ is longitude, μ is latitude):

$$\mathbf{r}_K = \mathbf{\Gamma}^{-1}\mathbf{R} = R\mathbf{e}_R, \ \mathbf{e}_R = (\cos\lambda\cos\mu; \sin\lambda\cos\mu; \sin\mu),$$
$$R = r_0 + h, \ h > 0. \quad (3.5)$$

Taking into account the conditions (3.2), the gravitational potential (3.1) linearized by the components of the vector **u** has the following form:

$$\Pi(\mathbf{R},t) = -\int_V \frac{f\rho dx}{|\mathbf{r}-\mathbf{\Gamma}^{-1}\mathbf{R}|} + \int_V \frac{(\mathbf{r}-\mathbf{\Gamma}^{-1}\mathbf{R},\mathbf{u})}{|\mathbf{r}-\mathbf{\Gamma}^{-1}\mathbf{R}|^3} f\rho dx. \quad (3.6)$$

Let us substitute in (3.6)

$$\mathbf{u}(\mathbf{r},t)=\frac{1}{E}\sum_{k=0}^{3}\mathbf{u}_{1k}(\mathbf{r},t),$$

where the vector function $\mathbf{u}_{1k}$ is defined by the formulas (2.14)–(2.16). Let us calculate the triple integrals in (3.6) using the values of the auxiliary integrals:

$$\int_V \frac{dx}{|\mathbf{r}-\mathbf{a}|}=\frac{V_0}{|\mathbf{a}|},\ \int_V \frac{(\mathbf{r}-\mathbf{a},\mathbf{r})dx}{|\mathbf{r}-\mathbf{a}|^3}=0,\ \int_V \frac{\mathbf{r}^2(\mathbf{r}-\mathbf{a},\mathbf{r})dx}{|\mathbf{r}-\mathbf{a}|^3}=0,$$

$$\int_V \frac{(\boldsymbol{\omega},\mathbf{r})(\mathbf{r}-\mathbf{a},\boldsymbol{\omega})dx}{|\mathbf{r}-\mathbf{a}|^3}=\frac{r_0^2V_0}{5}\left\{\frac{(\boldsymbol{\omega},\boldsymbol{\omega})}{|\mathbf{a}|^3}-\frac{3(\boldsymbol{\omega},\mathbf{a})^2}{|\mathbf{a}|^5}\right\},$$

$$\int_V \frac{(\boldsymbol{\omega},\mathbf{r})^2(\mathbf{r}-\mathbf{a},\mathbf{r})dx}{|\mathbf{r}-\mathbf{a}|^3}=\frac{2r_0^4V_0}{35}\left\{\frac{(\boldsymbol{\omega},\boldsymbol{\omega})}{|\mathbf{a}|^3}-\frac{3(\boldsymbol{\omega},\mathbf{a})^2}{|\mathbf{a}|^5}\right\},$$

$$\int_V \frac{\mathbf{r}^2(\boldsymbol{\omega},\mathbf{r})(\mathbf{r}-\mathbf{a},\boldsymbol{\omega})dx}{|\mathbf{r}-\mathbf{a}|^3}=\frac{r_0^4V_0}{7}\left\{\frac{(\boldsymbol{\omega},\boldsymbol{\omega})}{|\mathbf{a}|^3}-\frac{3(\boldsymbol{\omega},\mathbf{a})^2}{|\mathbf{a}|^5}\right\},$$

where $V_0=4\pi r_0^3/3$. After calculating triple integrals over the spherical area V we obtain the following expression for the gravitational potential:

$$\Pi=-\frac{fm}{R}-\frac{3fm^2r_0\Phi(\nu)}{140\pi ER^3}\left\{\omega^2-3(\omega,\mathbf{e}_R)^2\right\}+$$
$$+\sum_{k=1}^{3}\frac{9f^2m^2m_kr_0\Phi(\nu)}{140\pi Eq_k^3R^3}\left\{1-3(\xi_k,\mathbf{e}_R)^2\right\}\left(1+\frac{3\chi\dot{q}_k}{q_k}\right)+ \quad (3.7)$$
$$+\sum_{k=1}^{3}\frac{27\chi f^2m^2m_kr_0\Phi(\nu)}{70\pi Eq_k^3R^3}(\dot{\xi}_k,\mathbf{e}_R)(\xi_k,\mathbf{e}_R).$$

Here

$$R=|\mathbf{R}|,\ \mathbf{e}_R=\boldsymbol{\Gamma}^{-1}\frac{\mathbf{R}}{R},\ \Phi(\nu)=\frac{(1+\nu)(9\nu+13)}{(5\nu+7)},$$
$$q_k=|\mathbf{q}_k|,\ k=1,2,3.$$

The singular vector $\mathbf{e}_R$ in the moving coordinate system $Dx_1x_2x_3$ is given by the spherical coordinates λ and μ according to (3.5).

Let us express q_k through the orbital elements. According to (2.9)

$$\mathbf{q}_1=\boldsymbol{\Gamma}^{-1}\left(\mathbf{R}_1-\frac{m_2}{m+m_2}\mathbf{R}_2\right),$$
$$q_1=|\mathbf{q}_1|= \quad (3.8)$$
$$=R_1\sqrt{1-\frac{2m_2}{m+m_2}\frac{R_2}{R_1}\cos\gamma_{12}+\left(\frac{m_2}{m+m_2}\right)^2\left(\frac{R_2}{R_1}\right)^2},$$

where $\gamma_{12}=g_1+\vartheta_1-g_2-\vartheta_2$ is the angle between vectors $\mathbf{R}_1$ и $\mathbf{R}_2$, $R_1=|\mathbf{R}_1|$, $R_2=|\mathbf{R}_2|$.

Due to condition (1.1)

$$\frac{m_2}{m+m_2}\cdot\frac{R_2}{R_1}\ll 1.$$

Let us rewrite the formula (3.8) in the form:

$$q_1=\frac{a_1(1-e_1^2)}{(1+e_1\cos\vartheta_1)}F_{21},$$
$$F_{21}=\sqrt{1-2k_{21}h_{21}\cos\gamma_{21}+k_{21}^2h_{21}^2},$$
$$k_{21}=\frac{m_2}{m+m_2}\frac{a_2(1-e_2^2)}{a_1(1-e_1^2)},\ h_{21}=\frac{1+e_1\cos\vartheta_1}{1+e_2\cos\vartheta_2}. \quad (3.9)$$

Further:

$$q_2=\frac{a_2(1-e_2^2)}{(1+e_2\cos\vartheta_2)}, \quad (3.10)$$

$$q_3=\sqrt{R_1^2-2(\mathbf{R}_1,\mathbf{R}_3)+R_3^2}=\frac{a_3(1-e_3^2)}{1+e_3\cos\vartheta_3}F_{13},$$
$$F_{13}=\sqrt{1-2k_{13}h_{13}\cos\gamma_{13}+k_{13}^2h_{13}^2},$$
$$k_{13}=\frac{a_1(1-e_1^2)}{a_3(1-e_3^2)},\ h_{13}=\frac{1+e_3\cos\vartheta_3}{1+e_1\cos\vartheta_1}. \quad (3.11)$$

Let us find the coordinates of the vectors $\boldsymbol{\Gamma}^{-1}\mathbf{R}_k$, $k=1,2,3$:

$$\boldsymbol{\Gamma}^{-1}\mathbf{R}_k=\boldsymbol{\Gamma}_3(-\varphi)\boldsymbol{\Gamma}_1(-\theta_0)\mathbf{R}_k=$$
$$=R_k\boldsymbol{\eta}_k=\frac{a_k(1-e_k^2)}{(1+e_k\cos\vartheta_k)}\boldsymbol{\eta}_k, \quad (3.12)$$

$$\boldsymbol{\eta}_k=(\eta_{k1},\eta_{k2},\eta_{k3}), \quad (3.13)$$

$$\eta_{k1}=\cos\varphi\cos(g_k+\vartheta_k)+\sin\varphi\cos\theta_0\sin(g_k+\vartheta_k),$$

$$\eta_{k2}=-\sin\varphi\cos(g_k+\vartheta_k)+\cos\varphi\cos\theta_0\sin(g_k+\vartheta_k),$$

$$\eta_{k3}=-\sin\theta_0\sin(g_k+\vartheta_k).$$

Using (2.9) and (3.12), we find the coordinates of the vectors ξ_k:

$$\xi_1=\frac{1}{F_{21}}(\boldsymbol{\eta}_1-k_{21}h_{21}\boldsymbol{\eta}_2),$$
$$\xi_2=-\boldsymbol{\eta}_2,\ \xi_3=\frac{1}{F_{13}}(k_{13}h_{13}\boldsymbol{\eta}_1-\boldsymbol{\eta}_3). \quad (3.14)$$

Thus, the computation of scalar products $(\xi_k, \mathbf{e}_R)$ is reduced to the computation of scalar products $(\boldsymbol{\eta}_k, \mathbf{e}_R)$. Using (3.5), (3.13), (3.14), we obtain:

$$(\boldsymbol{\eta}_k, \mathbf{e}_R) = \left[\cos(\varphi+\lambda)\cos(g_k + \vartheta_k) + \right.$$
$$\left. + \sin(\varphi+\lambda)\cos\theta_0 \sin(g_k+\vartheta_k)\right]\cdot \cos\mu - \quad (3.15)$$
$$- \sin\theta_0 \sin(g_k+\vartheta_k)\sin\mu.$$

From (3.14) and (3.15) the following can be derived:

$$(\xi_1, \mathbf{e}_R) = \frac{1}{F_{21}}\left[(\boldsymbol{\eta}_1, \mathbf{e}_R) - k_{21}h_{21}\boldsymbol{\eta}_2\right],$$
$$(\xi_2, \mathbf{e}_R) = -(\boldsymbol{\eta}_2, \mathbf{e}_R), \quad (3.16)$$
$$(\xi_3, \mathbf{e}_R) = \frac{1}{F_{13}}\left(k_{13}h_{13}(\boldsymbol{\eta}_1, \mathbf{e}_R) - (\boldsymbol{\eta}_3, \mathbf{e}_R)\right).$$

Since $\boldsymbol{\omega} = (0, 0, \omega)$, then

$$(\boldsymbol{\omega}, \mathbf{e}_R) = \omega\sin\mu. \quad (3.17)$$

Taking into account that the influence of dissipative forces at time intervals commensurate with the period of the planet's revolution around its own axis is negligible, we transform formula (3.7) by putting $\chi = 0$:

$$\Pi = -\frac{fm}{R} - \frac{3fm^2 r_0 \Phi(\nu)}{140\pi E R^3}\left\{\omega^2 - 3(\boldsymbol{\omega}, \mathbf{e}_R)^2\right\} +$$
$$+\sum_{k=1}^{3}\frac{9f^2 m^2 m_k r_0 \Phi(\nu)}{140\pi E q_k^3 R^3}\left\{1 - 3(\xi_k, \mathbf{e}_R)^2\right\}. \quad (3.18)$$

According to formula (3.18), in order to estimate the contribution to the Earth's gravitational potential from the Sun, the Moon and other planets of the Solar System, it is necessary to estimate the value $\frac{m_k}{q_k^3}$. Index $k = 1$ corresponds to the influence of the Sun. Index $k = 2$ corresponds to the influence of the Moon, and $k = 3$ corresponds to the influence of the planet. Assuming all orbits to be circular, we obtain:

$$\frac{m_1}{q_1^3} \approx \frac{m_1}{R_1^3}, \quad \frac{m_2}{q_2^3} = \frac{m_2}{R_2^3},$$
$$\frac{m_3}{(R_1+R_2)^3} \le \frac{m_3}{q_3^3} \le \frac{m_3}{(R_1-R_2)^3}.$$

For the Sun and the Moon, the values of this quantity expressed in 10^{24} kg/(a.u.)^3 are as follows:

$$m_1/q_1^3 = 1.989\cdot 10^6, \quad m_2/q_2^3 = 4.332\cdot 10^6.$$

Table. Influence of the gravitational fields of the Solar System planets on the Earth's gravitational potential (measuring unit 10^{24} kg/(a.u.)^3)

Planets	$\frac{m_3}{(R_1+R_2)^3}$	$\frac{m_3}{(R_1-R_2)^3}$
Mercury	0.124	1.434
Venus	0.951	229.889
Mars	0.040	4.470
Jupiter	7.953	25.565
Saturn	0.486	0.914
Uranus	0.011	0.014
Neptune	$3.415 \cdot 10^{-3}$	$4.17 \cdot 10^{-3}$

The results of the calculations of the minimum and maximum values of the value m_3/q_3^3 corresponding to the planets of the solar system are presented in the table. The numerical values are expressed in 10^{24} kg/(a.u.)^3 (1 a.u. = $1.495978707 \cdot 10^{11}$ m). This is derived from the results obtained that the main contribution to the Earth's gravitational potential comes from the Moon and the Sun. The influence of other planets of the Solar System is not significant. The maximum value of the parameter m_k/q_k^3 is reached by Venus at the moment of its maximum approach to the Earth. However, even this value is of the order of 10^{-4}, when compared to the values of the corresponding numerical coefficients for the Moon and the Sun.

Let us transform the expression (3.18) by selecting dimensionless coefficients and taking into account (3.16)–(3.17), thus we obtain the following formula for the gravitational potential of a viscoelastic planet taking into account tidal effects:

$$\Pi = -\frac{fm}{R}\left\{1 + k_0(1 - 3\sin^2\mu) + \frac{k_1(1+e_1\cos\vartheta_1)^3}{F_{21}^3} + \right.$$
$$+\left(\frac{3}{F_{21}^2}\left[(\boldsymbol{\eta}_1, \mathbf{e}_R) - k_{21}h_{21}(\boldsymbol{\eta}_2, \mathbf{e}_R)\right]^2 - 1\right) +$$
$$+ k_2(1+e_2\cos\vartheta_2)^3\left(3(\boldsymbol{\eta}_2, \mathbf{e}_R)^2 - 1\right) + \quad (3.19)$$
$$+\frac{k_3(1+e_3\cos\vartheta_3)^3}{F_{13}^3}\times$$
$$\left.\times\left(\frac{3}{F_{13}^2}\left[k_{13}h_{13}(\boldsymbol{\eta}_1, \mathbf{e}_R) - (\boldsymbol{\eta}_3, \mathbf{e}_R)\right]^2 - 1\right)\right\},$$

where

$$k_0 = \frac{3mr_0\omega^2\Phi(\nu)}{140\pi E R^2},$$
$$k_j = \frac{9fmm_j r_0 \Phi(\nu)}{140\pi E R^2 a_j^3 (1-e_j^2)^3}, \quad j = 1, 2, 3. \quad (3.20)$$

Let us apply the obtained result to calculate the gravitational potential of the Earth moving in the gravitational field of the Sun, Moon and Venus. Let us take the following values of the parameters included in formulas (3.3), (3.9)–(3.11), (3.20) [23]:

$$r_0 = 6.378 \cdot 10^6\ \text{m},\ h = 3 \cdot 10^5\ \text{m},\ E = 1.2 \cdot 10^{11}\ \text{kg/(m} \cdot \text{s}^2),$$
$$\nu = 0.2,\ \omega = 7.2922 \cdot 10^{-5}\ \text{s}^{-1},$$

$$f = 6.672 \cdot 10^{-11}\ \text{m}^3/(\text{kg} \cdot \text{s}^2),\ m = 5.9736 \cdot 10^{24}\ \text{kg},$$
$$m_1 = 1.98911 \cdot 10^{30}\ \text{kg},\ m_2 = 7.349 \cdot 10^{22}\ \text{kg},$$
$$m_3 = 4.8685 \cdot 10^{24}\ \text{kg},$$

$$a_1 = 1.4959787 \cdot 10^{11}\ \text{m},\ a_2 = 3.844 \cdot 10^8\ \text{m},$$
$$a_3 = 108208627813\ \text{m},$$

$$e_1 = 0.01671022,\ e_2 = 0.0549,\ e_3 = 0.00676,$$
$$\theta_0 = 23.45° = 0.409280\ \text{rad},$$

$$T_1 = 365.26\ \text{days},\ T_2 = 27.321661\ \text{days},$$
$$T_3 = 224.7\ \text{days},$$

$$g_1 = 1.7967674\ \text{rad},\ g_2 = 0\ \text{rad},\ g_3 = 2.2956836\ \text{rad}.$$

Dimensionless coefficients included in (3.19) have the following values:

$$k_0 = 5.73271 \cdot 10^{-4},\ k_1 = 1.283118 \cdot 10^{-8},$$
$$k_2 = 2.817287 \cdot 10^{-8},\ k_3 = 8.2926 \cdot 10^{-14},$$
$$k_{21} = 3.114226 \cdot 10^{-5},\ k_{13} = 1.382169.$$

As dimensionless time, we take the number of revolutions of the Earth around its own axis:

$$\tau = \frac{\varphi}{2\pi} = \frac{\omega t + \varphi(0)}{2\pi}.$$

By denoting by the stroke the derivative of τ, we obtain from (3.3):

$$\vartheta_i' = N_i\left(1 + e_i \cos\vartheta_i\right)^2,\ N_i = \frac{2\pi T_{\text{rot}}}{\left(1 - e_i^2\right)^{3/2} T_i},\ i = 1, 2, 3,$$

where T_{rot} = 23.93419 h is the period of the Earth's revolution around its own axis. Values of dimensionless coefficients N_i:

$$N_1 = 0.017162,\ N_2 = 0.230381,\ N_3 = 0.027888.$$

Let us introduce into consideration a dimensionless function—the relative gravitational potential Π_1:

$$\Pi_1 = \frac{\Pi - \Pi_0}{\Pi_0},\ \Pi_0 = -\frac{fm}{R}.$$

According to (3.19)

$$\Pi_1 = \Pi_{10} + \Pi_{11},\ \Pi_{10} = k_0(1 - 3\sin^2\mu) = \text{const},$$

$$\Pi_{11} = \frac{k_1\left(1 + e_1\cos\vartheta_1\right)^3}{F_{21}^3} \times$$
$$\times\left(\frac{3}{F_{21}^2}\left[\left(\boldsymbol{\eta}_1, \mathbf{e}_R\right) - k_{21}h_{21}\left(\boldsymbol{\eta}_2, \mathbf{e}_R\right)\right]^2 - 1\right) +$$
$$+ k_2\left(1 + e_2\cos\vartheta_2\right)^3\left(3\left(\boldsymbol{\eta}_2, \mathbf{e}_R\right)^2 - 1\right) + \qquad (3.21)$$
$$+ \frac{k_3\left(1 + e_3\cos\vartheta_3\right)^3}{F_{13}^3} \times$$
$$\times\left(\frac{3}{F_{13}^2}\left[k_{13}h_{13}\left(\boldsymbol{\eta}_1, \mathbf{e}_R\right) - \left(\boldsymbol{\eta}_3, \mathbf{e}_R\right)\right]^2 - 1\right).$$

The Π_{10} summand is responsible for the perturbing part of the gravitational potential caused by the Earth's compression along the rotation axis, which does not change with time. The function Π_{11}, given by formula (3.21), is the time-dependent part of the gravitational potential caused by tidal effects.

Figures 2–4 show the graphs obtained using the *Octave*[1] mathematical package of the function $\Pi_{11} = \Pi_{11}(\tau)$ describing the Earth's gravitational potential at an external point over a period of 30 days at an altitude of h = 300 km from the Earth's surface at different latitudes (0°, 30°, 60°). At the initial moment of time, the following parameters are set:

$$\vartheta_1(0) = -0.0433335,\ \vartheta_2(0) = 0,\ \vartheta_3(0) = 0.8804619,$$
$$g_1 = 1.7967674,\ g_2 = 0,\ g_3 = 2.2956836,\ \lambda = 0.$$

One graduation on the abscissa axis corresponds to two days.

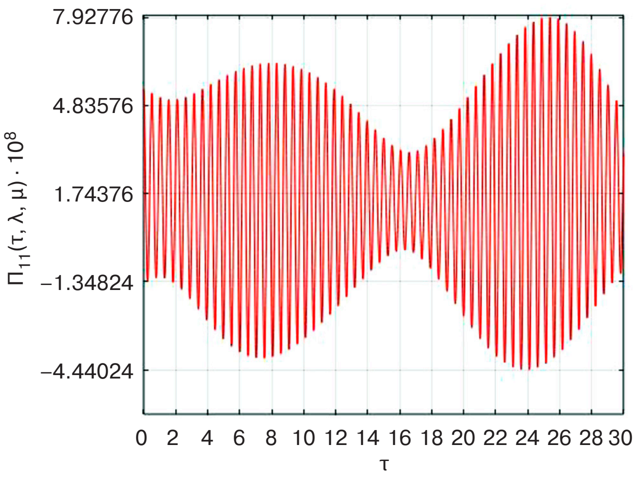

Fig. 2. Change in the Earth's gravitational potential at an external point with spherical coordinates $R = 6.678 \cdot 10^6$ m, $\lambda = 0$, $\mu = 0$ for 30 days

[1] https://octave.org/. Accessed May 16, 2023.

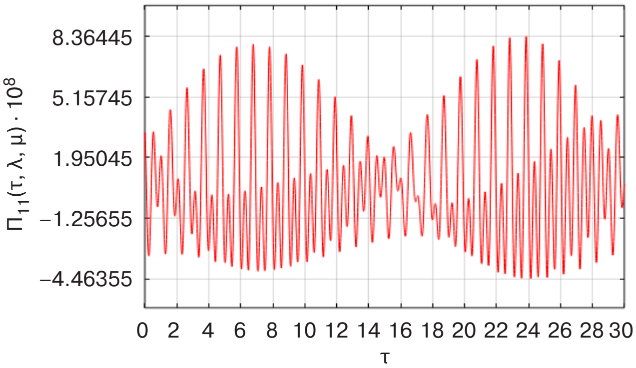

Fig. 3. Change in the Earth's gravitational potential at an external point with spherical coordinates $R = 6.678 \cdot 10^6$ m, $\lambda = 0$, $\mu = \pi/6$ for 30 days

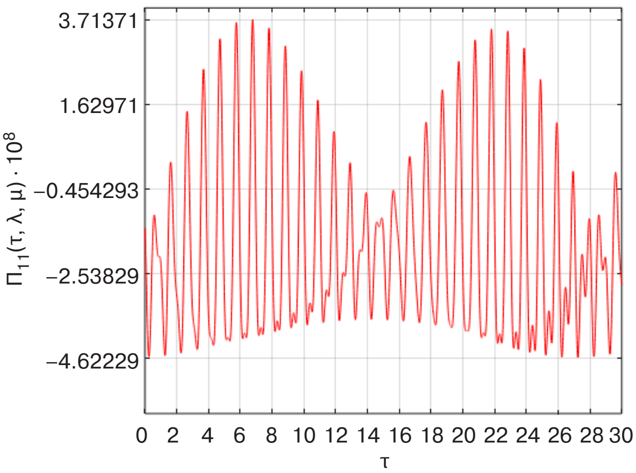

Fig. 4. Change in the Earth's gravitational potential at an external point with spherical coordinates $R = 6.678 \cdot 10^6$ m, $\lambda = 0$, $\mu = \pi/3$ for 30 days

As can be seen from the above graphs, the dependence of the gravitational potential on time has a complex oscillatory character. It depends significantly on the geographic latitude of the point over which it is measured.

CONCLUSIONS

In this article, a formula has been established for the gravitational potential of a planet modeled by a viscoelastic ball. It considers the tidal effects caused by the gravitational fields of its natural satellite, the attracting center (star) and another planet. Based on the model thus constructed, it is shown that the main contribution to the tidal component of the Earth's gravitational potential is made by the Moon and the Sun. The study also makes estimates of the influence of gravitational fields of the other planets of the Solar System on the gravitational potential of the Earth, modeled as a viscoelastic body. Graphs have been plotted of the time dependence of the tidal component of the gravitational potential at three different points in the Earth-related coordinate system located at different latitudes at an altitude of 300 km from the Earth's surface.

Authors' contribution. All authors equally contributed to the research work.

REFERENCES

1. Molodenskii M.S *Izbrannye trudy. Gravitatsionnoe pole. Figura i vnutrennee stroenie Zemli* (*Selected Works. Gravitational Field. The Figure and Internal Structure of the Earth*). Moscow: Nauka; 2001. 569 p. (in Russ.). ISBN 5-02-002331-0
2. Molodenskii S.M. *Prilivy, nutatsiya i vnutrennee stroenie Zemli* (*Tides, Nutation and the Internal Structure of the Earth*). Moscow: Institut fiziki Zemli im. O.Yu. Shmidta; 1984. 215 p. (in Russ.).
3. Efroimsky M., Williams J.G. Tidal torques. A critical review of some techniques. *Celest. Mech. Dyn. Astr.* 2009;104(3):257–289. https://doi.org/10.1007/s10569-009-9204-7
4. Darwin G.H. *Prilivy i rodstvennye im yavleniya v Solnechnoi sisteme (Tides and Kindred Phenomena in the Solar System)*: transl. from Engl. Moscow: Nauka; 1965. 252 p. (in Russ.).
   [Darwin G.H. *The Tides and Kindred Phenomena in the Solar System*. Boston: Houghton; 1899. 378 p.]
5. Zharkov V.N. (Ed.). *Prilivy i rezonansy v Solnechnoi sisteme:* sbornik statei (*Tides and Resonances in the Solar System:* a collection of articles). Moscow: Mir; 1975. 288 p. (in Russ.).
6. Petit G., Luzum B. (Eds.). *IERS Conventions* (2010). *IERS Technical Note 36.* Frankfurt am Main: Verlag des Bundesamts für Kartographie und Geodäsie; 2010. 179 p. ISBN 3-89888-989-6
7. Vil'ke V.G. Motion of a visco-elastic sphere in a central Newtonian force field. *J. Appl. Math. Mech.* 1981;44:280–284.
   [Original Russian Text: Vil'ke V.G. Motion of a visco-elastic sphere in a central Newtonian force field. *Prikladnaya Matematika i Mekhanika.* 1980;44(3):395–402 (in Russ.).]
8. Makarov V.V., Berghea C., Efroimsky M. Dynamical evolution and spin-orbit resonances of potentially habitable exoplanets. The case of GJ 581d. *Astrophys. J.* 2012;761(2):83–96. https://doi.org/10.1088/0004-637X/761/2/83
9. Sidorenkov N.S. *Fizika nestabil'nostei vrashcheniya Zemli* (*Physics of Earth Rotation Instabilities*). Moscow: Fizmatlit; 2002. 384 p. (in Russ.). ISBN 5-9221-0244-3

10. Baranova E.Yu., Vil'ke V.G. Rotation of elastic sphere around its center of mass in the gravitational field of two attractive centers. *Moscow Univ. Mech. Bulletin.* 2014;69(3):57–64. https://doi.org/10.3103/S0027133014030017
[Original Russian Text: Baranova E.Yu., Vil'ke V.G. Rotation of elastic sphere around its center of mass in the gravitational field of two attractive centers. *Vestnik Moskovskogo Universiteta. Seriya 1. Matematika. Mekhanika.* 2014;3:33–40 (in Russ.).]
11. Markov Yu.G., Perepelkin V.V., Rykhlova L.V., Filippova A.S. A Numerical-analytical approach to modeling the axial rotation of the Earth. *Astron. Rep.* 2018;62(4):299–308. https://doi.org/10.1134/S1063772918040042
[Original Russian Text: Markov Yu.G., Perepelkin V.V., Rykhlova L.V., Filippova A.S. Numerical-analytical approach to modeling the axial rotation of the Earth. *Astronomicheskii Zhurnal.* 2018;95(4):317–326 (in Russ.). https://doi.org/10.7868/S0004629918040047]
12. Sidorenkov N.S. Celestial-mechanical factors of the weather and climate change. *Geofizicheskie protsessy i biosfera = Geophysical Processes and Biosphere.* 2015;14(3):5–26 (in Russ.).
13. Sottili G., Martino S., Palladino D.M., Paciello A., Bozzano F. Effects of tidal stresses on volcanic activity at Mount Etna, Italy. *Geophys. Res. Lett.* 2007;34(1):L01311. https://doi.org/10.1029/2006GL028190
14. Aksenov E.P. *Teoriya dvizheniya iskusstvennykh sputnikov Zemli* (*Theory of Motion of Artificial Earth Satellites*). Moscow: Nauka; 1977. 360 p. (in Russ.).
15. Okhotsimskii D.E., Sikharulidze Yu.G. *Osnovy mekhaniki kosmicheskogo poleta* (*Fundamentals of Space Flight Mechanics*). Moscow: Nauka; 1990. 448 p. (in Russ.). ISBN 5-02-014090-2
16. Bordovitsyna T.V., Avdyushev V.A. *Teoriya dvizheniya iskusstvennykh sputnikov Zemli. Analiticheskie i chislennye metody* (*Theory of Motion of Artificial Earth Satellites. Analytical and Numerical Methods*). Tomsk: TSU; 2016. 254 p. (in Russ.). ISBN 978-5-9462-1607-4
17. Gusev I.V. Assessment of tidal effects on low Earth orbit satellites. *Izvestiya vysshikh uchebnykh zavedenii. Geodeziya i aehrofotosemka = Izvestia VUZOV. Geodesy and Aerophotography.* 2013;57(2):18–24 (in Russ.).
18. Vil'ke V.G. *Analiticheskie i kachestvennye metody mekhaniki sistem s beskonechnym chislom stepenei svobody* (*Analytical and Qualitative Methods of Mechanics of Systems with an Infinite Number of Degrees of Freedom*). Moscow: URSS; 2023. 200 p. (in Russ.). ISBN 978-5-9710-3847-4
19. Borets A.S., Shatina A.V. Gravitational potential of a planet modeled by a visco-elastic sphere. *J. Phys.: Conf. Ser.* 2020;1705:012001. https://doi.org/10.1088/1742-6596/1705/1/012001
20. Borets A.S., Shatina A.V. Mathematical model of the gravitational potential of the planet taking into account dissipation. In: *Fundamental'nye, poiskovye, prikladnye issledovaniya i innovatsionnye proekty sbornik trudov Natsionalnoi nauchno-prakticheskoi konferentsii = Fundamental, Exploratory, Applied Research and Innovative Projects: Proceedings of the National Scientific and Practical Conference.* Moscow: MIREA; 2022. P. 132–136 (in Russ.).
21. Vil'ke V.G. *Teoreticheskaya mekhanika:* uchebnik i praktikum dlya vuzov (*Theoretical Mechanics:* Textbook and Workshop for Universities). Moscow: Yurait; 2023. 311 p. (in Russ.). ISBN 978-5-5340-3481-3
22. Vil'ke V.G., Shatina A.V. Translational–Rotational Motion of a Viscoelastic Sphere in Gravitational Field of an Attracting Center and a Satellite. *Cosmic Research.* 2004;42(1):91–102. https://doi.org/10.1023/B:COSM.0000017567.89445.aa
[Original Russian Text: Vil'ke V.G., Shatina A.V. Translational–Rotational Motion of a Viscoelastic Sphere in Gravitational Field of an Attracting Center and a Satellite. *Kosmicheskie Issledovaniya.* 2004;42(1):95–106 (in Russ.).]
23. Murray C.D., Dermott S.F. *Dinamika Solnechnoi sistemy* (*Solar System Dynamics*). Moscow: Fizmatlit; 2010. 588 p. (in Russ.). ISBN 978-5-9221-1121-8
[Murray C.D., Dermott S.F. *Solar System Dynamics.* Cambridge University Press; 2000. 592 p. ISBN 9781139174817. http://doi.org/10.1017/cbo9781139174817]

СПИСОК ЛИТЕРАТУРЫ

1. Молоденский М.С. *Избранные труды. Гравитационное поле. Фигура и внутреннее строение Земли.* М.: Наука; 2001. 569 с. ISBN 5-02-002331-0
2. Молоденский С.М. *Приливы, нутация и внутреннее строение Земли.* М.: Институт физики Земли им. О.Ю. Шмидта; 1984. 215 с.
3. Efroimsky M., Williams J.G. Tidal torques. A critical review of some techniques. *Celest. Mech. Dyn. Astr.* 2009;104(3):257–289. https://doi.org/10.1007/s10569-009-9204-7
4. Дарвин Дж.Г. *Приливы и родственные им явления в Солнечной системе:* пер. с англ. М.: Наука; 1965. 252 с.
5. *Приливы и резонансы в Солнечной системе:* сборник статей: пер. с англ. под ред. В.Н. Жаркова. М.: Мир; 1975. 288 с.
6. Petit G., Luzum B. (Eds.). *IERS Conventions* (2010). *IERS Technical Note 36.* Frankfurt am Main: Verlag des Bundesamts für Kartographie und Geodäsie; 2010. 179 p. ISBN 3-89888-989-6
7. Вильке В.Г. Движение вязкоупругого шара в центральном ньютоновском поле сил. *Прикладная математика и механика.* 1980;44(3):395–402.
8. Makarov V.V., Berghea C., Efroimsky M. Dynamical evolution and spin-orbit resonances of potentially habitable exoplanets. The case of GJ 581d. *Astrophys. J.* 2012;761(2):83–96. https://doi.org/10.1088/0004-637X/761/2/83
9. Сидоренков Н.С. *Физика нестабильностей вращения Земли.* М.: Физматлит; 2002. 384 с. ISBN 5-9221-0244-3
10. Баранова Е.Ю., Вильке В.Г. Вращение упругого шара вокруг центра масс в гравитационном поле двух притягивающих центров. *Вестник Московского университета. Серия 1. Математика. Механика.* 2014;3:33–40.

11. Марков Ю.Г., Перепелкин В.В., Рыхлова Л.В., Филиппова А.С. Численно-аналитический подход к моделированию осевого вращения Земли. *Астрономический журнал.* 2018;95(4):317–326. https://doi.org/10.7868/S0004629918040047
12. Сидоренков Н.С. Небесно-механические причины изменений погоды и климата. *Геофизические процессы и биосфера.* 2015;14(3):5–26.
13. Sottili G., Martino S., Palladino D.M., Paciello A., Bozzano F. Effects of tidal stresses on volcanic activity at Mount Etna, Italy. *Geophys. Res. Lett.* 2007;34(1):L01311. https://doi.org/10.1029/2006GL028190
14. Аксенов Е.П. *Теория движения искусственных спутников Земли.* М.: Наука; 1977. 360 с.
15. Охоцимский Д.Е., Сихарулидзе Ю.Г. *Основы механики космического полета.* М.: Наука; 1990. 448 с. ISBN 5-02-014090-2
16. Бордовицына Т.В., Авдюшев В.А. *Теория движения искусственных спутников Земли. Аналитические и численные методы.* Томск: Изд. дом Томского гос. ун-та; 2016. 254 с. ISBN 978-5-9462-1607-4
17. Гусев И.В. Оценка влияния приливных эффектов на низкоорбитальные ИСЗ. *Известия высших учебных заведений. Геодезия и аэрофотосъемка.* 2013;57(2):18–24.
18. Вильке В.Г. *Аналитические и качественные методы механики систем с бесконечным числом степеней свободы.* М.: URSS; 2023. 200 с. ISBN 978-5-9710-3847-4
19. Borets A.S., Shatina A.V. Gravitational potential of a planet modeled by a visco-elastic sphere. *J. Phys.: Conf. Ser.* 2020;1705:012001. https://doi.org/10.1088/1742-6596/1705/1/012001
20. Борец А.С., Шатина А.В. Математическая модель гравитационного потенциала планеты с учетом диссипации. *Фундаментальные, поисковые, прикладные исследования и инновационные проекты: сборник трудов Национальной научно-практической конференции.* М.: РТУ МИРЭА; 2022. С. 132–136.
21. Вильке В.Г. *Теоретическая механика:* учебник и практикум для вузов. М.: Юрайт; 2023. 311 с. ISBN 978-5-5340-3481-3
22. Вильке В.Г., Шатина А.В. О поступательно-вращательном движении вязкоупругого шара в гравитационном поле притягивающего центра и спутника. *Космические исследования.* 2004;42(1):95–106.
23. Мюррей К., Дермотт С. *Динамика Солнечной системы:* пер. с англ. М.: Физматлит; 2010. 588 с. ISBN 978-5-9221-1121-8

About the authors

Albina V. Shatina, Dr. Sci. (Phys.-Math.), Professor, Department of Higher Mathematics, Institute of Artificial Intelligence, MIREA – Russian Technological University (78, Vernadskogo pr., Moscow, 119454 Russia). E-mail: shatina_av@mail.ru. Scopus Author ID 6506958326, RSCI SPIN-code 8714-6450, https://orcid.org/0000-0001-5016-5899

Alexandra S. Borets, Postgraduate Student, Department of Higher Mathematics, Institute of Artificial Intelligence, MIREA – Russian Technological University (78, Vernadskogo pr., Moscow, 119454 Russia). E-mail: borec@mirea.ru. Scopus Author ID 57221232991, RSCI SPIN-code 9669-2076, https://orcid.org/0000-0002-6878-0184

Об авторах

Шатина Альбина Викторовна, д.ф.-м.н., доцент, профессор кафедры высшей математики, Институт искусственного интеллекта ФГБОУ ВО «МИРЭА – Российский технологический университет» (119454, Россия, Москва, пр-т Вернадского, д. 78). E-mail: shatina_av@mail.ru. Scopus Author ID 6506958326, SPIN-код РИНЦ 8714-6450, https://orcid.org/0000-0001-5016-5899

Борец Александра Сергеевна, аспирант, кафедра высшей математики, Институт искусственного интеллекта ФГБОУ ВО «МИРЭА – Российский технологический университет» (119454, Россия, Москва, пр-т Вернадского, д. 78). E-mail: borec@mirea.ru. Scopus Author ID 57221232991, SPIN-код РИНЦ 9669-2076, https://orcid.org/0000-0002-6878-0184

Translated from Russian into English by Lyudmila O. Bychkova
Edited for English language and spelling by Dr. David Mossop

MIREA – Russian Technological University.
78, Vernadskogo pr., Moscow, 119454 Russian Federation.
Publication date March 31, 2024.
Not for sale.

МИРЭА – Российский технологический университет.
119454, РФ, г. Москва, пр-т Вернадского, д. 78.
Дата опубликования 31.03.2024 г.
Не для продажи.

https://www.rtj-mirea.ru